TECHNISCHE UNIVERSITÄT DRESDEN

Fakultät Forst-, Geo- und Hydrowissenschaften

Site Water Budget: Influences of Measurement Uncertainties on Measurement Results and Model Results

(Standortswasserbilanz: Einflüsse von Messunsicherheiten auf Mess- und Modellergebnisse)

Dissertation zur Erlangung des akademischen Grades
Doctor rerum naturalium (Dr. rer. nat.)

vorgelegt von
Dipl.-Hydrol. Uwe Spank
geboren am 02.08.1977 in Pirna

Gutachter:

Herr Prof. Dr. Christian Bernhofer
TU Dresden / Institut für Hydrologie und Meteorologie

Herr Prof. Dr. Konrad Miegel
Universität Rostock / Institut für Umweltingenieurwesen

eingereicht am: 31.08.2010

verteidigt am: 22.10.2010

Erklärung des Promovenden

Die Übereinstimmung dieses Exemplars mit dem Original der Dissertation zum Thema:

„Site Water Budget: Influences of Measurement Uncertainties on Measurement Results and Model Results“

wird hiermit bestätigt.

Uwe Spank

Tharandt, 24.11.2010

Abstract

The exact quantification of site water budget is a necessary precondition for successful and sustainable management of forests, agriculture and water resources. In this study the water balance was investigated at the spatial scale of canopies and at different temporal scales with focus on the monthly time scale. The estimation of the individual water balance components was primarily based on micrometeorological measurement methods. Evapotranspiration was assessed by the eddy-covariance (EC) method, while sap flow measurements were used to estimate transpiration. Interception was assessed by a combination of canopy drip, stem flow and precipitation (gross rainfall) measurements and soil moisture measurements were used to estimate the soil water storage.

The combination of different measurement methods and the derivation of water balance components that are not directly measurable e.g. seepage and soil evaporation is a very complex task due to different scales of measurement, measurement uncertainties and the superposition of these effects. The quantification of uncertainties is a core point of the present study. The uncertainties were quantified for water balance component as well as for meteorological variables (e.g. wind speed, temperature, global radiation, net radiation and precipitation) that served as input data in water balance models. Furthermore, the influences of uncertainties were investigated in relation to numerical water balance simulations. Here, both the effects of uncertainties in input data and in reference data were analysed and evaluated.

The study addresses three main topics. The first topic was the providing of reference data of evapotranspiration by EC measurements. Here, the processing of EC raw-data was of main concern with focus on the correction of the spectral attenuation. Four different methods of spectral correction were tested and compared. The estimated correction coefficients were significantly different between all methods. However, the effects were small to absolute values on half-hourly time scale. In contrast to half-hour data sets, the method had significant influence to estimated monthly totals of evapotranspiration.

The second main topic dealt with the comparison of water balances between a spruce (*Picea abies*) and a beech (*Fagus sylvatica*) site. Both sites are located in the *Tharandter Wald* (Germany). Abiotic conditions are very similar at both sites. Thus, the comparison of both sites offered the opportunity to reveal differences in the water balance due to different dominant tree species. The aim was to estimate and to compare all individual components of the water balance by a combination of the above mentioned measurement methods. A major challenge was to overcome problems due different scales of measurements. Significant differences of the water balances between both sites occurred under untypical weather conditions. However, under typical condition the sites showed a similar behaviour. Here, the importance of involved uncertainties deserved special attention. Results showed that differences in the water balance between sites were blurred by uncertainties.

The third main topic dealt with the effects of uncertainties on simulations of water balances with numerical models. These analyses were based on data of three sites (spruce, grass and

agricultural site). A kind of Monte-Carlo-Simulation (uncertainty model) was used to simulate effects of measurement uncertainties. Furthermore, the effects of model complexity and the effect of uncertainties in reference data on the evaluation of simulation results were investigated. Results showed that complex water balance models like BROOK90 have the ability to describe the general behaviour and tendencies of a water balance. However, satisfying quantitative results were only reached under typical weather conditions. Under untypical weather e.g. droughts or extreme precipitation, the results significantly differed from actual (measured) values. In contrast to complex models, it was demonstrated that simple Black Box Models (e.g. HPTFs) are not suited for water balance simulations for the three sites tested here.

Kurzfassung

Die genaue Quantifizierung des Standortswasserhaushalts ist eine notwendige Voraussetzung für eine erfolgreiche und nachhaltige Bewirtschaftung von Wäldern, Äckern und Wasserressourcen. In dieser Studie wurde auf der Raumskala des Bestandes und auf verschieden Zeitskalen, jedoch vorrangig auf Monatsebene, die Wasserbilanz untersucht. Die Bestimmung der einzelnen Wasserbilanzkomponenten erfolgte hauptsächlich mit mikrometeorologischen Messmethoden. Die Eddy- Kovarianz- Methode (EC- Methode) wurde benutzt zur Messung der Evapotranspiration, während Xylem- Flussmessungen angewendet wurden, um die Transpiration zu bestimmen. Die Interzeption wurde aus Messungen des Bestandesniederschlags, des Stammablaufs und des Freilandniederschlags abgeleitet. Messungen der Bodenfeuchte dienten zur Abschätzung des Bodenwasservorrats.

Die Kombination verschiedener Messmethoden und die Ableitung von nicht direkt messbaren Wasserhaushaltkomponenten (z.B. Versickerung und Bodenverdunstung) ist eine äußerst komplexe Aufgabe durch verschiedenen Messskalen, Messfehler und die Überlagerung dieser Effekte. Die Quantifizierung von Unsicherheiten ist ein Kernpunkt in dieser Studie. Dabei werden sowohl Unsicherheiten in Wasserhaushaltskomponenten als auch in meteorologischen Größen, welche als Eingangsdaten in Wasserbilanzmodellen dienen (z.B. Windgeschwindigkeit, Temperatur, Globalstrahlung, Nettostrahlung und Niederschlag) quantifiziert. Weiterführend wird der Einfluss von Unsicherheiten im Zusammenhang mit numerischen Wasserbilanzsimulationen untersucht. Dabei wird sowohl die Wirkung von Unsicherheiten in Eingangsdaten als auch in Referenzdaten analysiert und bewertet.

Die Studie beinhaltet drei Hauptthemen. Das erste Thema widmet sich der Bereitstellung von Referenzdaten der Evapotranspiration mittels EC- Messungen. Dabei waren die Aufbereitung von EC- Rohdaten und insbesondere die Dämpfungskorrektur (Spektralkorrektur) der Schwerpunkt. Vier verschiedene Methoden zur Dämpfungskorrektur wurden getestet und verglichen. Die bestimmten Korrekturkoeffizienten unterschieden sich deutlich zwischen den einzelnen Methoden. Jedoch war der Einfluss auf die Absolutwerte halbstündlicher Datensätze gering. Im Gegensatz dazu hatte die Methode deutlichen Einfluss auf die ermittelten Monatssummen der Evapotranspiration.

Das zweite Hauptthema beinhaltet einen Vergleich der Wasserbilanz eines Fichten- (*Picea abies*) mit der eines Buchenbestands (*Fagus sylvatica*). Beide Bestände befinden sich im Tharandter Wald (Deutschland). Die abiotischen Faktoren sind an beiden Standorten sehr ähnlich. Somit bietet der Vergleich die Möglichkeit Unterschiede in der Wasserbilanz, die durch unterschiedliche Hauptbaumarten verursacht wurden, zu analysieren. Das Ziel was es, die einzelnen Wasserbilanzkomponenten durch eine Kombination der eingangs genanten Messmethoden zu bestimmen und zu vergleichen. Ein Hauptproblem dabei war die Umgehung der unterschiedlichen Messskalen. Deutliche Unterschiede zwischen den beiden Standorten traten nur unter untypischen Wetterbedingungen auf. Unter typischen Bedingungen zeigten die Bestände jedoch ein ähnliches Verhalten. An dieser Stelle erlangten Messunsicherheiten beson-

dere Bedeutung. So demonstrierten die Ergebnisse, dass Unterschiede in der Wasserbilanz beider Standorte durch Messunsicherheiten verwischt wurden.

Das dritte Hauptthema behandelt die Wirkung von Unsicherheiten auf Wasserbilanzsimulationen mittels numerischer Modelle. Die Analysen basierten auf Daten von drei Messstationen (Fichten-, Grasland- und Agrarstandort). Es wurde eine Art Monte-Carlo-Simulation eingesetzt, um die Wirkung von Messunsicherheiten zu simulieren. Ferner wurden auch der Einfluss der Modellkomplexität und die Effekte von Unsicherheiten in Referenzdaten auf die Bewertung von Modellergebnissen untersucht. Die Ergebnisse zeigten, dass komplexe Wasserhaushaltsmodelle wie BROOK90 in der Lage sind, das Verhalten und Tendenzen der Wasserbilanz abzubilden. Jedoch wurden zufriedenstellende quantitative Ergebnisse nur unter üblichen Wetterbedingungen erzielt. Unter untypischen Wetterbedingungen (Dürreperioden, Extremniederschläge) wichen die Ergebnisse deutlich vom tatsächlichen (gemessenen) Wert ab. Im Gegensatz zu komplexen Modellen zeigte sich, dass Black Box Modelle (HPTFs) nicht für Wasserhaushaltssimulation an den drei genannten Messstandorten geeignet sind.

Contents

1 Introduction and Overview

1.1 General Introduction

Water balance is determined by the interaction of a huge number of biotic and abiotic parameters (Barner 1987, Dyck and Peschke 1995, Baumgartner and Liebscher 1996). Abiotic parameters (such as meteorological conditions, geological and hydro-geological properties, soil and relief) as well as biotic parameters, (such as composition of species, form, height and vitality) are mutually dependent and interact in a complex way. Most of this interaction is different for different scales of space and time. Generally speaking, abiotic parameters define the potential limits of the water balance and the biotic parameters modify the characteristics inside these limits. However, in a more detailed view there are also feedbacks from biotic to abiotic parameters, which change the potential limits and even modify abiotic conditions (Rios-Entenza and Miguez-Macho 2010).

Additionally, the complex interaction between abiotic and biotic parameters is overlain by anthropogenic effects, which affects the water balance directly and indirectly at any scale of space and time. Direct effects of anthropogenic impacts are typically limited to small areas or to short time periods up to centuries. However, the total effect of anthropogenic impacts can cause long-lasting effects or even irreversible changes of water balance characteristic at large spatial scales. Further anthropogenic effects can influence regions which are far way from direct impacts because of indirect feedbacks and because of a combination of different anthropogenic effects.

A well-known example is related to increasing desertification in Sub-Saharan Africa (Sahel region), which is caused by a combination of direct and indirect anthropogenic effects. Direct effects are related to a change in the use of water resources, overgrazing and soil erosion. Indirect effects are related primary to effects of land use changes at the local scale (local scale: 100 m up to 100 km according to Oke, 1987) and eventually to global warming as a consequence of increased CO_2 emissions on global scale (IPCC 2007). However, the overlap of all anthropogenic effects and the (typically positive) feedbacks with effects of global warming cause changes at the macro scale (macro scale: > 100 km according to Oke 1987) and cause changes related to geological periods of time, which means the changes are practically irreversible.

1.2 Study Intentions

In contrast to dramatic example of Sahel region, the present study is related to investigations of water balance in the temperate zone and is restricted to areas of around 0.75 km². Further, the investigations are related exclusively to test sites in the *Erzgebirge* (Ore Mountains, Germany). The investigated time scales reaches from 30 minutes (estimated fluxes of eddy covariance system device) and days (typical resolution of input data) to months and years (balances). The analyses are restricted to direct effects of human activity at the same scales of space and time. However, long-lasting effects, indirect feedbacks and complex interactions with bigger scales of space and time are disregarded. An area of 0.75 km² is the change from

micro to local scale (micro scales: < 1 km according to Oke 1987) and is related to the canopy as typical unit of landscape. In this context the scale of space is also called canopy scale.

A canopy is represented by widely homogeneous properties of biotic parameters, at which the biotic parameters are representative for properties of predominate vegetation. But also the most abiotic parameters such as climate, slope, aspect and micro relief are similarly homogenous at the spatial scale of canopy, at which especially variations of meteorological conditions can be ignored for an area < 0.75 km². However, soil properties and some related hydrological characteristics such as infiltration, preferential flow and creation of perched water are often very heterogeneous within areas of 0.75 km². In this context the description of geological and soil properties must be accumulated to a set of representative parameters, which describes all hydrological relevant characteristics. With the above limitations, it becomes possible to describe the behaviour of the water balance on a canopy scale through a one-dimensional column model. However, the interaction with neighbouring columns must be treated appropriately, which is especial important in case of sloping terrain, where lateral exchanges and lateral flows are relevant hydrological processes.

Almost all canopies in Central Europe (with the exception of some isolated nature reserves) are cultural areas. That means, the current characteristic was not created before or created only due to human activities (Larcher 1976, Ellenberg 1996). For stands in the *Erzgebirge*, human activities - in terms of agricultural and forest management - are decisive, at which changes of biotic properties (biotic parameters) are typically related to changes of land use and soil management. In this way the water balance, which is characterized by the complex interaction between biotic and abiotic parameters, is also influenced and determined by these anthropogenic effects. In context to investigated sites and in relation to predominate activities in the *Erzgebirge*, the impacts on vegetation (species composition, height and form) and the impacts on soil properties (sealing, consolidation, ploughing and drainage) are most relevant for the characteristics of the water balance.

The effects of anthropogenic management on water balance, as well as the interaction between management and water balance, are important for both forest and agricultural sites. Successful and sustainable management is only possible due to sufficient and careful consideration of present general conditions, which determine the available water resources and determine the individual water balance components. It should be noted that agricultural and forest management is actually facing significant changes of water balance components. This is due to the predicted and ongoing climate change in Central Europe, with lower precipitation sums in summer months, more rainfall extremes, shorter periods with snow cover and a changing growing season (Beck et al. 2007, Franke et al. 2006b, Franke and Köstner 2007, Schönwiese and Janoschitz 2008a, Schönwiese and Janoschitz 2008b)

The empirical experiences in context to interrelationships between agricultural and forest management, utilization and management of present water resources and optimal yield of crop and timber have lost their validity in many cases because of changed general conditions resulting from climate change. This circumstance is especially important for forests, where

practical experiments and accumulation of practical experiences for finding optimal strategies of management are excluded or only possible in very restricted ways because of the long growing time of trees. However, for agriculture, practical experiments are often also not the optimal way to find useful strategies for agricultural management because of high costs and time consumption to arrive at reliable results.

A possible way to optimize strategies of management is offered by the application of numerical water balance models. These models offer the opportunity to predict the behaviour of the water balance (and the behaviour of individual water balance components) for different scenarios of land use, for different scenarios of agricultural and forest management, and for different scenarios of climate and climate change respectively. In this way, it is possible to give an estimate of the effects of management and of climate change. It is possible to optimize strategies of management to reduce crop failure and to sustain and create stable and healthy forests.

The evaluation of water balance and subsequently the classification of water supply are much more difficult for forest sites than agricultural sites. In particular, the coupling between biotic and abiotic parameters is significantly more complex in forests because of height, form, multi-layered structure, depth of roots and plant physiological behaviour. Additionally, the growing time before harvest is significantly longer. Management mistakes may cause significantly higher economic and ecological damages.

1.3 Background and Special Topics

The DFG (German Science Foundation) supported the "Model Based Classification of the Water Balance of Forest Sites in Low Mountain Areas (FE 504/2-2)" project, which dealt with the classification and evaluation of water balance of forest sites. This project was the basis of the present study. The objectives of the project were to indicate and to analyze the basics for objective evaluation of water balance, at which the objective evaluation of water supply of forest sites was the primary focus. The investigations and analyses were based on combinations of different measurement methods (micrometeorological, plant physiological and soil hydrological methods) and based on investigations in different spheres (atmosphere, biosphere, hydrosphere and soil). In this context the project was divided into four subprojects: (1) Atmosphere, (2) Soil, (3) Plant, and (4) Integration.

(1) Atmosphere was responsible for providing meteorological input data and reference data of evapotranspiration (by eddy covariance measurements). Furthermore, the subproject investigated the interaction between atmosphere and biosphere on a canopy scale; the main focus of this was in particular plant physiology behaviour in relation to meteorological conditions.

(2) Soil was focussed on estimating and providing soil parameters by investigating soil water movement and soil water storage (infiltration, root water uptake and seepage). Furthermore, it was responsible for measuring soil moisture and matrix potential and for providing this data. In another perspective this subproject investigated the spatial distribution and heterogeneity of soil characteristics at a canopy scale.

(3) Plant investigated plant physiology behaviour in relation to meteorological and soil hydrological conditions. The measurements were related at first to the scale of individual trees. However, in a second step the results were raised to canopy scale, which was a second main task. Furthermore, the subproject was responsible for providing plant physiological structure parameters and measuring transpiration via sap flow measurements.

(4) Integration was the interface between all subprojects. It was responsible for combining and integrating results at different levels. It had the task of regionalizing the results with a GIS based application. In this way, this subproject was primary responsible for the increase from canopy scale to landscape scale.

The subprojects focused on investigations and analyses of individual components of the water balance. However, the subprojects focused on the water balance from another perspective. So, it was possible to identify and to analyze all processes, which are relevant for the water balance on a canopy scale.

The analyses and investigations of the present study are primary related to the subproject Atmosphere. However, the present study is also related to other subprojects, especially Soil and Plant. The soil-vegetation-atmosphere interaction and the water balance respectively are analyzed with a multidisciplinary approach, although from a meteorological perspective. In detail the present study deals with three special topics:

Chapter 3 deals with the measurement of reference data of evapotranspiration. Evapotranspiration was measured using the eddy covariance (EC) technique. The EC technique is the state-of-the-art method to estimate mass and energy fluxes at a canopy scale (Foken 2006). However, measured raw fluxes often differ significantly from actual fluxes and require complex and extensive post processing to get correct fluxes (Aubinet et al. 2000, Lee et al. 2004). One special task of post processing is the correction of the spectral attenuation in EC measurements, which is the primary topic of this chapter (already published in Spank and Bernhofer, 2008).

The following Chapters 4 and 5 focuses on the combination and integration of measurement of precipitation, canopy drip, stem flow, transpiration and soil moisture. The behaviour and the characteristic of two different canopies (a Beech and a Spruce canopy) were investigated and compared. In Chapter 4 the net precipitation was primarily investigated, where net precipitation means the percentage of precipitation which becomes potential available for plants. Chapter 5 is primarily related to investigations of individual components of evapotranspiration. Secondly, Chapter 5 deals with the closure of the water balance on a canopy scale, addressing the approximation of seepage by a combination of micro-meteorological measurements, plant physiological measurements and measurements of soil moisture.

Chapter 6 is related to simulations of evapotranspiration and seepage with numerical water balance models. The focus of investigations was to estimate measurement uncertainties and to estimate the effects of model complexity on simulation results. It was possible to identify

sources for uncertainties in water balance investigations and it was possible to quantify their effects at the canopy scale.

2 Materials

2.1 Test sites

2.1.1 Overview

The intention of the following chapters is to give an overview of the test sites and applied methods. However, detail descriptions of methods are given in specific context in special chapters of investigation. The investigations are based on tests sites, located in or in the immediate vicinity of the *Tharandter Wald* (Tharandt Forest, Germany). *Tharandter Wald* is the biggest closed forest in Saxony (Germany). It is part of the foreland of the *Erzgebirge* (Ore Mountains). The average altitude is between 350 and 400 m above sea level. Thus, the relief is a gentle, hilly plateau with some deep valleys. The climate is categorized as sub-oceanic, for which the average annual air temperature is 7.8 °C and average annual precipitation is 823 mm (Grünwald and Bernhofer 2007). The main test sites are located at four places with different types of land use (Spruce forest, Beech forest, Grassland and Agriculture land). So, the vegetation and hydrologic relevant properties of vegetation are significant different at all four sites. However, climatic conditions and soil properties are similar and comparable.

Three of the test sites (Spruce, Grassland and Agricultural) are part of the European measurement programme for carbon dioxide fluxes EUROFLUX (CarboEurope-IP 2008a) and part of the framework for integration of worldwide carbon dioxide measurements FLUXNET (FLUXNET, 2007). In this context, in addition to standard meteorological measurement devices such as rain gauges, humidity sensors, thermometers etc., all three sites were equipped with closed-path eddy covariance system devices for measurements of sensible heat flux, latent heat flux, carbon dioxide flux and momentum flux. Furthermore all sites are equipped with radiation sensors for measurement of radiation balance, components of radiation balance and photosynthetic active radiation.

As well as the sites of FLUXNET/ EUROFLUX programme, a fourth site was installed in a Beech canopy. Therefore, the instrumentation was similar to the other. However, an open-path eddy covariance system device was used, because this site was equipped with an autarkic power supply (solar panels); all other test sites have access to mains electricity. Some additional measurements which are worth mentioning are the measurements of sap flow and of canopy drip at both forests sites. Furthermore, it is referred to the measurements of stem flow at Beech site

Beside the actual test sites, data from the climate station Grillenburg (750 m from the Grassland site) was fundamental for the present study. It was primarily used for reference and for categorization of climate within the *Tharandter Wald*. Furthermore, the precipitation measurement network in the Wernersbach catchment was important (consisting of six rain gauges, N1 to N6). In particular, it was used as a reference in context to the Beech site. In context to the precipitation measurement network, it is also pointed to hydrological measurements (three water gauges) in the Wernersbach catchment. However, hydrological measurements at a

catchment scale were unimportant for the present study. Therefore, the Wernersbach catchment is only referred to for completeness.

However, another and very important test site was the International Phenological Garden of Tharandt, near Hartha. The phenological observations at this site were used as a reference for phenological development and delimitation of growing seasons. The history of this site began in 1962 in the context of the Global Phenological Monitoring Project. The monitoring of leaf status of European Beech trees (*Fagus sylvatica* Dän.) was especially important for investigation of the present study. However, this site has also been equipped with standard measurement devices for climate observations since 2005. Therefore, the site gives an additional reference of the climate of *Tharandter Wald*.

The position of all called test sites within Tharandt Forest is shown in Figure 2.1 with the exception of the Agricultural site. The Agricultural site is located about 6 km south of the Grassland site near Klingenberg.

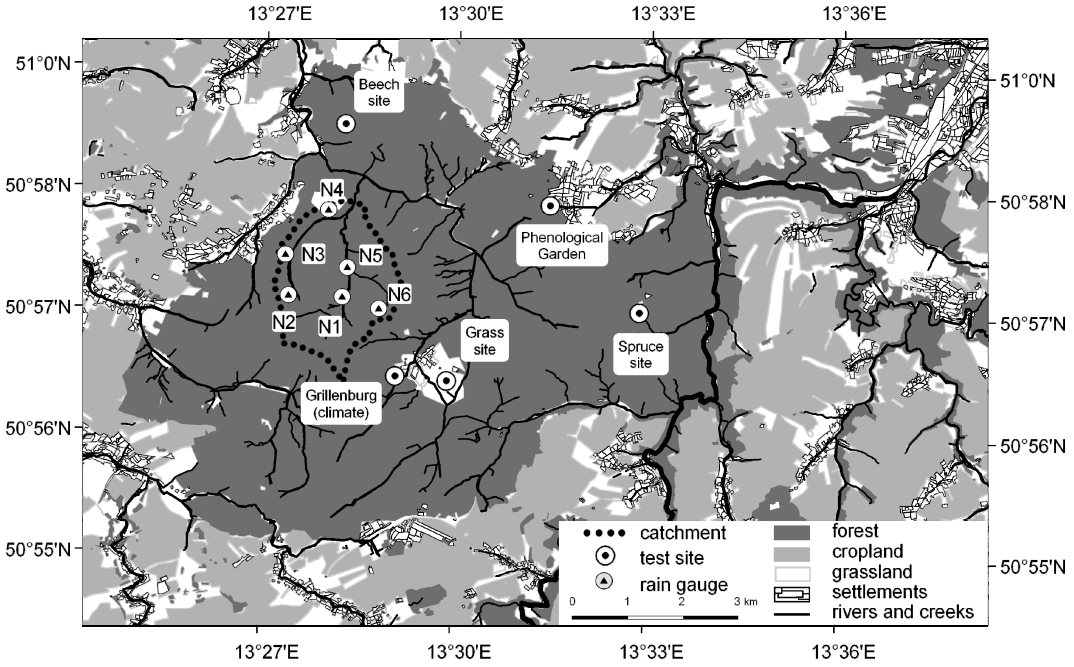

Figure 2.1 Location of test sites, rain gauges and catchment area (Wernersbach) within the *Tharandter Wald* (The Agricultural site is located about 6 km south of the Grassland site)

2.1.2 The Spruce Site and the Beech Site

The Spruce and Beech sites are the most important test sites of the present study. Both sites are located in forests, which are influenced by forestry management and forestry operations. The Beech site is at an autochronous pure European Beech stand (*Fagus sylvatica*) in the north-western part of *Tharandter Wald*. The height of the trees is around 30 m and the age of predominant adult trees is approximately 100 years. An understory is no-existent, with the exception of some isolated young-growth Beech trees. The depth of roots is atypical low for Beech trees; excavations found a root depth of only around 0.5 m. It is to be noted that the results of excavations were confirmed by some trees in the surrounding area of the test site,

which were overturned (including their root plate) by the winter storm *Kyrill* on January 18th and 19th 2007. The LAI (leaf area index) is 3.9 and the percentage of crown closure is 88 %, which was recorded in a measurement campaign in 2009.

The Spruce site is located in the eastern part of *Tharandter Wald*. The canopy trees were sowed in 1887. So, the age of trees is around 120 years. The height of adult trees is about 29 m. The dominating tree species is Norway Spruce (*Picea abies*) with 72 % of all adult trees. Other species of trees are Scots Pine (*Pinus sylvestris*, 15 %), European Larch (*Larix decidua*, 10 %) and subordinated different deciduous trees (3 %) like Silver Birch (*Betula pendula*), Norway Maple (*Acer platanoides*) and Horse Chestnut (*Aesculus hippocastanum*). The depth of roots is on average between 30 and 40 cm due to the predominant Spruce trees. However, other tree species e.g. Pine and Larch have much deeper roots, but they are less important for the characteristics of the site. The canopy was thinned three times (1983, 1988 and 2003) in context to forestry operations and was replanted with European Beech (*Fagus sylvatica*) in 1995 (Gerold, 2004). Those Beech trees have reached a height about 3 to 4 m (measured 2007). Besides young growing Beech trees, the understory is represented by Wavy Hair-grass (*Deschampsia flexuosa*). A complete overview of the most important characteristics of location and vegetation for both sites is given in Table 2.1.

Table 2.1 Most important parameters of location and vegetation of Spruce and Beech sites (Parameters for Spruce site estimated by Grünwald and Bernhofer, 2007; otherwise marked)

attribute	Spruce site	Beech site
position	50°57'49" N 13°34'01" E	50°59'33" N 13°29'25" E
altitude	380 m a.s.l.	392 m a.s.l.
species composition of adult trees	Norway spruce (*Picea abies*) 72 % Scots pine (*Pinus sylvestris*) 15 % European Larch (*Larix decidua*) 10 % other (different deciduous species) 3 %	European Beech (*Fagus sylvatica*) 100 %
species composition of understory	Wavy Hair-grass (*Deschampsia flexuosa*) European Beech (*Fagus sylvatica*)	some isolated young-growth Beech trees
tree age (2007)	~ 120 years (homogenous)	~ 100 years in average (variable)
tree height	29 m	30 m
sky view coefficient	15 % (estimated in 2009)	12 %
leaf area index (LAI)	7.6	3.9 (maximal)
above ground woody elements (SAI) [m²/m²]	1.43	0.94
averaged tree diameter in breast height	≈ 0.361 m	≈ 0.345 m
stem density	477×10^{-4} m^{-2}	331×10^{-4} m^{-2}

The climatic conditions are almost identical at both sites because the spatial separation is small (~6.5 km) and both sites are about the same altitude. Beside similar climatic conditions, soil properties are also comparable. The soil was classified as loamy-skeletal podsol-brown earth (WRB: Dystric Cambisol) on rhyolite at the Spruce site and as loamy podsol-brown earth (WRB: Endostagnic Cambisol) on rhyolite at the Beech site (Schwärzel et al 2009a;

Schwärzel et al 2009b). The texture is typically a sequence of humus top layer (Aeh horizon), mineral layer with entry of loam (Bv) and alteration zone (Cv). However, the Bv horizon is bordered from Cv horizon by a water affected horizon (Bv-Sw/ Bv-Sd) at some places at the Beech site.

High rock content is typical for soils at both sites. The estimated content of rock was dependent on depth: 2 to 10 % in Aeh, 10 to 25 % in Bv and 50 to 75 % in Cv at the Spruce site (Schwärzel et al 2009b). At the Beech site, the content of rock was similar but lower in Bv (2 to 10 %). In general, the depth of soil layers, soil consistency, rock content and (consequently) all hydraulic properties of soil are very heterogeneous on a small scale at both sites. However, it was assumed according to Schwärzel et al (2009b): a thickness of about 5 cm for Aeh and of about 85 cm for Bv. So, the approximated content of plant-available water was between 39 and 65 mm with regard to the rooting depth of the predominant Spruce trees at the Spruce site (Schwärzel 2009c). At the Beech site, the plant-available water was significantly higher because of the deeper Beech roots and lower rock content. The approximated plant-available water was between 125 and 145 mm within rooting depth according to Ad-hoc-AG Boden (2005).

2.1.3 The Grassland Site

The Grassland site is in the centre of *Tharandter Wald* in an area which is used for pasture and forage production. The relief is relative flat and homogenous within a radius of 0.5 km. However, the area is a cold air pocket as a consequence of ambient forests and of slightly convex relief. So, the daily minima air temperature is often significant lower than the other sites. The difference to the Spruce site can increase 4 K in windless nights. In this way, the site is vulnerable to frost and fog.

The grass is usually cut twice a year (occasionally three times). Thereby, the dates of swaths are typically at the beginning of summer (end of May or start of June) and at the beginning of autumn (end of August or in September). In the case of three swaths, the second swath is typically inserted in July. Because of cutting, the vegetation height and LAI (leaf area index) have significant yearly courses, which must be considered in the exact parameterization of models. The vegetation height was measured once per week. Thereby, lowest values (5 to 10 cm) were at the beginning of the growing season or after cutting. However, the highest values (typically 30 to 40 cm, recorded maximum 80 cm) were in the summer before cutting. The LAI was only measured sporadically. However, it was possible to interpolate the yearly course due to a significant correlation between vegetation height and LAI. So, the range of LAI was between 0.46 and 4.69 in the yearly course.

The soil was classified as pseudo-gleysol according to Ad-hoc-AG Boden (2005) (Prescher et al. 2010). The material is silty clay or silty clay loam. By means of an excavation the layering was found to be a humus top layer (Ap) and a mineral layer (Sg). Thereby, the Ap horizon had a thickness of about 25 cm and was well rooted. In the Sg horizon, roots were founded up to depths of 60 cm. However, the number of roots was significant lower than in the Ap horizon. The approximated plant-available water is between 70 and 100 mm. In this context, it is

noted, the site was always well supplied with water; stress due to water shortage could be excluded even in extremely dry summers.

2.1.4 The Agricultural Site

The Agricultural site is situated 4km south of *Tharandter Wald* and about 6 km southern to the Grassland site. The area was once grassland, which was changed into arable land in 1975. Changing crops is typical for this site. During the entire period of investigation, the following crops were cultivated: Winter Barley (*Hordeum vulgare*, 2003/2004), Rapeseed (*Brassica napus*, 2004/2005), Winter Wheat (*Triticum aestivum*, 2005/2006), Maize (*Zea mays* 2007) and Spring Barley (*Hordeum vulgare*, 2008) (Prescher at al. 2010). In this context, vegetation height, LAI and rooting depth were very variable between different periods.

The soil is under strong anthropogenic influence, in contrast to the soils at the other test sites. Ploughing and application of organic and mineral fertilizers have significant effects to soil properties and characteristic of run off at this site. In according to Ad-hoc-AG Boden (2005) the soil was classified as drained Gleysol (Prescher et al. 2010). The founded material was predominately loam in layers within the ploughing zone. However, it was sandy clay or sandy clay loam in zones below. The quantification of plant available water was based on the average rooting depth and the depth of ploughing. So, the plant available water was assumed in range between 100 and 170mm in according to Ad-hoc-AG Boden (2005).

2.2 Measurements

2.2.1 Measurements of Water Balance Components

Primarily, three different methods were used and combined for the estimation of water balance components: eddy covariance (EC) measurements, sap flow measurements and interception measurements. However, the exact interception was estimated as the difference between measured precipitation and estimated sum of measured canopy drip and measured stem flow. However, it should be noted that not all methods were applied at all sites. So, sap flow and interception were only measured at the forests sites (Spruce and Beech sites). Further, stem flow was only necessary for estimation of interception at the Beech site because stem flow is negligible on Spruce (Benecke 1984, Benecke and Ellenberg 1986). In addition, it is referred to measurements of soil moisture at all sites. However, data of soil moisture measurements were only relevant for investigation at forest sites (Chapter 4 and Chapter 5) in the present study.

The EC measurements were primary used for the estimation of complete evapotranspiration. EC measurements are the state-of-the-art micrometeorological method to measure the latent heat fluxes and the evapotranspiration of a canopy or rather of an area, which is called footprint (Foken 2006, Gash 1986). So the EC measurements defined the maximal dimension of the area of investigation, which was in relation to the specific height of measurements and in relation to predominant weather conditions at test sites around 0.75 km².

Besides evapotranspiration, EC data were used for the estimation of aerodynamic conductance g_a and canopy conductance g_c. Those parameters are used to characterize the vegetation

in a big leaf model (Monteith and Unsworth 1990). In the present study (Chapter 5), an inverse solution of the model algorithm was used to distinguish between periods with predominant interception and periods with predominant transpiration. In this way, it was possible to estimate the transpiration from EC data, or rather it was possible to estimate the total transpiration of adult trees, transpiration of understory and soil evaporation.

The transpiration was also measured by sap flow measurements according to Granier (1985, 1987). As opposed to the transpiration, which was derived from EC data, this method directly measured the transpiration of individual trees. However, the transpiration of individual trees was averaged and raised to canopy scale to reduce the effect of errors from individual sensors. At the same time, it was possible to estimate representative data of transpiration of trees (adult trees) at the canopy scale.

The measurements of soil moisture were used for the estimation of charge and discharge of soil water storage. Thereby, changes of soil water storage $\Delta\Theta$ represent the superposition of inputs due to net precipitation and withdrawals due to transpiration, soil evaporation and run off in terms of seepage. In this way, measurements of soil moisture were necessary for validation and cross-check on the one hand. On the other hand, they were necessary for estimation of water balance components, which are not measurable directly.

2.2.2 Measurements of Meteorological Standard Variables and Ancillary Measurements

In addition to measurements of evapotranspiration and its components, the measurements of meteorological standard variables (such as air temperature, air humidity, wind speed, precipitation, global radiation and net radiation) were fundamental for the present study. Furthermore, the data of photosynthetic active radiation (PAR), soil heat flux and soil temperature at all sites and of snow at the Spruce site were used. The estimation of meteorological standard variables was possible directly at specific sites in the case of the Grassland and Agricultural sites. However, a spatial separation was necessary in the case of the Spruce and Beech sites because of vegetation height.

In the case of the Spruce site, temperature, air humidity and precipitation were measured at a clearing in the immediate vicinity. This data were used as reference for meteorological standard. Furthermore, temperature and air humidity were also measured within the canopy. The net radiation and all components of radiation balance were measured at the top of a 42 m scaffolding tower, which was also used as platform for the eddy covariance (EC) system device. Furthermore, the tower was a platform for measurement of PAR, measurement of wind speed and measurements of gradients of temperature, air humidity, PAR and wind speed.

Meteorological standard measurements were not possible in the direct vicinity of the Beech site. So, the data of climate station (Grillenburg), which is around 5 km away, were used as reference for temperature and air humidity. In addition, a 37 m scaffolding tower (similar to the Spruce site) was built as a platform for the EC system device and for measurements of radiation, PAR and wind speed. Moreover, gradients of temperature, air humidity and PAR were measured at the tower of site.

In addition, a rain gauge was installed at the top of the tower. However, this device was not useable for quantification of precipitation, because data were significant affected by measurement errors. These errors were identified by regression analyses with neighbouring rain gauges (N3, N4, N5) and were caused by massive effects due to wind and turbulence. So, the tower measurements of precipitation were only usable for indication of individual precipitation events. However, the quantification of precipitation was done with data from rain gauge N4, which was located at a clearing in a distance of around 0.75 km.

2.2.3 Measurements to Estimate Interception

The interception was estimated as the remainder between precipitation and the sum of canopy drip and stem flow at forest sites. Thereby, the sum of canopy drip and stem flow is called net precipitation. The reference of precipitation (measurements according to meteorological standards) was estimated in the case of the Spruce site at the above mentioned rain gauge in the immediate vicinity. The devices used were a weighing rain gauge (Ott Pluvio) and a tripping bucked rain gauge (Theis); the temporal resolution of measurements was 10 minutes. However, the data in high temporal resolution were complemented by measurements with totalizators (construction according to Hellman) and by measurements of snow depth.

At the Beech site, the rain gauge at the top of tower was a tripping bucked rain gauge (Theis). However, this instrument was only used for identification of rain events because of significant wind induced measurement errors. The devices used for quantification of reference were a bucked rain gauge (Theis) with a temporal resolution of 10 minutes and completing a totalizator (Hellman), which were installed at N4.

Canopy drip was measured with two throughfall troughs at both forest sites. The two throughfall troughs were positioned orthogonally. The length of an individual trough was 10 m and the opening width was 0.159 m. So, the total collection area was 3.18 m² for canopy drip at each site. The collected water was directed into a storage tank, which was equipped with a pressure sensor. So, the canopy drip was estimable by the filling level. In addition, some bucked rain gauges were positioned randomly in both canopies to detect the spatial distribution and variability of canopy drip. However, only the throughfall troughs were used for quantification.

The measurements of stem flow were only necessary at the Beech site. However, stem flow was negligible for Spruce (Benecke 1984, Benecke and Ellenberg 1986). The stem flow was measured according to Reynolds and Henderson (1967) with spiralled collectors, which were installed at three trees at the Beech site. These collectors directed the water flowing on stems into storage tanks with a volumetric capacity of 220 L. The filling level of the storage tanks was measured in the same way as in case of the canopy drip measurements by pressure sensors. It was observed that even 15 mm precipitation was sufficient to create more than 100 L stem flow on an individual tree. In that context, all storage tanks were equipped with automatic emptying, which drain the tanks in rainless periods.

In addition to the three stem flow collectors with storage tanks, a fourth measurement device was installed, where the stem flow was directed into a tripping bucked rain gauge instead of storage tanks. However, this device proved itself only at small precipitation intensities with small stem flow, because the access to the counter was often blocked or the maximal counting rate was exceeded in the case of high flow rates of stem flow. So, the data of this device were used only for cross-checking and were not included in quantitative analyses.

A final overview of canopy drip measurements and stem flow at the Beech site is given in Figure 2.2. Furthermore the measurements of canopy drip at the Spruce site are shown in Figure 2.3. In addition these figures illustrate the characteristics of both forest sites.

Figure 2.2 Measurements of canopy drip and stem flow at the Beech site (visible: throughfall troughs with storage tank as well as spiralled collectors and storage tanks of stem flow measurements)

Figure 2.3 Measurements of canopy drip at the Spruce site (visible: throughfall troughs with storage tank and one of additional bucked rain gauges for estimation of spatial distribution of canopy drip)

2.2.4 Eddy Covariance Measurements

The eddy covariance (EC) method is used to measure the turbulent exchange between canopy and atmosphere. In detail, EC measurements are used to estimate latent heat flux (energy equivalent of evapotranspiration), sensible heat flux, wind speed, wind direction and friction velocity. In relation to the principle of measurement, the estimated data are the spatial average of a base area, which is called the footprint. The exact dimension and location of the footprint is very dynamical. It depends on wind speed, wind direction and atmospheric stability. Furthermore, the footprint is determined by the height of measurement and the roughness of surface. A rough approximation of location and dimension of footprint is given by Gash (1986). According to Gash (1986), and in relation to predominant weather conditions, it was possible to evaluate the spatial composition of EC data. It was found that the maximal percentage of measured EC signal was from areas within a radius of 30 up to 250 m to the EC sensors at all sites. Thereby, it is noted that these results widely conform to approximations of footprint according to Rebmann et al. (2005) and Göckede et al. (2008).

Two different types of EC systems devices were used: closed-path EC system devices and open-path EC system devices. Closed-path EC system devices were installed at the Spruce, Grassland and Agricultural sites. An open-path system device was used at the Beech site. A closed-path system is characterised by a spatial separation between anemometer and gas analyzer. In the special case of the Spruce site, an ultra sonic anemometer Solent Gill R2 (since May 2006 replaced by a Solent Gill R3) and a gas analyzer LI-COR LI 6262 (since November 2006 replaced by a LI-COR LI 7000) were used. The anemometer was installed at the top of the scaffolding tower, while the gas analyzer was in a container on the ground.

The gas analyzer was supported by an air stream from the point of the anemometer with a tube system. Thereby, the main distance (59 m) was bridged by a primary tube with a high flow rate (about 60 L min^{-1}). However, this flow rate was too high for the gas analyzer. So, an air stream with a lower flow rate (4-6 L min^{-1}) was bypassed with a second tube to support the gas analyzer. The signal recording (which means the logging of measured gas concentration, wind speed and sonic temperature) was done by a PC using the recoding software EdiSol for Windows (The University of Edinburgh 2001), at which the recording interval was 0.048 s (≈ 20.8 Hz).

The fundamental construction was similar for the closed-path EC system devices at the Grassland and Agricultural sites. However, the spatial separation was smaller between ultra sonic anemometer (Solent Gill R3 at both sites) and gas analyzer (LI-COR LI 7000 at both sites). So it was possible to supply the gas analyzer directly by an air stream with a low flow rate (3-5 L min^{-1}) and only one tube was necessary instead of a tube system. Thereby, the lengths of tubes were 3.8 m at the Grassland site and 7.8 m at the Agricultural site.

In contrast to closed-path systems, anemometer and gas analyzer are installed at the same location in the case of open-path systems. That means there is no spatial separation between anemometer and gas analyzer. The open-path system consisted of a sonic anemometer (Campbell CSAT3) and an open-path gas analyzer (LI-COR LI 7500) at the Beech site. Both devices

were installed at the top of the 37 m scaffolding tower and so were 7 m above the treetops. Another special difference to EC systems at other sites is related to signal recording at Beech site; this was done by a data logger Campbell CR 5000, for which the recording interval was 0.1 s (= 10 Hz).

The calculation of fluxes (flux processing) was done on the basis of half-hourly record sets. In this way, the estimated fluxes and estimated wind data were available in temporal resolution of 30 minutes. In the case of the Grassland and Agricultural sites, it was possible to access already processed fluxes (CarboEurope-IP 2008b, Grünwald 2008). However, the fluxes were processed in the case of the Spruce and Beech sites with a self-written flux processing programme. The results were compared and cross-checked with fluxes, which were calculated with the flux processing software EdiRe (The University of Edinburgh 2007). Significant differences were not found between both programmes. However, the quality of estimated fluxes was significantly affected by the correct application processing steps. All relevant and applied processing steps are listed in chronological order in Appendix A1. The lists for the self-written programme and for EdiRe were identical. However, the processing steps were slightly different for closed-path and open-path EC system devices. Furthermore, an overview about technical details of EC system devices is included in Appendix A2.

2.2.5 Sap Flow Measurements

The estimation of tree transpiration was done by sap flow measurements according to Granier (1985, 1987), which was measured on 9 trees at the Spruce site and on 8 trees at the Beech site with 2 sensors (west/east) on each tree. In detail, Granier style probes (Granier 1985, 1987) were used, which were 20 mm long with a diameter of 2 mm. A complete sensor consisted of two probes, with each probe inserted radially into the stem 2 m high with a vertical distance of 150 mm. Each probe consisted of two thermocouple junctions (copper-constantan). The upper probe was heated by a heating wire (Constantan) with a constant 0.2 W. However, the lower probe was used as a reference and measures the temperature of the passing sap flow.

The actual measurement of sap flow was based on the temperature difference between the upper and the lower probe. The temperature differences were monitored in 10 second intervals and the 10 minute average were stored on a data logger. Subsequently, the sap flow densities were calculated in according to Granier (1985, 1987) in half-hour intervals by,

$$FD = 0.0119 \cdot \left(\frac{\Delta T_{\max} - \Delta T_i}{\Delta T_i} \right)^{1.231} \qquad (2.1)$$

Thereby, FD is the sap flow density in [g m^{-2} s^{-1}]; ΔT_{max} is the maximal temperature difference (by night or after rainfall) in [K]; and ΔT_i is the actual measured temperature difference between upper and lower probe in [K].

The estimation of night-time sap flow was done according to Lu et al. (2004). Hereby, ΔT_{max} was determined over a period of 10 days. In addition, missing data were primary replaced by

data of the opposite sensor of the tree. Secondly, missing data were performed by regressions to sensors on other trees.

The estimated sap flow density seemed to be independent from the diameter of stems at the Spruce site. In particular, a clear interrelationship was not found between sap flow density and diameter of stems at breast high for the measured Spruce trees. In this context, it was possible to estimate the stand transpiration T_{SF} [mm] by the product of the averaged sap flow density of all measured trees, the cumulative area of sapwood $A_{s,cum}$ and the time period t,

$$T_{SF} = FD_{avg} \cdot A_{s,cum} \cdot t \; . \tag{2.2}$$

In equation (2.2) it has to be considered that $A_{s,cum}$ was related to the area of sapwood, which was normalized by the base area of the site. The required information about the cumulative area of sapwood was estimated from the sum of sapwood areas of all individual trees at the site. The sap flow area of individual trees can be estimated due to a fundamental interrelationship between the circumference of a tree at breast height (C_{BH} in cm) and the corresponding area of sapwood A_s. The interrelationship, which was valid for the Spruce site, was found due to analyses of stem disks (Clausnitzer 2008), and is,

$$A_s = 0.158 \cdot C_{BH}^{\;1.684} \; . \tag{2.3}$$

The procedure at the Beech site was similar to that at the Spruce site. However, in contrast to Spruce, where the sap flow density was widely homogenous within the area of sapwood, the sap flow density decreases radially within the sapwood of a stem from outer to inner parts (Granier et al. 2000, Hölscher et al. 2005, Lüttschwager and Remus 2007). The available measurements were restricted to estimations of the integrated sap flow density within the outer 2 cm of a stem. In this context, information about sap flow density in deeper parts of sapwood and information about the distribution of sap flow density within sapwood were not available. So, it was necessary to use results from other Beech stands, which were comparable in structure, age and height, and which were affected by similar climate conditions. In context to the present study, the results of Geßler et al. (2005) were used.

In this way, it was possible to calculate the ratio of sap flow density from deeper xylem to the outermost. In addition, it was possible to estimate the area of sapwood A_s from circumference at breast high (C_{BH}). For actual calculation of sap flow density per tree, the estimated sap flow density of each pair of sensors was multiplied with the corresponding sapwood area. Afterwards all densities were summed and normalized to the related sapwood area of the tree. For up scaling to stand transpiration, several methods were possible. Usually the trees were divided into C_{BH} classes and the mean sap flow densities per class were multiply with the associated sapwood. Finally, to obtain transpiration of stand T_{SF}, all C_{BH} classes were summed. However, no clear interrelationship between weighted sap flow density and diameter at breast high was found at the investigated Beech stand. In this context, the weighted mean sap flow density of all trees was multiplied with $A_{s,cum}$ as described in Equation (2.2).

2.2.6 Measurements of Soil Moisture

Measurements of soil moisture were especially necessary for investigation at the forest sites. However, the soil moisture was measured at all four sites. The soil moisture was measured in three different layers continuously in temporal resolution of 10 minutes at the Beech site. Thereby, the depths of measurements were 0-10 cm (litter and humus layer), 15 cm and 35 cm. The upper sensor was installed vertically, whereas the others were installed horizontally. At the Spruce site, continuous measurements were done in two layers, at which one of the sensors was installed vertically in the humus layer (depths of measurement 0-10 cm) and the other horizontally below the humus layer at a depth of 10 cm. Besides continuous measurements, the soil moisture was also measured with a TDR-tubular-probe twice a week at the Spruce site. Thereby, the soil moisture was measured between 20 and 100 cm in a vertical resolution of 10 cm.

In addition to described measurements (point measurements), the soil moisture was also measured at two special transects in the immediate vicinity of both test sites (Schwärzel et al. 2009b). At the Spruce site, the transect consisted of 51 FDR-sensors, which were arranged in 9 different columns. Thereby, the soil moisture was measured in each column in 5 to 6 different layers, at depths between 0 and 90 cm. At the Beech site, the transect consisted of 64 TDR-sensors, with the configuration similar to the Spruce site. However, it was measured in 11 columns.

Both transects were significantly more representative for the canopy than the point measurements, because the heterogeneity of soil properties was better attended due to the higher number of sensors. In this way, the derived change of soil water storage $\Delta\Theta$ would also be more representative, if data of transects were used. However, the data of transects were not continuously available. In particular, the data series were interrupted for a long time in 2006. In this context, it was decided to use primarily the data of point measurements. However, the soil moisture as well as $\Delta\Theta$ were compared with transects in periods, when data were available.

In addition, the heterogeneity of soil moisture was investigated by manual measurements with portable TDR instruments. The estimated heterogeneity of soil moisture was significant higher in dry periods than in humid periods. However, it was not possible to quantify the effects of heterogeneity. So, it was not possible too to approximate neither the representativeness of used soil moisture nor the uncertainty of $\Delta\Theta$.

2.3 Periods of Investigation

2.3.1 General Information

Meteorological as well as hydrological and silvicultural measurements and investigation have a long tradition in *Tharandter Wald* (Bernhofer 2002, Grünwald und Bernhofer 2007). So, continuous data series of precipitation, air temperature, air humidity and radiation (rather sunshine duration) are available from the climate station in Grillenburg and from the Spruce site since the 1950s. In that way, the availability of climate data was not a limitation of investiga-

tions. However, the availability of eddy covariance data, sap flow data and data of interception was restrictive for investigation.

The periods of investigation were different for the individual parts of the present study. In Chapter 3 and Chapter 6, the periods of investigations were only restricted due to the availably of eddy covariance (EC) data at the respective test sites. So, the investigations were limited to the period 1997 until 2008 in Chapter 3 due to the availably of EC-data at the Spruce site. In the same way, the investigations were restricted in Chapter 6. However, there the individual periods of investigation were related to periods starting on April 1st and finishing on March 31st of the following year (Wessolek et al. 2008). In detail, complete data series were available from 1997 until 2008 at the Spruce site, from 2004 until 2009 at the Grassland site and from 2005 until 2009 at the Agricultural site for investigation in Chapter 6. It is noted that data from the Beech site were not useable for investigations in Chapter 6 because the applied open-path EC system device often failed in the winter season.

In contrast to investigations of Chapter 3 and Chapter 6, where periods of investigation were only restricted due to the availability of EC data, the investigations of Chapter 4 and Chapter 5 were restricted due to the availably of sap flow data and data of interception, as well as the availability of EC data. Furthermore it was necessary that required data were available from the Beech site as well as from Spruce site. Thereby, two major problems occurred; one was related to massive data gaps of EC system device in winter season at the Beech site; the second was related to autarkic power supply (solar cells) at the Beech site.

The autarkic power supply had insufficient power to heat the storage tanks of stem flow and canopy drip measurements. So, it was not possible to protect the pressure sensors against frost, which prevented measurements of canopy drip and measurements of steam flow in winter. This circumstance restricted the investigation to frost-free periods. Finally, complete data series for comparative investigations were available from April until October 2006 and from April until October 2007.

2.3.2 Climatic Conditions within Investigation Periods

The most important investigation periods in the present study were 2006 and 2007. In this context, they are introduced in detail following. The weather conditions of both periods as well as the climatic conditions of both sites (Spruce and Beech) are analysed in Figure 2.4 and Figure 2.5. They show the monthly mean temperature and the monthly sum of precipitation in comparison to the long-term average of the climate period from 1961 until 1990. It is conspicuous that the monthly mean temperatures were clear higher in both investigation periods than in the long-term average (Figure 2.4). Particularly in summer, autumn and winter 2006, as well as in spring 2007, monthly mean temperatures increased significantly above the long-term average. However it is assumed that temperatures of 2006 and 2007 are typical for the expected future climate.

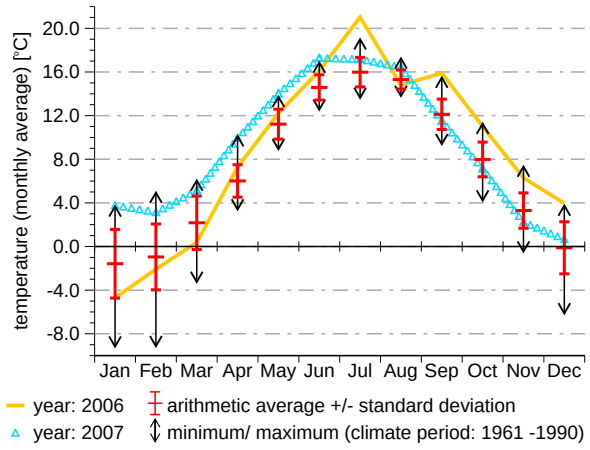

Figure 2.4 Monthly mean temperatures in the *Tharandter Wald* for 2006 and 2007 compared to the climate period 1961 – 1990 (arithmetic mean, standard deviation, minimum and maximum concerning monthly averages of temperatures for 1961 – 1990)

In contrast to temperatures, the monthly sums of precipitation (Figure 2.5) were within normal variations of climate in both investigation periods. The months where the precipitation was below average were July 2006, September 2006 and April 2007. April 2007 was an absolute anomaly. In this month only 0.2 mm was measured during a six week drought. Opposed to the untypically dry months, the measured precipitation was above average in March 2006, August 2006, May 2007, September 2007 and November 2007. In general, two scenarios are derivable from climate conditions: a dry and hot scenario (2006) and a cooler and rainier scenario (2007).

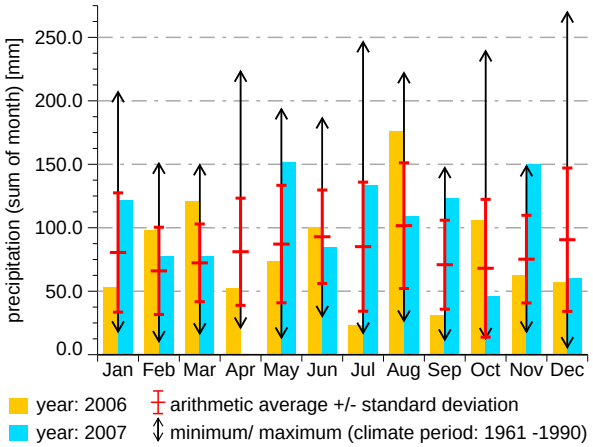

Figure 2.5 Monthly sums of precipitation in the *Tharandter Wald* for 2006 and 2007 in comparison to the climate period 1961 – 1990 (arithmetic mean, standard deviation, minimum and maximum related to monthly sums of precipitation for 1961 – 1990)

An important weather event during the period of investigation was the winter storm *Kyrill* on January 18th and 19th 2007. Although no trees were blown down on test sites, the storm damaged trees at both sites; many branches and twigs were broken, the bark of several trees was injured and heavy losses of needles were observed on Spruce trees. Although damage to trees was severe at both sites, it was clear that trees were more affected at the Spruce site than at

the Beech site. In this context it is assumed, that in particular the loss of needles affects the productivity of Spruce over several years.

2.3.3 Effects of Weather Conditions on Phenological Phases

The effects of weather on phenological phases of vegetation are clarified with Table 2.2. Time points of phenological phases are listed which are related directly to weather conditions: start of foliation (shoot of spruces), autumn colouring and fall of leaves. It is noticeable that the growing season started earlier in both investigation periods than in the long time average. That means the start of foliation of Beech in the Phenological Garden was significantly earlier than usual because of the warm weather in springtime in both investigation periods.

Particularly in 2007, the growing season started around two weeks earlier than usual because of extreme hot temperatures in spring (especially in April). Furthermore, a clear delay of the autumn colouring was observed in 2006, which was due to the untypically warm autumn. In contrast to 2006, the autumn colouring started earlier than usual in 2007 because of quite cool temperatures in August and September. However, the fall of leaves was at quite similar times in both periods and was in the range of normal variations.

The comparison between Beech trees at Phenological Garden and at the Beech site showed; the start of foliation was around 5 days earlier at the Beech site. However, the times of autumn colouring and fall of leaves were quite similar. Particularly, the small differences in times of fall of leaves were probably created by subjective sensation of observer. Generally and simplified the growing season of Beeches can be assumed from end of April until middle of October in both investigation periods, at which the periods with full foliation were approximately from June until September.

Table 2.2 Phenological observations of investigated Beech and Spruce stands in 2006 and 2007 compared with phenological observations of the Phenological Garden as well as long-time averages (observed at Phenological Garden, Tharandt)

attribute, phenological phase	2006	2007	long time average ± standard deviation
(*Fagus sylvatica* Dän., Phenological Garden)			
start of foliation	29Apr	18Apr	03May ± 7 days
autumn colouring	19Oct	30Sep	11Oct ± 7 days
fall of leaves	28Oct	21Oct	26Oct ± 6 days
start of foliation at Beech site			
start of shoots	23Apr	13Apr	
approx. 90% of foliation	03May	20Apr	
autumn colouring at Beech site			
start	23Oct	01Oct	
broad	28Oct	15Oct	
fall of leaves at Beech site			
generally fall down	01Nov	22Oct	
approx 90% bare-branched	23.Nov	08Nov	
shoot of spruce (Spruce site)	06May	26Apr	

2.3.4 Evaluation of Water Supply in 2006 and 2007

The water supply of canopies, that is the water which is available for plants, was evaluated by the measured soil moisture Θ within the main rooting zone at both forest sites. In a broader sense, the canopy water supply was also representative for inputs in terms of net precipitation and snowmelt. For an overview and classification, the measured soil moisture and estimated net precipitation (estimation of P_n is special object of investigation in Chapter 4) are shown in Figure 2.6 from the Spruce and Beech site. In addition, the depth of snow was measured at the Spruce site.

The net precipitation P_n was slightly higher at the Beech site than at the Spruce site in most months within main investigation periods (April-October). However, the differences were not caused by a higher percentage of net precipitation. The percentage of net precipitation related to precipitation measured according to meteorological standard was around two-thirds at both sites (for details see Chapter 4). So, the higher amount of net precipitation was caused only by more precipitation at the Beech site, which was due to the exposed location at northern end of *Tharandter Wald*. In another aspect, it is noted that net precipitation consisted to one-third out of stem flow at the Beech site.

The total of net precipitation at the Beech site was 367 mm in 2006 and 446 mm in 2007. However at the Spruce site, P_n was only 312 mm in 2006 and 283 mm in 2007. That means, at the Spruce Site, P_n was 85.2 % (2006) and 73.9 % (2007) respectively related to P_n at the Beech site. Thereby, significant differences (> 20 mm) between both sites were in May 2006, July 2006, May 2007, June 2007, July 2007 and September 2007. In this context, it is noted that the difference in July 2006 (21.1 mm) was caused only by two thunderstorms. However, there were also months where the sum of precipitation and net precipitation respectively was very similar at both sites.

Besides net precipitation, soil moisture and canopy water supply respectively were affected by snowmelt. Large amounts of water were discharged by snowmelt in March 2006, which caused a significant increase of measured soil moisture and ensured good water supply at the beginning of the growing season in 2006. However, the missing snowmelt and, in particular, the abnormal drought in April 2007 caused very low soil water contents at the beginning of the 2007 growing season. Thereby, it is noted again that the spring of 2007 (and there especially April 2007) was an absolute anomaly of climate.

However, in general the canopy water supply was significantly better in 2007 than in 2006. So, the measured soil moisture was typically higher in 2007 than in 2006 because of more precipitation and more net precipitation respectively. The months of July 2006 and September 2006 were especially interesting. In those months, the lowest soil moistures were measured because of a long period of fair weather conditions. It can be assumed that water stress certainly occurred at the Spruce site in those months. Moreover, water stress can also not be completely excluded for the Beech site. However, such low soil moisture did not occur in 2007. In this way, water stress was excluded for 2007, even for spring and in particular in April.

August 2006 was also especially interesting. A significant increase of soil moisture in curve course was observed, which was caused by above average precipitation. Furthermore, low soil moisture is conspicuous in the period between the end of January and the middle of February 2006 (outside the actual periods of investigation). However, these low values were caused by heavy soil frost and they were not related to the actual (total) water content. However, they were related to the content of available (liquid) water. In general, the conditions of climate and water supply were quite different between 2006 and 2007. So, two scenarios were affirmed (dry 2006 and wet 2007).

The comparison between the Spruce and Beech sites showed that the measured soil moisture was typically lower at the Spruce site than at the Beech site. An exception was spring 2006 (especially April 2006). However, this exception was caused only by snowmelt. In this context it is noted that the snow cover was very heterogenic within both canopies before. So, the higher soil moisture at the Spruce site was an effect of inhomogeneous snowmelt and was not a specific characteristic of climate or soil.

However, the general characteristic with respect to higher soil moisture at the Beech site was caused by the special characteristics of sites. On the one hand, the higher totals of precipitation and net precipitation respectively were a reason. But on the other hand, slightly different soil properties were a second reason. In this context, the rock fragment was the decisive parameter (evaluation of soil properties was given by Schwärzel et al 2009b). So, probably the higher rock fragment at the Spruce site caused higher seepage and in consequence lower soil moisture.

In another context, the soil moisture Θ was represented primarily by measurements at a single point at each test site. In this context, the differences between both forest sites were within the range of uncertainty, which was related to the representativeness of measurements. Thereby, the high spatial heterogeneity of Θ was proved by manual measurements. Variations were found of Θ up to ± 4 % within a radius of 250 m at both sites. However, the maximal variations (± 4 %) were found only after small events of precipitations in general dry periods. The differences and the heterogeneity of Θ were significant lower after long and intensive precipitation.

A special problem, which was related to the representativeness of Θ, was caused by stem flow at the Beech site. So, significant percentages of precipitation were infiltrated along of roots, which acted as a preferential flow path. This process was investigated by tracer experiments by Ebermann (2010). Significant radial diffusion was found. Thus, the distance between sensor and stem and the distances between sensor and primary roots significantly affect the representativeness of measured soil moisture Θ. In a similar way, the measured Θ and representativeness of Θ was affected by the free throughfall P_t. However, this effect was less significant, because of lower amounts of P_t and because of wider distribution. In general, the measured soil moisture Θ was an indicator and was a value for qualitative evaluations. However, Θ was not a representative value for quantitative analyses.

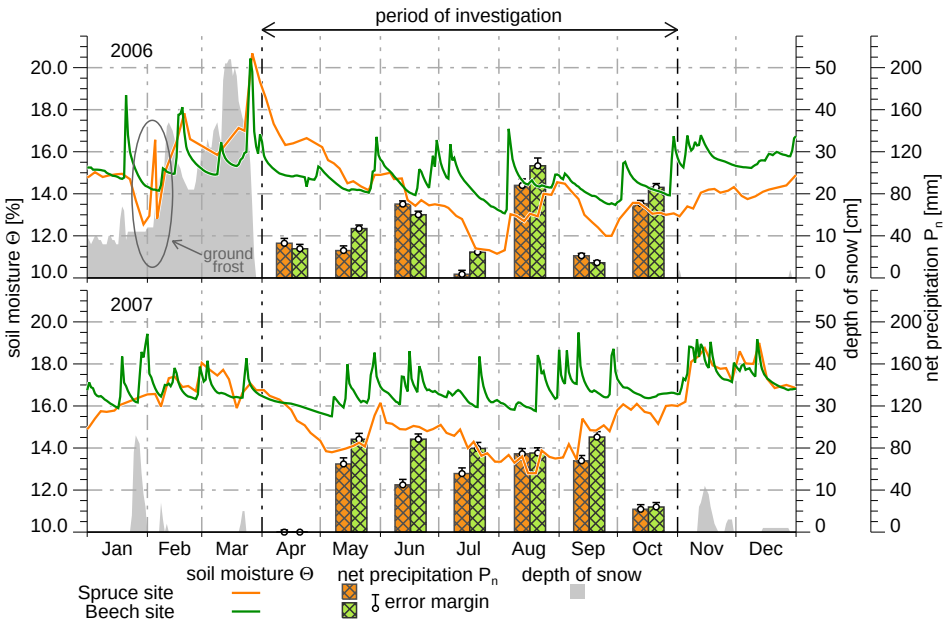

Figure 2.6 Soil moisture Θ in main rooting zone (average of measured Θ between 30 and 40 cm at Spruce site; 35 cm at Beech site); net precipitation with associated range of uncertainty in periods of investigation (April-October); snow cover and depth of snow measured at Spruce site (ground frost deeper than 35 cm is marked); upper diagram 2006, lower diagram 2007

3 Influences of Spectral Correction on Estimated Fluxes and Estimated Balances Derived from Eddy-Covariance Measurement*

3.1 Role of Post-processing in Eddy Covariance Measurements

At present, eddy covariance (EC) is the most accurate method which is used to measure vertical fluxes of mass, energy, and momentum (Foken 2006, Lee et al. 2004), but even so, such fluxes often differ significantly from *actual* or *expected* fluxes. This becomes notably evident in monthly or yearly totals or when turbulent heat fluxes are compared with available energy in the energy balance (Wilson et al. 2002).

The list of reasons for the deviation between actual and measured EC fluxes starts with the fact that perfect stationary conditions are rarely observed, and the theoretical background of the Reynolds decomposition (basis of the EC method) is typically violated. An additional real world restriction is that no measuring site can be regarded as an ideal plane surface with infinite fetch. For excellent general advice and details of state-of-the-art EC techniques and analyses, see Lee et al. (2004).

Due to instrument levelling deficiencies and sloping terrain the measured vertical wind speed contains always a horizontal component too, so the averaged vertical wind speed differs sometimes significantly from zero. This violation of the EC fundamentals must be corrected by a so called tilt correction. Widely used algorithms for the tilt correction are: double rotation, triple rotation, and planar-fit (McMillen 1988, Wilczak et al. 2001, Finnigan 2003). However, each has specific shortcomings and consequences for the derived fluxes, e.g. after a planar fit a mean residual vertical wind speed is typically present, and this needs further consideration (as input to the calculation of vertical advection).

Non-flat orography and heterogeneities of the land cover cause a diffraction of streamlines, and this diffraction or deflection of the streamlines leads to an insufficient detection of the vertical wind component (Foken 2006). Also, related to orography or to heterogeneities of the vegetation, mean vertical and mean horizontal fluxes occur, which have to be considered (Aubinet et al. 2003, Feigenwinter et al. 2004). A typical source of advection is a non-zero mean vertical wind speed, which in turn violates standard EC prerequisites.

Advective transports those are not covered by an EC measuring system may represent a significant fraction of the complete exchange (Aubinet et al. 2003, Moderow et al. 2007, Feigenwinter et al. 2008). Such advection effects probably cause deviations of the measured flux spectra from idealized spectra in the low frequency region (Thomas et al. 2006).

* Content of this chapter is already published in: "Spank U, Bernhofer C (2008): Another simple method of spectral correction to obtain robust eddy-covariance results. Boundary-Layer-Meteorology, 128(3): 403-422"

Another major cause for systematic differences between measured and actual fluxes that relates to the fact that only eddies of a defined scale are observed by the EC method; all eddies beyond this range, very large and very small eddies, respectively, are not detected. This leads to both low frequency (longwave) and high frequency (shortwave) attenuation. The low frequency attenuation is mainly defined by the averaging interval of the Reynolds decomposition (Sakai et al. 2001, Foken et al. 2006), while the high frequency attenuation is caused by the resolution deficits of the hardware.

In summary, the absolute derivation between measured and actual fluxes is unknown; this derivation is a superposition of different systematic and unknown random errors. However, it is possible to minimize these errors through an optimal equipment configuration and through application of adequate correction methods. The typical steps are: tilt correction, buoyancy correction (also Schotanus correction, see Schotanus et al. 1983), density correction (also WPL correction, see Webb et al. 1980) and damping (attenuation) correction.

Particularly in closed-path systems the high frequency attenuation leads to a significant underestimation of the actual flux, and depending on the measurement configuration this can amount to 30 % (Eugster and Senn 1995) or even over 100 % (Massman 2000). Additionally to the hardware, atmospheric conditions may also influence the attenuation. Stable stratification and strong winds lead to high frequency attenuation. In periods with stable stratification or periods with strong wind only small eddies occur (Kaimal and Finnigan 1994). Because EC systems damp small eddies more than bigger ones, attenuation will increase.

Even though numerous studies, e.g.: Moore (1986), Eugster and Senn (1995), Horst (1997), Laubach and McNaughton (1998), have dealt with the problem of spectral attenuation, there still is a lack of a simple and universal correction method. Especially the attenuation in closed-path systems with long tube lengths is not described satisfactorily. The often unknown actual flow velocity in the tubing system is only scarcely tackled. Usually the effective flow rate is estimated using the time delay between sonic anemometer and gas analyser, as detected by maximization of the cross-covariance. The influence of tube curves, bends, branch connections, variable tube diameters, and the influence of the filters necessary (i) to keep the tube clean, and (ii) to protect the gas analyser, are not precisely known. Especially the particle filters, arranged at both ends of the tube, are significant flow barriers, and it is possible that they (both, in clean condition and contaminated with particles) have a large influence on attenuation. In this article, a robust easy-to-handle correction method referring to high frequency attenuation of closed-path systems is introduced and tested.

3.2 Measurements

Collection of data used in this chapter has been started 1996 in the framework of the project Euroflux and is continued until today (CarboEurope-IP 2008a) at the Anchor Station Tharandter Wald, which is called Spruce site in nomenclature of present study. The station's EC system device is a closed-path system with a relatively long tube and high flow velocity. The sonic anemometer (Solent Gill R2, since May 2006 replaced by a Solent Gill R3) and the inlet of the main tube are mounted on a 42 m scaffolding tower, approximately 13 m above the

canopy, while the gas analyser (LI-COR, LI 6262) is situated in a container on the forest floor. The tube length is 59 m, and the pump produces a typically high flow rate of ≈ 60 L min^{-1}. A secondary tube probes the primary tube with a lower flow rate ≈ 4-6 L min^{-1} and feeds into the gas analyser. A more detailed site description can be found in the FLUXNET data base (Bernhofer 2003) or in Bernhofer et al. (2003a) and Grünwald and Bernhofer (2007). Appendix A2 summarizes the configuration of the EC system. Furthermore the list of required processing steps to obtain correct energy and mass fluxes is shown in Appendix A1.

3.3 Established Methods for Correction of High Frequent Attenuation

3.3.1 The Method According to Moore (1986)

The first substantial practical correction method can be found in Moore (1986). The application was restricted earlier to open-path systems and was adapted later by the introduction of additional terms describing the attenuation of closed-path systems (Leuning and Moncrieff 1990, Lenshow and Raupach 1991, Massman 1991, Leuning and King 1992, Leuning and Judd 1996, Moncrieff et al. 1997).

The Moore correction is based on a description of all attenuation components by transfer functions, and combines all relevant transfer functions to generate theoretical damped cospectra. Finally, the correction coefficient K (or the damping coefficient D) can be estimated through the ratio between these damped cospectra and theoretical undamped cospectra. In this fundamental relation, $Co_{Mod}(f)$ symbolises the theoretical cospectrum and T(f) the transfer function of the whole EC device, T(f) itself is the product of all component or process specific sub-transfer functions $T_i(f)$. All $T_i(f)$ considered for correction of data from the test site are listed with the corresponding equations in Appendix A3. Note, f symbolises the spectral frequency, so

$$\frac{1}{K} = D = \frac{\int_{f=0}^{\infty} T(f)\, Co_{Mod}(f)\, df}{\int_{f=0}^{\infty} Co_{Mod}(f)\, df} \quad . \tag{3.1}$$

For theoretical cospectra, model spectra are used that are adjusted to measurements of the Kansas and Minnesota experiments. Here, the model equations published in Aubinet et al. (2000), were adapted so that $Co_{Mod}(f)$ results directly instead of $f\,Co_{Mod}(f)$. For unstable atmospheric conditions this yields,

$$Co_{Mod}(f) = \frac{\frac{z-d}{u}}{0.284\,\Theta^{0.75} + 9.345 \cdot \Theta^{-0.825} \left(f\,\frac{z-d}{u} \right)^{2.1}} \quad , \tag{3.2}$$

where z is the measurement height (= 42 m), d is the zero-plane displacement (approximately 20.6 m), and u is the wind speed at height z. The calculation of parameter Θ is based on,

$$\Theta = 1 + 6.4\,\frac{z-d}{L}\ . \tag{3.3}$$

For stable conditions, the model cospectra are split into two terms depending on a threshold frequency:

$$Co_{Mod}(f) = \begin{cases} \dfrac{12.92\,u^{-1}(z-d)}{\left(1+26.7\ f\ u^{-1}(z-d)\right)^{1.375}} & f < 0.54\,u\,(z-d)^{-1} \\ \dfrac{4.378\,u^{-1}(z-d)}{\left(1+3.8\ f\ u^{-1}(z-d)\right)^{2.4}} & f \geq 0.54\,u\,(z-d)^{-1} \end{cases}\ . \tag{3.4}$$

In many cases the correction factors derived after Moore (1986) turned out to be too small (Eugster und Senn 1995, Aubinet et al. 2000, Bernhofer et al. 2003b), for two probable reasons: on the one hand, the model spectra used do not correspond necessarily to the actual spectra and cospectra, occurring at the site (Eugster and Senn 1995, Laubach and McNaughton 1998, Bernhofer et al. 2003b, Massman and Clement 2004). On the other hand, it is not made sure through the applied transfer functions that all attenuation processes are adequately considered. In particular, the calculated tube attenuation turned out to be too low (Aubinet et al. 2000).

Two correction approaches have been suggested. The first is a correction method independent of the spectrum or cospectrum (Laubach and McNaughton 1998). The second is to replace the model of the spectrum (cospectrum) by an undamped spectrum (cospectrum) for the measurement site (Eugster and Senn 1995, Bernhofer et al. 2003b). The latter method is based on the assumption that the cospectrum of the sensible heat measured with an ultra sonic anemometer can be considered as undamped. Furthermore, similarity is assumed between the cospectrum of the sensible heat flux and the undamped cospectrum of any mass flux. However, the Moore correction is the most commonly used correction method, and it is used as reference in the following.

3.3.2 The Method Similar to Eugster and Senn (1995)

In analogy to Eugster and Senn (1995) a simple correction method was developed for the calculation of corrected water and carbon fluxes at Spruce site (Bernhofer et al. 2003b). The correction depends on atmospheric stability and amounts to about 20 % for unstable and 40 % for stable stratification. Its application improved the energy balance closure considerably and yielded ecologically sound carbon fluxes (Grünwald and Bernhofer 2007). This method was developed using data from the Spruce site, and is useful for closed-path systems with long tube lengths. The basis is a comparison between the cospectrum of the sensible heat flux $Co^{w'T'}(f)$ and the cospectrum of any mass flux $Co^{w'x'}(f)$, where x stands for water vapour or

carbon dioxide concentration. Other parameters are: the spectral frequency f, the covariance $\overline{w'T'}$ between vertical wind w and sonic temperature T, the covariance $\overline{w'x'}$ between vertical wind w and mass concentration c. Co_{max} symbolises the maximum in the cospectrum, f (Co_{max}) the frequency at Co_{max}. According to Bernhofer et al. (2003b), the calculation of the spectral damping D or the correction coefficient K uses

$$\frac{1}{K} = D = \frac{f\left(Co_{\max}^{w'T'}\right) Co_{\max}^{w'T'}}{f\left(Co_{\max}^{x'T'}\right) Co_{\max}^{x'T'}} \int_{f>0}^{\infty} \frac{f\ Co^{w'x'}(f)}{\overline{w'T'}} d\log f \quad . \tag{3.5}$$

It is assumed that the measuring EC system device captures the whole frequency range, which is relevant for turbulent exchange. Due to Reynolds averaging,

$$\overline{w'x'} = \int_{f=0}^{\infty} Co^{w'x'}(f) df = \int_{f>0}^{\infty} f\ Co^{w'x'}(f) d\log f \quad , \tag{3.6}$$

the integral in this equation can be replaced by the covariance $\overline{w'x'}$,

$$\frac{1}{K} = D = \frac{f\left(Co_{\max}^{w'T'}\right) Co_{\max}^{w'T'}}{f\left(Co_{\max}^{x'T'}\right) Co_{\max}^{x'T'}} \frac{\overline{w'x'}}{\overline{w'T'}} \quad . \tag{3.7}$$

The application of this method is described in Grünwald (2002) where the spectral frequency range was divided into 20 frequency groups (classes). The classification was done logarithmically. Consequently, the cospectrum within one class corresponds to the arithmetic average of all values inside the class borders. Further, damping coefficient calculations are processed on the basis of the classified values. For the determination of correction factors, a pre-selection of applicable cospectra and a plausibility check were done.

Bernhofer et al. (2003b) were able to demonstrate a relation between the atmospheric stability ς and spectral attenuation at Spruce site. Thereby, the dimensionless parameter ς is derived from the Monin-Obukhov length L,

$$\varsigma = (z - d)/L \quad . \tag{3.8}$$

Figure 3.1 shows the correction coefficient K for water vapour and carbon dioxide fluxes depending on the stablility class, where Bernhofer et al. (2003b) choose six stability classes between strong unstable and strong stable. The lowest K occurs among slightly unstable condition. At almost neutral conditions K changes rapidly. Generally, it is shown that the correction coefficient of water vapour flux is higher than that of carbon dioxide flux.

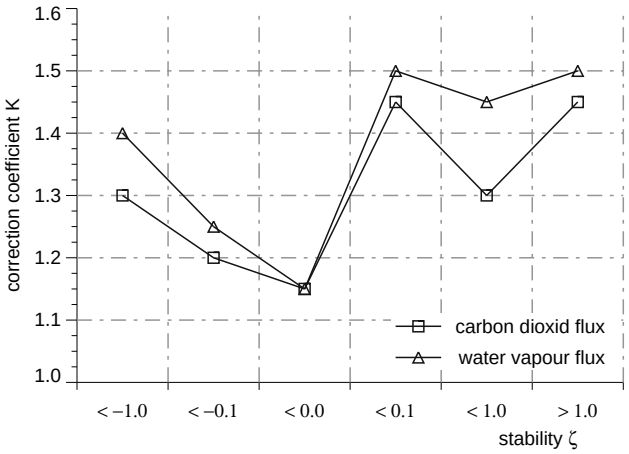

Figure 3.1 Correction coefficient for carbon dioxide and water vapour fluxes in dependency on atmospheric stratification at Spruce site (according to Bernhofer et al. 2003c)

3.3.3 The Method According to Aubinet et al. (2000)

Another method based on comparison between the cospectrum of the sensible heat flux and the cospectrum of mass flux can be found in Aubinet et al. (2000), and in this case a specific transfer function $T_{Spez}(f)$ for high frequency damping is derived from,

$$T_{spez}(f) = \frac{\dfrac{Co^{w'x'}(f)}{\int_{f>0}^{\infty} Co^{w'x'}(f)df}}{\dfrac{Co^{w'T'}(f)}{\int_{f>0}^{\infty} Co^{w'T'}(f)df}} = \frac{\overline{w'T'}}{\overline{w'x'}} \frac{Co^{w'x'}(f)}{Co^{w'T'}(f)} \quad . \tag{3.9}$$

Furthermore, several specific transfer functions are used to calculate the cut-off frequency f_{co} of the EC system. (f_{co} is, where is $T(f) = 2^{-½}$.) Finally, the cut-off frequency enables to deduce a characteristic transfer function for the eddy covariance system $T_{sys}(f)$,

$$T_{spez}(f) \rightarrow T_{Sys}(f) = \exp\left(-0.347 \cdot \left(\frac{f}{f_{co}}\right)^2\right) , \tag{3.10}$$

which can be used analogously to T(f) in Equation (3.1). In theory, it is possible to use additionally the cospectra of the sensible heat flux instead of the models in Equation (3.1) to consider special features of the test site according to,

$$D = \frac{\int_{f>0}^{\infty} T_{Sys}(f) \cdot Co^{w'T'}(f)df}{\int_{f>0}^{\infty} Co^{w'T'}(f)df} \quad . \tag{3.11}$$

This method was also applied to the test site. However, the cospectra derived from sensible heat fluxes are often not well defined. In consequence, direct application of this approach can produce implausible values.

3.4 An Alternative Method for Spectral Correction

3.4.1 Technical Background and Derivation of Fundamental Equations

Hardware shortcomings and characteristics of turbulent transport can equally affect the measured fluxes. At Spruce site, a Solent Gill R2 sonic anemometer was used until May 2006, a sonic anemometer known to produce significant errors during the determination of the sonic temperature at wind speeds above 3 m s^{-1} (Grelle and Lindroth 1996; Grünwald 2002). In consequence, the cospectra of the sensible heat flux are also subject to errors. An additional problem exists generally at very low wind speeds. Gusts combined with nonstationary turbulence cause irregular spectra and cospectra (Foken 2006), and consequently, during these conditions with their higher demand for correction, it is not possible to calculate plausible spectra or cospectra. A similar situation exists during strong-wind periods. To avoid problems with irregular sensible heat flux cospectra, the measured cospectrum in Equation (3.9) was replaced by a model,

$$T_{spez}(f) = \frac{1}{Co^{Mod}(f)} \cdot \frac{Co^{w'x'}(f)}{\overline{w'x'}} \quad . \tag{3.12}$$

It is well known that under highly stable conditions the commonly applied models are rather a guiding principle (Su et al. 2003, Massman and Clement 2004). However, as alternative models are missing they are still widely used as a reference (Aubinet et al. 2000; The University of Edinburgh 2007).

In the following step, a model to describe the attenuation is derived from the computed specific transfer function. It was attempt to fit the specific transfer function through a two parameter (a and b) exponential function,

$$T_{spez}(f) \rightarrow T_{Mod}(f) = \exp\left(-a \cdot f_N{}^{b}\right) . \tag{3.13}$$

It has been found, that the optimization of the parameter shows better results, if the normalised frequency f_N is used instead of the frequency f,

$$f_N = f \cdot \frac{z-d}{u} \quad . \tag{3.14}$$

However, exponential fitting of two parameters was shown to be extremely critical in a routine application. Often, the applied regression algorithm (Fuchs and Lutz 1999) failed and led to implausible values, so to overcome this problem and in reference to Equation (3.10) we fixed b = 2 during further analysis. Finally, the optimization was adjusted to the square root of the reciprocal of a (= α) instead of just a, improving the numerical stability of the optimization algorithm,

$$T_{Mod}(f_N) = \exp\left(-a \cdot {f_N}^2\right) = \exp\left(-\left(\frac{f_N}{\alpha}\right)^2\right) . \quad (3.15)$$

Eventually, the only remaining step is to estimate the parameter α to describe the attenuation of a single data record. Here, a linearization of the Kerrich algorithm (Sachs 1999) was used for the approximation of α, and should be noted that, in advance of the calculation process to derive α, it is necessary to check values of the transfer function calculated using Equation (3.12). In the following, it is appropriate to limit the frequency range to avoid potential problems in consequence of scattering in the low frequency range and of aliasing in the higher frequency range.

3.4.2 A Comparison between Moore's Correction and the Individual Correction

With the correction method described it is easy to find a correction coefficient for any specific EC station and any specific record. In particular, the dynamics of the tube attenuation is considered, especially with regard to the effective attenuation by the particle filter. In the following text this correction method is called individual correction. Figure 3.2 shows a typical example for the comparison between correction coefficients according to Moore and according to the individual correction for the carbon dioxide flux. The results for the water vapour flux (not shown) are very similar. The chronological sequence of the stability parameter ς is also shown.

The typical correction coefficients using an individual transfer function are significantly higher than according to Moore (1986), and is explained by the specifically adapted attenuation description. Furthermore, typical diurnal cycles of K can be observed, which strongly depend on the diurnal cycle of the stratification. Under stable conditions with low turbulence only small-sized eddies occur. And in consequence, as smaller eddies are damped more than larger eddies, the attenuation increases. After sunrise, the stratification becomes more unstable and K decreases rapidly; note that civil sunrise (which includes twilight) is roughly at 03 45 UTC and civil sunset is roughly at 20 15 UTC.

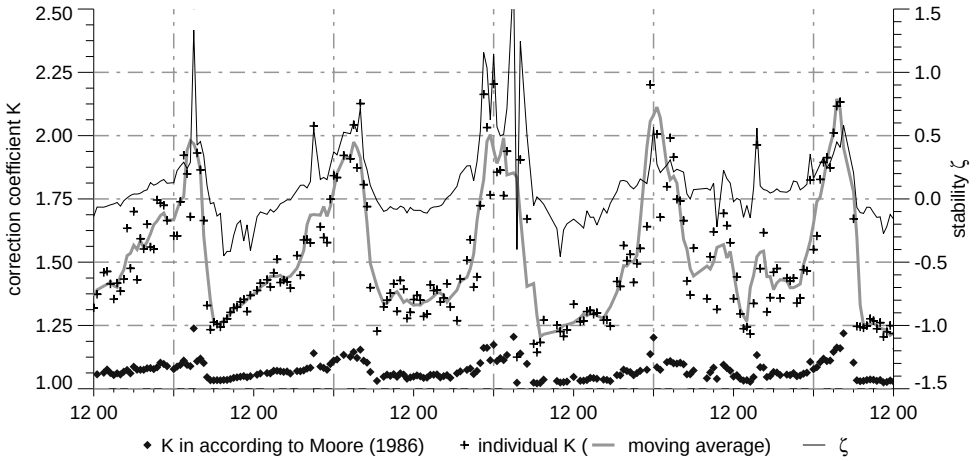

Figure 3.2 Time dependent characteristics of the correction coefficient at Spruce site (carbon dioxide flux, 4 to 9 May 1999, time in UTC)

3.4.3 The Relationship between the Correction Coefficient and Atmospheric Conditions

The relationship between K and the wind speed, and the relationship between K and the atmospheric stratification, respectively, will be the focus of the following investigations. The clear dependence of K on the wind speed is shown in Figure 3.3. Under unstable conditions (left) a strong linear dependence is observed. Under stable conditions (right), the dependence on the wind speed is overlaid by influences of the stratification. However, in the case of limiting ς, there is also a linear dependence. This specified effect concerns both the individual and Moore's correction, but it is more obvious for the individual correction.

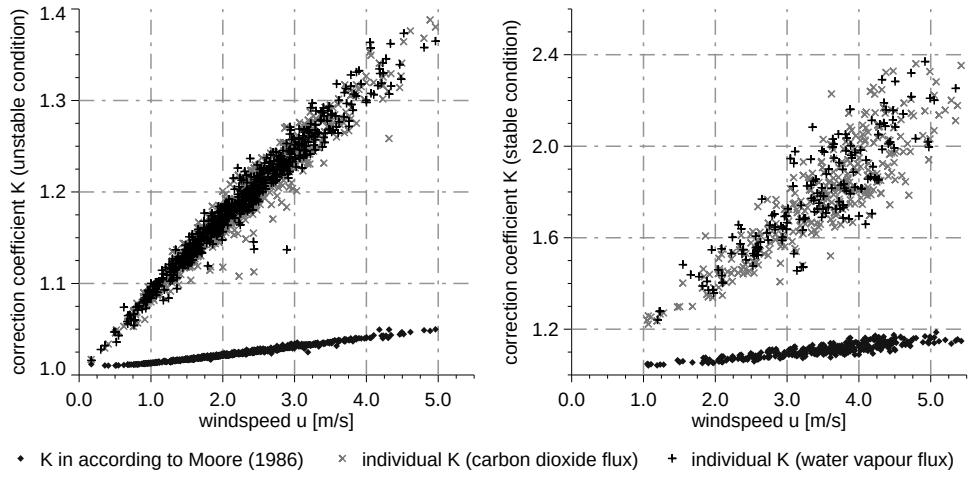

Figure 3.3 Correction coefficients dependent on wind speed for unstable conditions ($\zeta < -0.25$, left panel) and stable conditions (stable conditions $0.25 < \zeta < 0.5$, right panel); time delay between 6 and 11 s, all data of 1999

The relationship between K and the atmospheric stratification is shown in Figure 3.4 for all u between 1.5 and 3 m s^{-1}. Under stable conditions a linear relationship with stratification is observed; but under unstable conditions this effect is negligible. It should be pointed out that stratification itself depends on wind speed. For the test site, wind speeds above 2.5 m s^{-1} are related to near neutral stratification.

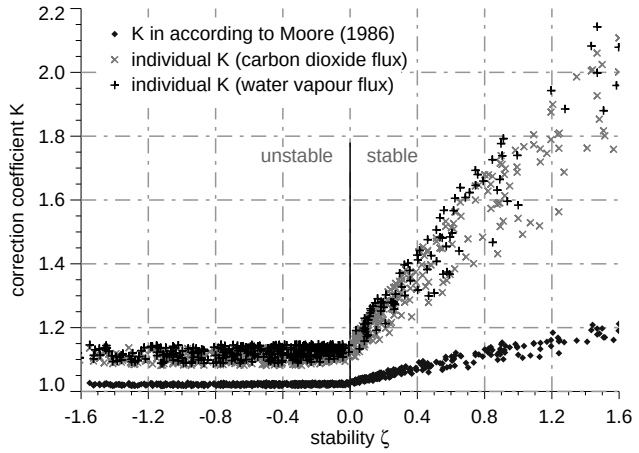

Figure 3.4 Correction coefficients dependent on atmospheric stratification ς (wind speed 1.5 – 3.0 m s^{-1}, time delay 6 – 11 s, all data of 1999)

A statistical investigation was conducted with the intention of identifying the dependency of the individual correction coefficient on wind speed and atmospheric stratification. It was demonstrated that the correction coefficient can be described by a two-dimensional linear regression,

$$K = Au + B\varsigma + C \ , \tag{3.16}$$

with the regression parameters for Spruce site listed in Table 3.1.

Table 3.1 Parameters to describe the correction coefficients in relation to wind speed and atmospheric stratification; the coefficients of determination are valid in the stable case for $\varsigma > 0.1$ und in the unstable case for $\varsigma < -0.1$

flux	atmospheric stratification	A	B	C	coefficient of determination
CO_2	unstable	0.07	0.0	1.02	0.97
CO_2	stable	0.15	0.79	0.86	0.87
H_2O	unstable	0.07	0.0	1.03	0.97
H_2O	stable	0.21	0.83	0.71	0.88

Except for near-neutral conditions ($-0.1 < \varsigma < 0.1$) the two-dimensional regression function describes K very well, and the coefficients of determination were between 0.88 and 0.97. For unstable stratification, even a simple linear correlation exists between wind speed and K. In that case it is possible to neglect parameter B.

The coefficient of determination is quite high, which suggests that the dynamics of the tube attenuation only has a small influence on the correction coefficient K, meaning that the degree of pollution of the particle filter and the associated change of flow rate in the tube has also only a small influence. However, the tube attenuation is of major influence.

3.4.4 Investigation of Parameter α and Derivation of the α*-correction

The following section describes a closer investigation of the parameter α. In this analysis the cospectrum of the sensible heat flux has been included to determine the specific transfer func-

tion. So, the specific transfer function on one hand is calculated as described in Equation (3.9) with the reference spectrum of the sensible heat flux. On the other hand, it is calculated as described in Equation (3.12) with a model as reference. The attenuation was approximated as described in Equation (3.15).

As the applied optimization is based on the normalised frequency, parameter α shows a functional dependency on the reciprocal of wind speed. Accordingly, through renormalisation of parameter α, it is possible to get a parameter α* which is independent of wind speed,

$$\alpha^* = \alpha \cdot \frac{u}{z-d} \ . \tag{3.17}$$

Parameter α* is a near constant value, describing the attenuation of the eddy covariance system well. In Table 3.2, the following parameters are listed for parameter α*: the arithmetic average (mean), the median, and the standard deviation. Additionally listed are equivalent statistical variables related to the reciprocal (1/α*).

Table 3.2 Statistical variables of α* and its reciprocal 1/α*

flux	reference	mean (α*)	standard deviation (α*)	median (α*)
CO_2	Sensible heat	0.168	0.031	0.164
CO_2	Model	0.109	0.012	0.108
H_2O	Sensible heat	0.160	0.035	0.154
H_2O	Model	0.108	0.014	0.105
flux	reference	mean (1/α*)	standard deviation (α*)	median (α*)
CO_2	Sensible heat	6.1	0.99	6.1
CO_2	Model	9.2	0.98	9.3
H_2O	Sensible heat	6.5	1.11	6.5
H_2O	Model	9.4	1.15	9.5

The attenuation of the water vapour flux turned out to be higher than the attenuation of the carbon dioxide flux, an effect that appears whatever reference is used: a model cospectrum or the measured cospectrum of the sensible heat flux. This confirms the conclusion drawn in Aubinet et al. (2000) and Grünwald (2002).

The calculated attenuation is significantly higher if a model cospectrum is used as reference. Aubinet et al. (2000) and Bernhofer et al. (2003b) assume that the spectrum of the sensible heat flux measured with an ultrasonic anemometer can be taken as undamped. However, even sonic anemometers create a small attenuation, particularly related to path averaging, choice of high pass filter, and discretisation of the measurement signal. Furthermore, as mentioned above, the applied sonic anemometer Solent Gill R2 delivers inaccurate temperature information at wind speeds above 3 m s^{-1}. Hence, also the calculated cospectra of the sensible heat flux are inaccurate above 3 m s^{-1}. Consequently, the small attenuation could be due to a slightly damped cospectrum as reference.

In the next step of investigation, it was attempted to explain the small scatter of α* through fluctuations of the tube flow rate, or rather by the time lag of the signals. However, it was not possible to find a clear functional dependency on either of the two. This fact supports the earlier statement, that the flow rate dynamics has only a small influence.

Resuming the former statements, here the possibility is given to use an averaged transfer function for all records instead of an individual transfer function for each individual record. This mean transfer function based on α* is described by,

$$T(f) = \exp\left(-\left(\frac{1}{\alpha^*}\cdot f\right)^2\right) . \tag{3.18}$$

The corresponding correction method is referred to as α*-correction, and is similar to the correction method according to Aubinet et al. (2000), although with a different statistical background.

3.4.5 Consequences for the Calculated Mass Fluxes and Balances

In consequence of a higher K, the alternatively corrected fluxes are always higher (absolute values) than the fluxes corrected according to Moore (1986). Furthermore, the values of the alternatively corrected fluxes are quite close to each other. In comparison with fluxes corrected according to Bernhofer et al. (2003b), the α*-correction creates slightly lower values. The individual correction causes slightly higher values. Those effects are more significant under stable and near-neutral conditions than under unstable conditions. For stable conditions, the comparison between the different alternative correction methods and Moore‘s correction is shown in Figure 3.5.

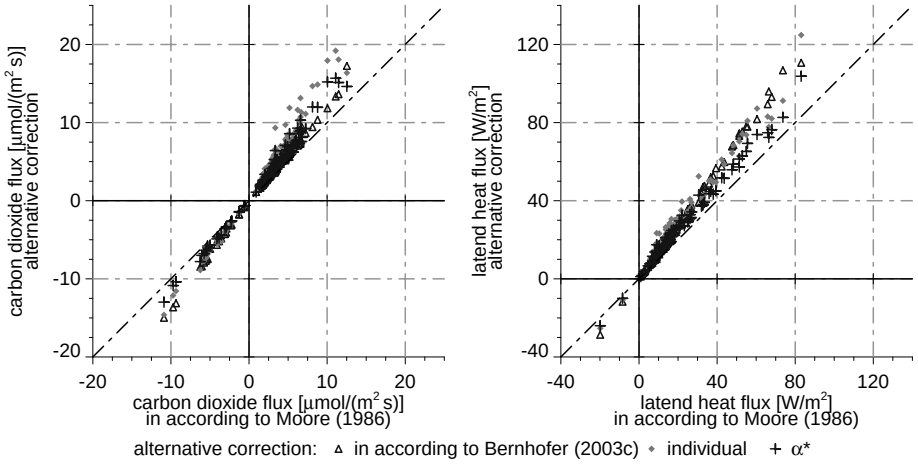

Figure 3.5 Comparison of fluxes corrected according to Moore (1986) and fluxes corrected alternatively (carbon dioxide flux left, latent heat flux right, stable stratification, data base: May 1999)

The influence of the different correction methods on the balance is shown in Figure 3.6 for carbon dioxide exchange and in Figure 3.7 for evapotranspiration for the year 1999. With the intention of comparing the different correction procedures all acceptable measured data were summed up monthly. It has to be noted that no gap filling was applied, and consequently the

cumulative carbon exchange and the cumulated water vapour transport is different from the expected total after gap filling.

Although the individual monthly sums of the individual years differ from each other, the statements concerning the correction methods are equal for all years. Concerning carbon exchange, the correction method according to Bernhofer (2003b) creates significantly higher sums than all other correction methods. Particularly during the main growing season (May until September) a considerably higher carbon sink was calculated (about 90 g C m^{-2} more than with the α* method in 1999). In contrast, the individual and the α*-correction are in the same range and predict a lower carbon sink. Despite a considerable damping of both negative (sink) and positive (source) carbon fluxes with the application of the Moore correction, the cumulative monthly values are similar to the other correction methods due to compensating effects.

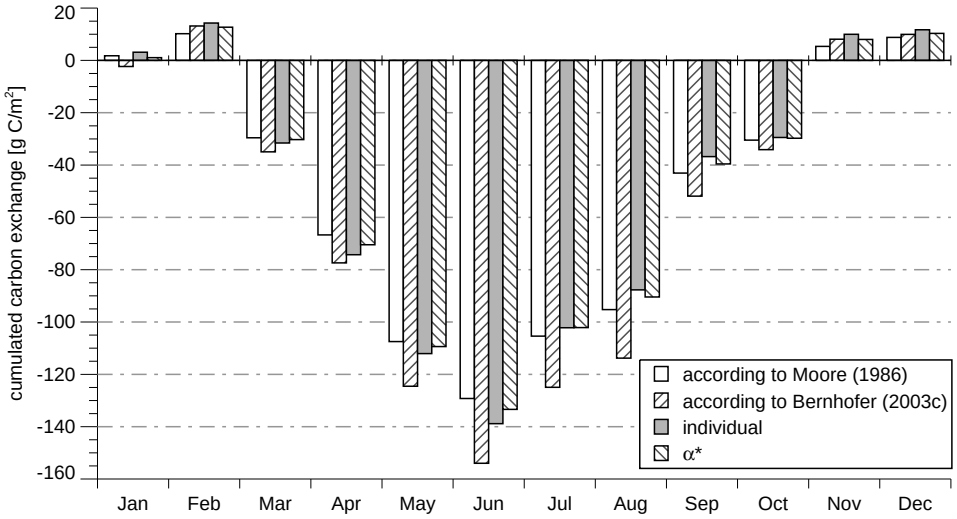

Figure 3.6 Cumulative monthly carbon exchange dependent on correction method (Data base: certified measured data of 1999, no gap filling)

Concerning water vapour fluxes all site-specific correction methods produce a higher cumulated evapotranspiration than fluxes corrected according to Moore. The correction method according to Bernhofer (2003b) and the individual correction method lead to very similar results. They are only slightly higher than the fluxes corrected according to the α* method.

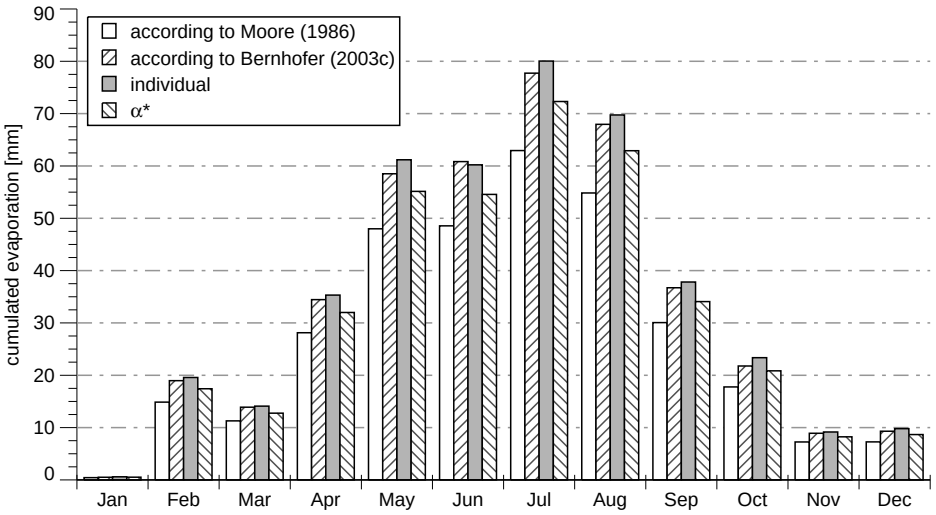

Figure 3.7 Cumulative monthly evapotranspiration dependent on correction method (Data base: certified measured data of 1999, no gap filling)

Generally, the influence of the different correction methods on the monthly sums is more significant in summer months than in winter months. This effect is connected with the fact, that during the cold season (November until March) only small fluxes occur. In winter, also the absolute differences between the methods are small, although the biggest differences of K appear especially in this season. This is caused by the typically stable atmospheric stratification and frequent high wind speeds.

3.5 Concluding Remarks on Post-Processing of Eddy Covariance Measurements

The correction of spectral attenuation in EC systems is an important processing step in the calculation of mass fluxes. Particularly closed-path systems with long intake tubes need special attention. Here four different methods to correct the spectral attenuation were introduced and compared: the correction method according to Moore (1986); the method according to Bernhofer et al. (2003b); the individual (adapted from Aubinet et al. 2000) and the α*-correction method.

The method according to Moore is based on various theoretical transfer functions, that describe almost every individual damping component of the EC system device. However, it is known that this method underestimates the spectral attenuation of closed-path systems. In consequence, the absolute values of the calculated mass fluxes are too low. It is likely that the description of the tube attenuation is not sufficient (e.g., due to flow restrictions by the particle filters or branch connections).

The three alternative correction methods overcome this problem in different ways. However, all estimate the device attenuation directly from the observed spectra. So, site and device specifics of the EC-system device (including the tube attenuation) are considered implicitly. The core of Bernhofer's (Bernhofer et al. 2003b) method is the estimation of an empirical relationship between correction coefficient and atmospheric stratification. The individual and the α*-

correction are based on a device and site specific transfer function. In the case of the individual correction this transfer function is calculated for each individual dataset. Thus, it is possible to consider the effective flow rate and its influence on the tube attenuation. The flow rate through the intake tube is strongly influenced by the changing conditions of the particle filter. However, the change of the tube attenuation (not the tube attenuation itself) has only a small influence on the whole device attenuation. Therefore, it is possible to work with an averaged transfer function as used for the α*-correction.

Generally, all correction methods include a relationship between correction demand and atmospheric stratification as well as a relationship between correction demand and wind speed. Only Bernhofer et al. (2003b) disregards the influence of the wind speed, but its influence is included implicitly by the relationship between wind speed and stratification. Anyway, higher wind speeds and stable stratification increase the correction coefficient.

Although the correction coefficients of the alternative correction methods are always higher than the correction coefficient according to Moore, and the correction coefficients of alternative corrections are in a comparable range, the effect on budgets is different for carbon and water. Concerning the carbon balance the Moore correction, the individual correction, and the α*-correction produce similar results. Bernhofer's correction algorithm produces a somewhat higher carbon sink. However, all alternative correction methods calculate a higher evapotranspiration, at which Bernhofer's and the individual correction produce the highest water flux.

Both, the individual correction and the α*-correction method are easy-to-handle. Site specifics and device specifics are considered though the direct estimation of attenuation. The straightforward derivation of the correction coefficient via spectral analysis allows an easy application to any EC system. These methods represent a simple and robust way to calculate and to correct the inevitable attenuation prominent in any EC system (including those with the new closed-path gas analyser LI-7000 or even the open-path LI-7500), but most prominent in those with close-path gas analysers.

4 Estimation and Comparison of Site Water Budget at a Spruce and a Beech Canopy – Estimation of Net Precipitation

4.1 Importance of Net Precipitation

The quantification of water balance and its components is a necessary precondition for successful forest management. The availability of water determines the assessment of forests in terms of stability, productivity and risk load (Wagner 2004, Rennenberg et al. 2004, Ammer et al 2005, Kölling et al 2005, Kölling et al 2007). This is especially important in the face of an ongoing and future climate change with lower precipitation sums in summer months, more rainfall extremes, shorter periods with snow cover and a changing growing season in Central Europe (Niemand et al. 2005, IPCC 2007, Beck et al. 2007, Schönwiese and Janoschitz 2008a, Schönwiese and Janoschitz 2008b, Franke 2009). In this context the replacement of coniferous monocultures by forests which are better adapted to individual location characteristics is essential for creating stable and productive forests (Hanewinkel 1996, Butter 2001, Leder 2002, Fürst et al. 2004).

The transfer from Spruce monocultures into natural Beech stands is a typical example for forests in Central Europe (Benecke und Ellenberg 1986). Besides the different root systems between Spruce and Beech trees (which affects the root water uptake and hence influences transpiration) differences in interception storage capacity cause significant differences in the amount of water which becomes available for Spruce and Beech respectively (Weihe 1984, Weihe 1985, Benecke 1984). The effects of interception on water balance are especially important, because the interception (or rather the percentage of precipitation) which becomes available for plants (net precipitation) is controllable by forest operations and forest management. Particularly changes of canopy density and changes of species composition cause significant changes in crown cover and LAI (leaf area index) which directly affect interception. Thus, net precipitation (and hence the complete water balance) is also directly affected by forest operations. It is assumed that forest operations (which are adjusted to the specific condition of site) are an option to reduce stress due to water deficiency in droughts.

Although many studies have dealt with interception in Spruce and Beech stands (a list of studies can be found e.g. in Llorens and Domingo, 2007), comparative investigations between Spruce and Beech stands are rare. Two examples of comparative investigations over long time periods are Benecke (1984) and Tužinský (2000). The typical problem is that sites are often not comparable because of different site conditions. Particularly the climatic conditions are often different because of spatial separation, altitude, exposure and because of other parameters, which influence the microclimate e.g. wind effects. In this chapter, two adjacent forest sites (a Spruce stand and a Beech stand) were investigated and compared in terms of interception, stem flow, canopy drip and net precipitation over a period of two growing seasons. Be-

cause of the short distance and comparable altitude, the climatic gradient is not significant between the sites. Therefore, both canopies can be compared directly.

The analyses of this chapter are focused on two different time scales. On one hand the investigations are related to individual precipitation events, and on other hand the investigations are related to monthly totals. Special attention is given to the quantification of balance errors, which are caused by uncertainties of measurements. In particular, this aspect was often neglected in former studies, although those uncertainties cause a noticeable vagueness in the evaluation of water balance. The focus of this chapter is neither to present a model of interception nor its application. Rather the presentation and the interpretation of measurement data are the primary focus. In this context, the study demonstrates the importance of exact knowledge about the partitioning of precipitation in forests in the context of applications of water resource and forest management. In relation to primary fields of application, the study is focused on estimations of water which is available for the forest stand, and is thus primarily related to the net precipitation rather than to the "interception loss".

4.2 Material and Methods for Investigation of Net Precipitation

4.2.1 Theory and Fundamentals

The amount of water which falls during an event of precipitation on a canopy is divided into four components in a forest stand. One component means the percentage which falls directly through gaps of crown cover to the ground. This component is called (free) throughfall P_t in accordance with Rutter et al. (1971). P_t depends primarily on degree of crown cover and so on the sky view coefficient. Secondly, P_t is affected by the incidence angle, which results from wind speed, size and phase of droplets. However, the second effect is typically negligible. So, it is assumed that P_t is a fixed percentage of measured precipitation P (Rutter et al. 1971),

$$P_t = p_t \, P \ . \tag{4.1}$$

Thereby, p_t denotes the (free) throughfall coefficient, which is derivable from the sky view coefficient and so from the percentage of gaps in crown area. So the throughfall coefficient (or rather the percentage of throughfall related to precipitation) is controllable by forestry operations such as thinning and cutting of several trees. These operations cause an increase in the sky view coefficient and consequently an increase in the throughfall coefficient.

The other components of precipitation are temporary storage on leaves or branches in the crown area. Later, they evaporate, drip down or they are shifted laterally. The laterally shifted water can induce stem flow P_s. Stem flow being water which runs on trunks to the forest floor and so becomes available for plants. P_s is significant for some species of broadleaf trees like Beech, Maple and Eucalyptus. However P_s is insignificant for most coniferous trees like Spruce, Fir and Pine (Reynolds and Henderson 1967, Falkengren-Grerup 1989).

The component of temporary stored water, which drips down with some delay, is called canopy drainage P_d. However, the component of temporary stored water, which evaporates and does not arrive on the forest floor, is called interception I. The partitioning of temporary

stored water into interception and canopy drainage depends on the one hand on individual canopy characteristics such as LAI (leaf area index), form of trees and canopy density. Cumulated, these plant characteristics are quantified by the canopy storage capacity (also named as interception storage capacity). On the other hand, the partitioning into interception and drainage is affected by meteorological conditions such as wind, radiation, temperature and vapour pressure (Rutter et al. 1971, Gash 1979).

Fundamentally the partitioning of precipitation P (P being the precipitation measured according to meteorological standards) into four components, namely throughfall P_t, stem flow P_s, drainage P_d and interception I can be described by the precipitation balance,

$$P = P_t + P_d + I + P_s \ . \tag{4.2}$$

However, typically drainage and throughfall are summarized to canopy drip P_c, because it is not possible measure both components separately. Furthermore, the total amount of precipitation which reaches the forest ground (sum of canopy drip and stem flow) is called net precipitation P_n. So, the net precipitation defines the amount of water which is potentially available for plants.

4.2.2 Measurements

The investigations of this chapter were primary related to the test sites at the Spruce and the Beech stands. Thereby, the measurements of precipitation (according to meteorological standards), canopy drip and stem flow were most important. However, it is noted again that stem flow was only relevant at the Beech site. The precipitation (according to meteorological standards) was measured in the case of Spruce site at a rain gauge on a clearing in the immediate vicinity. However, in the case of Beech site, the data of station N4 were used primary for quantification of precipitation.

The periods of investigation were delimited to frost-free season of 2006 and 2007 because of autarkic power supply at the Beech site. So, the primary periods of investigation were arranged for the periods April to October 2006 and 2007. However, some special investigations were delimited to periods where Beech trees were foliated completely. That means in detail the periods June to September.

4.2.3 Uncertainties of Measurement

It is well known that precipitation is the most heterogeneous meteorological variable on a scale of time but also on a scale of space. So, the distance between site of measurement and site of investigation must be as small as possible to minimise effects of spatial heterogeneity. In context to the investigation of this chapter, this fact is related to the distances between rain gauges and measurement of canopy drip and to the distances between rain gauges and measurement of stem flow respectively.

The spatial separation was negligible at the Spruce site. However, the spatial separation between rain gauge and measurement of canopy drip and stem flow was around 1.5 km at the Beech site. That means that the effects of spatial separation were not excludable. However, it

was possible to identify the times of precipitation events due to measurements directly at the test site (rain gauge installed at top of tower). Furthermore, a strong correlation was found between N4 and other rain gauges (N2, N3, N5) in the near vicinity. It was possible to transpose those correlations and to quantify the precipitation at the Beech site. In this way, the effects of spatial separation of measurement devices were reduced, and it was assumed, they were unimportant in context to the objects of investigation.

In context of representativeness of measurements of canopy drip and measurements of stem flow, it must be ensured that measurements of are representative samples of the complete characteristics of the canopy. So, it must be ensured that the canopy is in a range of measurements widely homogenously related to LAI (leaf area index), sky view coefficient, form of trees, density of trees and composition of tree species. Furthermore, the throughfall troughs must be positioned in representative areas, and stem flow measurements must be installed on representative tress. The arrangement of throughfall troughs and stem flow measurement devices at the test sites is shown in Figure 4.1, at which the devices are shown in context to structure and characteristic of surrounding trees.

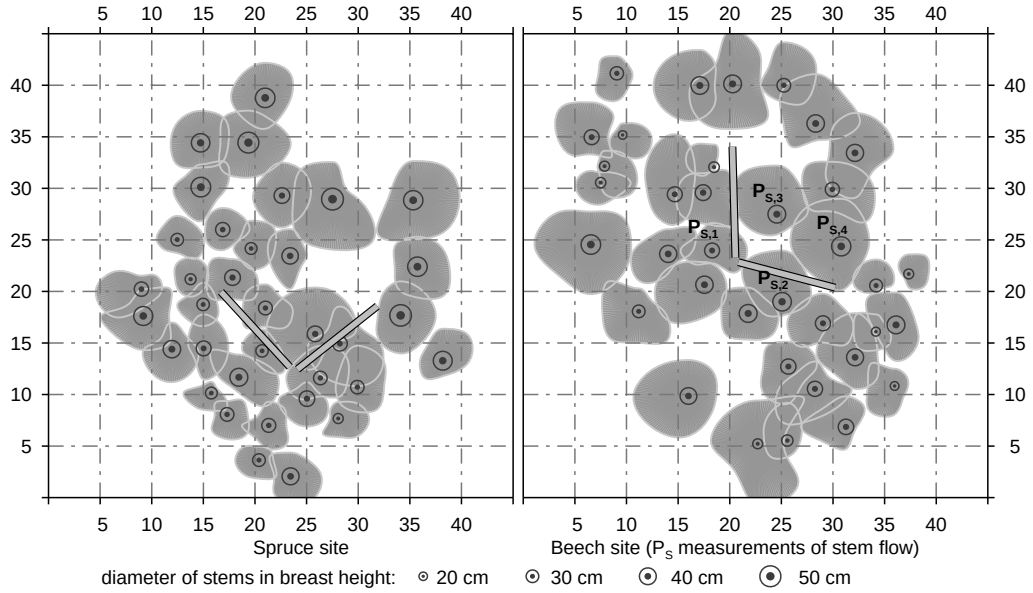

Figure 4.1 Position of throughfall troughs and position of stem flow measurements at test sites; also displayed are position, diameter (measured at breast height) and area of crowns of surrounding trees

Other sources of uncertainties, which are relevant for measurements of canopy drip and stem flow, are related to the measuring principles. A detailed overview is given in Crockford and Richardson (1987). In the context of this study, the uncertainties are primary related to percentages of stem flow and other lateral flows, which are misled due to branches and crotches respectively. That means that some parts of stem flow are forced to drip down. This effect causes two major problems: (i) It is possible that significant percentages of precipitation drip down but they are measured neither as stem flow nor as canopy drip; (ii) It is possible that important parts of stem flow fall into the throughfall troughs, so the measured canopy drip does not represent the actual conditions. In the worst case, it is possible that the measured canopy drip increases precipitation (measured outside) due to funnelled stem flow.

Another type of uncertainty is related to the approximated interrelationships between precipitation and canopy drip and precipitation and stem flow. Although, these uncertainties are not actual measurement uncertainties, it is necessary to consider these effects in subsequent analyses. In principle, it means effects of wind on net precipitation and on canopy drip. So, the strong correlation between precipitation and canopy drip and the strong correlation between precipitation and stem flow are blurred due to the effects of wind.

Finally, a type of uncertainty which must be discussed is related to initial wetness of the canopy at the start of a precipitation event. So, it was found that the amount of canopy drip and stem flow depends significantly on the wetness of leaves, twigs, braches and trunks at the beginning. A check of initial wetness was only possible visually and it was also done only sporadically for some selected periods. But, it was not possible to quantify the initial wetness. So, it was typically unknown. However, it was possible to minimize effects of initial wetness due to the separation of precipitation events by a four-hourly period (see Chapter 4.2.5). In this way, it was assumed that the canopy was dried completely before another event started.

4.2.4 Quantification of Uncertainties of Measurement

Besides uncertainties related to representativeness and weather conditions, there are also actual measurement uncertainties. In contrast to other uncertainties, it was possible to approximate their magnitude. In general, there are two major sources for uncertainties: (i) there are uncertainties due to wind induced turbulence around the rain gauges, which shift precipitation droplets beside the collector (Richter 1995, Nešpor and Sevruk 1999, Yang et al. 1999); (ii) there are uncertainties due to moistening deficits of measurement devices (Groisman and Legates 1994, Richter 1995). Another uncertainty, which is often referred to, is related to evaporation out of storage vessels. However, it is negligible in this study because of to the high temporal resolution (10 minutes) of primary devices.

The uncertainties caused by turbulence and wind were assumed to be 5 % for all rain gauges used, according to Richter (1995) and other authors (Rodda and Smith 1986, Groisman and Legates 1994, Yang et al. 1999). In this context, it is noted that periods of investigation were completely in frost-free seasons and were primarily in the summer season. In this way, the uncertainty of 5 % is related predominately to convective rain events. In addition, all stations are well protected against wind. For canopy drip, effects of turbulence and wind were completely negligible because of low wind speed within the canopy and because of the large collection area of throughfall troughs.

The uncertainties caused by moistening deficits were measureable by empirical observations and practical experiments (Eichelmann and Prasse 2008). Typically effects of moistening deficits were around 0.1 mm per event in the case of tripping bucked rain gauge (Theis, N4). However, uncertainties due to moistening deficits were excludable for weighing rain gauges (Pluvio, Spruce site). For the throughfall troughs and so for canopy drip, the uncertainties due to moistening deficits were approximated at 0.2 mm.

A similar quantification was not possible for measurements of stem flow. However, it is assumed that moistening deficits at collectors are negligible in two ways. So, moistening deficits are insignificant for moderated and large precipitation events because of a large volume of stem flow. But, the moistening deficits are also negligible in the case of small events. Here, it is assumed that the moistening demand of trunks below collectors, which is normally necessarily for creation of stem flow to forest floor, is significant higher than the moistening deficits of the collector. In that way, the moistening deficits are negligible for stem flow measurements.

In general, all uncertainties cause an underestimation of measured precipitation and measured canopy drip respectively. Consequently the range of accuracy can be assessed by a minimum, which is represented by measured value, and by a maximum, which is represented by the sum of measured value and superposed uncertainties. It is possible to approximate the range of uncertainty for individual devices. In the case of weighing rain gauge (Spruce site), the range of uncertainty is between P and 1.05 P. (P being precipitation measured according to meteorological standards.) However, the range of uncertainty increases in the case of tripping bucked rain gauge (N4) due to the additional uncertainty of moistening deficit. So, the uncertainty is between P and 1.05 P + 0.1 mm related to individual events. For canopy drip, the range of uncertainty is between P_c and P_c + 0.2 mm related to individual events. (P_c being measured canopy drip.) The differences between maximum and minimum are abbreviated by ΔP for precipitation and by ΔP_c for canopy drip in the following text.

Uncertainties, which were not possible to regard, were related to very small events such as drizzle, fog or dew. It was not possible to measure these events. So, it was also not possible to regard their effects. However, it is assumed that they affect the moistening deficits of devices and the wetness of canopies. Other uncertainties, which were not possible to regard, were related to short drying periods within precipitation events. It was not possible to consider and quantify those effects because of the method for separation of individual precipitation events (see the next Chapter 4.2.5). In this context, it is assumed, when an event last a long time and is interrupted severally by short periods of drying (< 4 h), that the actual moistening deficit is significant higher than assumed (0.1 mm for ΔP and 0.2 mm for ΔP_c). However, the derived uncertainties due to moistening deficits are reliable approximations for a general and objective evaluation of measurement uncertainties.

4.2.5 Separation of Individual Events of Precipitation

The investigations of this chapter are related to two time scales: months and individual events. A special task was the separation of precipitation events on basis of data in temporal resolution of 10 minutes. In principle, a period of 4 hours was assumed for complete drying after a recorded event. So, it was assumed that when the period between recoded precipitations was longer than 4 hours, there were two independent events. Otherwise, it was assumed that the recorded precipitations belong together. The time of 4 hours was derived from empirical observations, historical measurements with wetness grids (artificial leaves) and cross checks with eddy covariance measurements (derivation of canopy conductance). It was found that 4

hours are a reliable period for the typical duration of complete drying after wetting due to rain in the summer season.

The numbers of all events of precipitation identified in both periods of investigation (April until October) are listed in Table 4.1. The number of recorded events was lower at the Beech site than the Spruce site. However this circumstance concerns primarily only small events with an amount of precipitation less than 1 mm. The reason is found in the method of separation, where sometimes an interrelated event was assumed at the Beech site, but independent event was assumed at the Spruce site.

Table 4.1 Number of recorded precipitation events during investigation periods (April-October); values in brackets are related to periods with complete foliation of beech trees (period June - September)

period	Spruce site	Beech site
2006 all	159 (91)	147 (90)
events > 1 mm	73 (47)	69 (41)
2007 all	186 (125)	177 (126)
events > 1 mm	85 (67)	86 (65)

4.3 Analyses and Investigations on Scale of Individual Events

4.3.1 Investigations of Stem Flow at the Beech site

The analyses of stem flow were restricted to periods when full foliation was assumed for Beech trees (June until September). This restriction was necessary to ensure widely homogeneous properties of canopy in context to phenological phase, LAI (leaf area index) and percentage of crown closure. The interrelationship between measured precipitation and measured stem flow on a scale of individual events is shown in Figure 4.2. The left side of Figure 4.2 shows the volume of stem flow, which was measured at individual trees ($P_{s,1}$, $P_{s,2}$, $P_{s,3}$). Thereby, it is clear that events with more than 1.0 to 1.5 mm caused measurable stem flow. Events with around 10 mm cause on average more than 50 L stem flow per tree. However, there were also events with 10 mm which caused stem flow rates higher than 100 L.

The measured stem flow was quite variable in dependence to the characteristics of precipitation events. Two examples therefore are highlighted by rectangles in Figure 4.2 (left side) and are related to two events with about 25 mm measured precipitation. There are two reasons for variations of stem flow: (i) the initial wetness of trunk, braches and leaves before an event and (ii) the characteristic course of event. In the case of small events the variations are caused predominately by different initial wetness of trunk and other plant parts. So, they are also related to the method of separation of individual events. However, the initial wetness is insignificant in the case of bigger events (like the marked examples). There, the variations are caused by the course and characteristics of events. In context to the example, the small stem flow was caused by an event which lasted around 23 hours and was interrupted by many short (< 2 hours) periods of drying. In contrast, the high stem flow was created by an event, which lasted only 4 hours and was nearly continuously.

Besides the variability between individual events, there were also differences of measured stem flow between individual trees. The differences between trees were significantly for individual events. However, the trees have comparable parameters (height, age, crown diameter, LAI). The biggest observed differences were 86.7 L (measured precipitation 17.2 mm) and 62.1 L (measured precipitation 31.2 mm). Both events are highlighted by ellipses (Figure 4.2, left side). However, there were also events with almost identical stem flow at all trees. Two examples therefore are marked by grey bolt arrows. On average, the difference between individual trees was around 15 % in relation to the arithmetic mean of all three trees.

The differences between individual trees were not systematic. Rather, the differences between trees were random. However, the statistical interrelationship between precipitation and stem flow was very similar for all three trees. The estimated regression lines have very similar slopes and offsets. In particular, the regression lines of trees 2 and 3 ($P_{s,2}$, $P_{s,3}$) are almost identical. In addition, the coefficient of determination $\Re^2$ is around 0.85 for all three trees, which means linear regressions are sufficient for description of general behaviour and practical applications.

The up-scaling of stem flow from tree scale to canopy scale was done by averaging and weighting measured stem flow, at which the weighting coefficient was the number of trees per m² base area (stem density). The resulting interrelationship between precipitation and stem flow per m² (stem flow at canopy scale P_s) is shown on the right side of Figure 4.2. (Note: P_s without index means stem flow at canopy scale.)

It was possible to describe the statistical interrelationship between stem flow and precipitation at a canopy scale similar to an individual tree scale using a linear regression. The regression line has a slope of 0.23 and an offset of -0.19, at which the coefficient of determination $\Re^2$ is 0.88. The coefficient of determination is relatively high, although two events (marked by bold orange arrows) differ significantly from all other observations. Those outliers were caused by unusually long lasting precipitation events, which were interrupted by several periods of drying. One such event has already been discussed in the former example. In addition to the coefficient of determination, the confidence interval was also calculated. It is shown as grey area in the background of Figure 4.2 (right side).

It can be concluded for water balance and for net precipitation P_n respectively at the Beech site that events of precipitation greater than 1 mm cause stem flow. In these cases the stem flow is between 20 to 25 % of precipitation, measured according to meteorological standards. Finally, it is noted that the percentage of stem flow and also the statistical interrelationship between stem flow and precipitation were almost identical in both investigation periods. In particular, an effect of the storm *Kyrill* was not detectable.

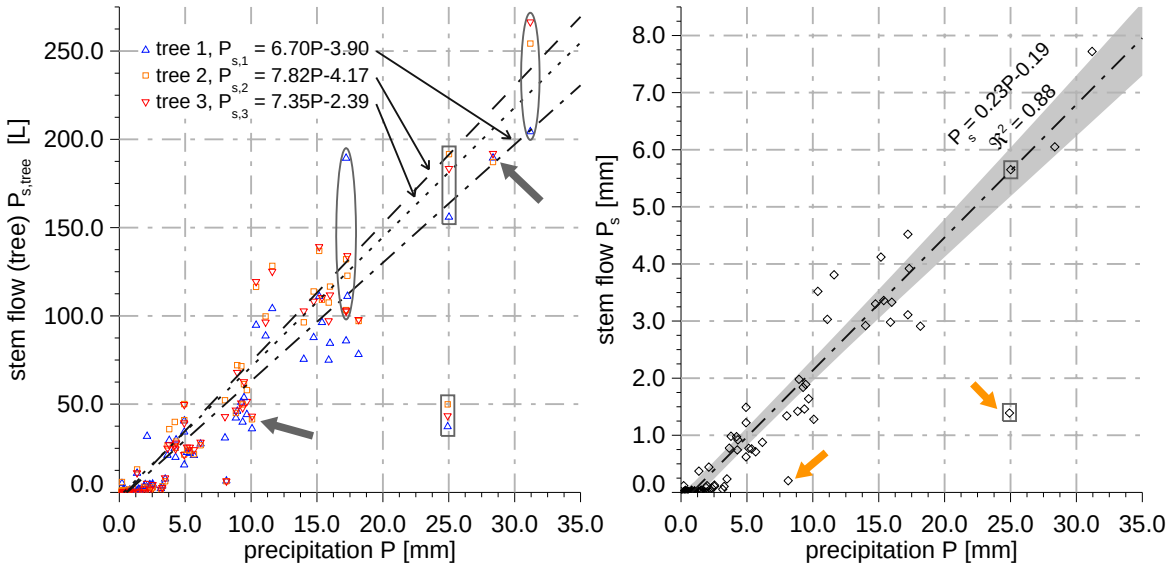

Figure 4.2 Interrelationship between measured precipitation and measured stem flow on scale of individual events of precipitation and associated regression lines; left: measured volume of stem flow at individual trees; right: stem flow up-scaled to canopy scale (grey background marks confidence interval of regression line); rectangles, ellipses, bold arrows: special examples (see text)

4.3.2 Investigations of Net Precipitation

The objective of this particular chapter was to estimate the percentage of precipitation which reaches the forest floor on a scale of individual events. That means to estimate the net precipitation P_n (and hence the percentage of precipitation) which becomes potentially available for plants in individual precipitation events. The net precipitation is equal to the canopy drip P_c at the Spruce site. However P_n is the sum of canopy drip and stem flow at the Beech site. Similar to the former investigations of stem flow also the investigations of net precipitation are restricted to the period when complete foliation of Beech trees is assumed (June until September) to ensure temporal homogeneity of canopies.

The interrelationships between net precipitation and measured precipitation are shown in Figure 4.3 for both canopies (left: Spruce; right: Beech). The calculated regression lines are fairly similar between both sites and the coefficient of determination $\mathfrak{R}^2$ is greater than 0.8. In particular, the slopes of regression lines are nearly identically and are around 0.6. In context to the approximated confidence intervals (shown as grey background) the percentage of net precipitation is around 60 % of measured precipitation at both sites in the statistical average.

Separated measurements of throughfall P_t and of canopy drainage P_d are not possible. However, this separation is possible using statistical analyses as described in Rutter et al. (1971). In this context, the separation and quantification of P_t and P_d are important preconditions for the parameterisation of different interception models (e.g. Rutter et al. 1971, Gash 1979, Valente et al. 1997). However, here the derivations of throughfall coefficient and canopy storage capacity are especially important to the evaluation of canopy water supply.

According to Rutter et al. (1971), the percentage of throughfall (and hence the throughfall coefficient) p_t is determinable by a regression between precipitation events with less than

1 mm and associated canopy drip. It is assumed for such small events that the percentage of canopy drainage P_d related to entire canopy drip P_c is negligible. Accordingly, the canopy drip is created only by throughfall P_t. In that way, the slope of regression line (which is forced through the origin and is related to precipitation events < 1 mm) represents the percentage of throughfall and the throughfall coefficient respectively.

The estimated throughfall coefficients p_t were 0.12 at the Spruce site and 0.14 at the Beech site. These rates agree very well with expectations, derived from sky view coefficient (see Table 2.1). However, differences between both canopies are also marginal. So, it is assumed that differences between both sites were caused by uncertainties of representativeness of measurements. However, the differences do not indicate significant and systematic differences between both canopies. In context to practical applications of forest management, it is assumed that 10 to 15 % of precipitation reached the forest floor directly in terms of throughfall at both sites. Furthermore, this percentage is caused by gaps in the crown cover.

Another important parameter is the canopy storage capacity S_c, which is also called interception storage capacity. The canopy storage capacity being the amount of water which is maximally storable in leaves, needles, twigs and branches. To estimate this parameter, a line with a slope of 1 was fitted through the data points with the highest ratio (P_n/P). The resulting offset of this line matches the canopy storage capacity according to Rutter et al. (1971).

The estimated canopy storage capacity was about 1.18 mm at the Spruce site. This value represents a typical canopy storage capacity of coniferous forests, which is around 1.2 mm according to Shuttleworth (1993). At the Beech site, the estimated canopy storage capacity was 0.92 mm. This value is somewhat higher than usual for deciduous forests, for which an average of 0.8 mm is assumed according to Shuttleworth (1993). It seems to be a special characteristic of Beech trees at the Beech site. A normalisation of canopy storage capacity with LAI (leaf area index) results to the storage capacity per leaf area. The normalised storage capacity was 0.24 mm m^{-2} at the Beech site and 0.16 mm m^{-2} at the Spruce site. So, the storage of precipitation per leaf area was almost one and a half times higher on Beech trees than on Spruce trees.

Special attention was given to analyse the effects of storm *Kyrill*. It was assumed that significant losses of twigs and branches and losses of needles from Spruce trees have a significant influence on net precipitation. However, effects were not observed. In this context, it is noted that significant effects were observed in measured transpiration (see Chapter 5). It is assumed that effects of storm damage to net precipitation were overlaid due to effects of more precipitation in 2007. In this way, the effects of *Kyrill* were probably compensated due to the effects of initial wetness, which caused unquantifiable uncertainties in relationships between precipitation and net precipitation.

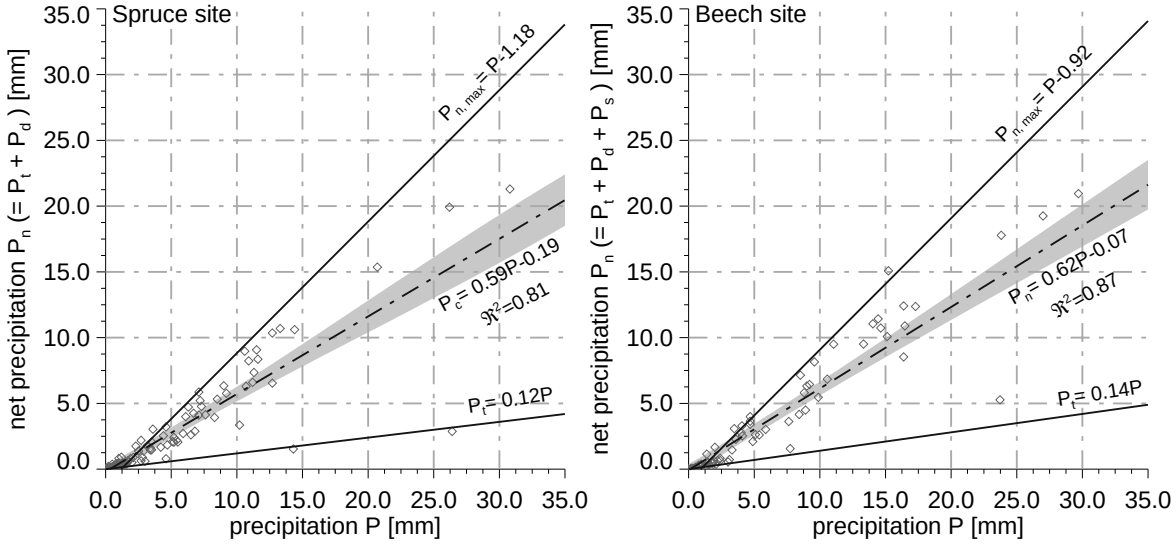

Figure 4.3 Interrelationship between net precipitation and precipitation related to events during periods with complete foliation (June – September) at Spruce and Beech sites; associated regression lines and confidence intervals (grey background); approximations of canopy storage capacity and throughfall coefficient (further details see text)

4.3.3 Effects of Measurement Uncertainties

The effects of measurement uncertainties to regression lines between precipitation and net precipitation were marginal compared to general variability of the data. Some special cases for effects of measurement uncertainties are listed in Table 4.2. There are shown as slopes and offsets of regression lines in dependence to differently considered measurement uncertainty.

The standard case (i) means slope and offset of regression line without considered measurement uncertainties and is identical to the regression lines in Figure 4.3. In case (ii), it was assumed measured precipitation was correct. However, canopy drip was underestimated maximally. So, case (ii) means the regression between P and $P_c + \Delta P_c$. In contrast to case (ii), it was assumed in example (iii) that the measurement of canopy drip was correct. However, precipitation was underestimated maximally. So, it means the regression between $P + \Delta P$ and P_c. The last case (iv) means a situation where precipitation as well as canopy drip underestimate actual values maximally. So, case (iv) means regression between $P + \Delta P$ and $P_c + \Delta P_c$.

All observed effects were small and insignificant for regression lines. That means that slopes a and offsets b were very similar and were inside the confidence interval shown in Figure 4.3. So, compared to the standard case (i), the differences of slopes were maximally ± 0.03. That means the variations in slope were smaller than ± 5% related to the standard case (i). The maximal difference of offset was caused by maximal uncertainty due to moistening deficits. Therefore, the maximal difference to standard case was 0.2 mm.

Table 4.2 Slope and offset of the regression lines between precipitation and net precipitation in dependence to different consideration of measurement uncertainties

regression		Spruce site	Beech site
(i)	$P_n = P_c + P_s = a \cdot P + b$	a = 0.59, b = -0.19	a = 0.62, b = -0.07
(ii)	$P_{n,\min} = P_c + P_s = a \cdot (P + \Delta P) + b$	a = 0.57, b = -0.25	a = 0.59, b = -0.08
(iii)	$P_{n,\max} = P_c + \Delta P_c + P_s = a \cdot P + b$	a = 0.59, b = +0.01	a = 0.62, b = +0.13
(iv)	$P_n = P_c + \Delta P_c + P_s = a \cdot (P + \Delta P) + b$	a = 0.57, b = -0.05	a = 0.59, b = +0.12

4.4 Analyses and Investigations on Monthly Scale

4.4.1 Estimation of Monthly Balances

The monthly totals and the effects of measurement uncertainties were investigated similar to individual events. The monthly totals of precipitation P, canopy drip P_c and stem flow P_s as well as the totals of periods of all variables are shown in Figure 4.4 for 2006 and in Figure 4.5 for 2007. Additionally, the interception is shown as the difference between precipitation and net precipitation (sum of P_c and P_s). Finally, the associated uncertainties are shown for all variables. The uncertainty of interception results from measurement uncertainties of precipitation and of measurement uncertainties canopy drip. So, the range of uncertainty is between $I_{max} = I + \Delta P$ (maximum) and $I_{max} = I - \Delta P_c$ (minimum). Thereby, ΔP and ΔP_c means maximal uncertainties of measurements of precipitation and canopy drip respectively.

The monthly sums of precipitation P were fairly similar at both sites in investigation 2006. A bigger difference was only seen in July and was caused by two heavy thunderstorms at the Beech site. So, P was 38 mm at the Beech site but only 10 mm at the Spruce site in this month. However, other bigger differences of P were not observable between both sites in 2006. However, significant differences occurred between both sites in 2007. This is surprising, because 2007 was dominated by long lasting moderate events of precipitation. However, precipitation was dominated by short and heavy events in 2006.

In this context, it is typically assumed that spatial heterogeneity of precipitation P decreases in relation to the duration of events. Additionally it is assumed that spatial heterogeneity increases with increasing intensity of P. However, effects of spatial heterogeneity were more significant for 2007 than for 2006. Thereby, the difference of P was higher than 20 mm between both sites in May, June and August. For the complete period, the difference was 54 mm in 2006 and 118 mm in 2007. So, P at the Spruce site was 91 % in 2006, but only 84 % in 2007 related to precipitation of the period at the Beech site. That means, P was around 10 % lower at the Spruce site than at the Beech site, although the distance between both sites was only 6.5 km. In this context, both sites are approximately at the same altitude and effects due to slope and aspect are excludable.

To avoid problems due to different precipitation, the investigations were delimited to months when precipitation was similar at both sites. It was observed in those months that the net precipitation was also fairly similar at both sites. However, it must be considered that the net precipitation was composed completely differently at both sites. So, stem flow was negligible

at the Spruce site. However, it was a major component of net precipitation at the Beech site. The percentage of stem flow varied between 27 % (September 2006) and 43 % (September 2007) on a monthly scale. The percentage was 32 % in 2006 and 36 % in 2007 related to entire periods. So, the stem flow was around one-third of net precipitation on average at the Beech site.

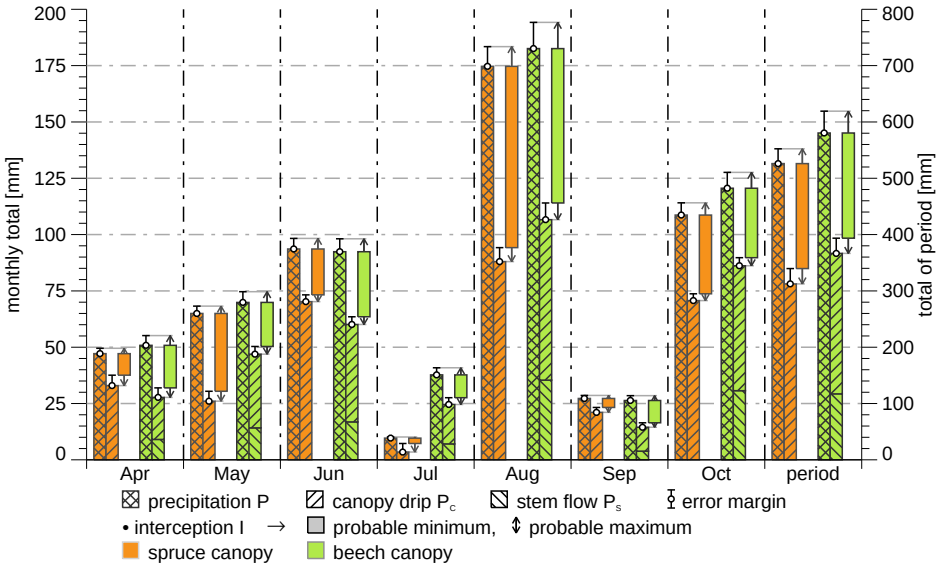

Figure 4.4 Monthly totals (left axis) and totals of period (right axis) of precipitation, stem flow, canopy drip and interception in 2006 (April – October)

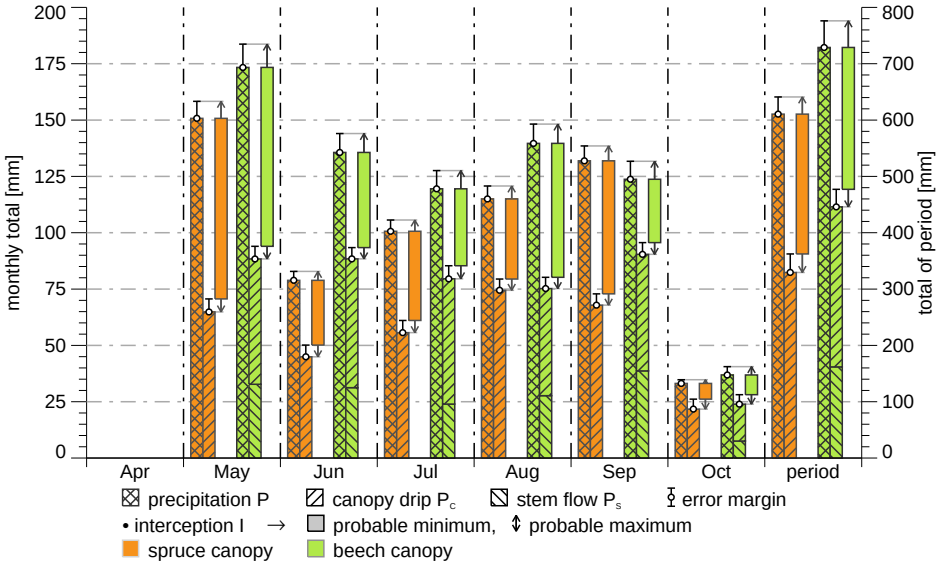

Figure 4.5 Monthly totals (left axis) and totals of period (right axis) of precipitation, stem flow, canopy drip and interception in 2007 (April – October); note: missing bars in April 2007 are caused by extreme dry weather conditions, when measured P was only 0.2 mm.

4.4.2 General Evaluation of Measurement Uncertainties to Long Time Observations

In contrast to investigations on a scale of individual events, measurement uncertainties have significant importance for investigations and analyses of long time periods. Here, the superposition and addition of systematic measurement uncertainties cause significant uncertainties

in totals of precipitation and canopy drip, which must be considered. The approximated uncertainties (absolute and relative) of precipitation P and canopy drip P_c are listed together with the associated totals of period in Table 4.3 for both periods and both test sites. In addition, the totals of stem flow P_s and net precipitation P_n are listed.

It must be considered that the uncertainty of P_n is actually defined due to the superposition of uncertainties of P_c and P_s. However, it was not possible to quantify the uncertainty of P_s. It was assumed that it is negligible in context to uncertainties of P_c. So the absolute uncertainty of P_n is identical to the absolute uncertainty of P_c at the Spruce site. But the relative uncertainty is different at the Beech site because it is related to the sum of P_c and P_s.

Table 4.3 Totals of periods of precipitation P, canopy drip P_c and stem flow P_s at both sites and associated uncertainties of precipitation ΔP, canopy drip ΔP_c and net precipitation ΔP_n (note: absolute uncertainty of net precipitation was assumed as similar to uncertainty of canopy drip, uncertainty of stem flow was neglected)

test site (year)	P [mm]	P_c [mm]	P_s [mm]	P_n [mm]	ΔP [mm]	ΔP_c [mm]	ΔP_n
Beech (2006)	580.4	249.4	117.2	366.4	38.3 (6.6%)	26.8 (10.7%)	7.3%
Spruce (2006)	526.0	312.5	---	312.5	26.3 (5.0%)	27.8 (8.9%)	8.9%
Beech (2007)	728.9	284.0	161.9	445.9	49.6 (6.8%)	34.0 (12.0%)	6.2%
Spruce (2007)	610.5	329.5	---	329.5	30.5 (5.0%)	33.2 (10.0%)	10.0%

4.4.3 Evaluation of Uncertainties in Totals of Precipitation

The uncertainties of precipitation were higher at the Beech site than at the Spruce site. The higher absolute uncertainty was primary caused by more precipitation at the Beech site. However, effects of higher uncertainty of used measurement device were secondary. That is different in the case of relative uncertainty. Here, the higher (relative) uncertainty at the Beech site was caused by the higher uncertainty of the rain gauge used. So, tripping bucked rain gauges (Beech site/ N4) have a higher uncertainty than weighting rain gauges (Spruce site) because of an additional uncertainty due to moistening deficits, which can be ignored for weighting rain gauges.

The absolute uncertainty of precipitation P was only defined due to the amount of P at the Spruce site. So, the relative uncertainty was 5 % constantly related to measured P. However, the uncertainties (both absolute and relative) are affected by the amount of P as well as by the number of precipitation events within a period at the Beech site. An increasing number of events cause an increase of uncertainty. In average, the relative uncertainty of precipitation was 6.7 % in period April until October at the Beech site. So it was 1.7 % higher than at the Spruce site.

Similar to totals of periods, also total of months are affected significantly by the superposition of measurement uncertainties. It was observable that an increase of P causes an increase of

absolute uncertainty (compare Figure 4.4 and 4.5). Consequently, the biggest uncertainties occurred in months with highest precipitation P (August 2006 and May 2007). There, the absolute uncertainty was 11.6 mm (August 2006) and 10.3 mm (May 2007) at the Beech site and 8.7 mm (August 2006) and 7.5 mm (May 2007) at the Spruce site respectively.

The relative uncertainty was because of measuring principle only variable at the Beech site. However, it was constant (5 %) at the Spruce site. The typical range of relative uncertainty was 6 up to 10 % at the Beech site. Thereby, the variation was caused by the different number of events in individual months. An exception and absolute extreme was April 2007. In this month, only one event with 0.2 mm precipitation was recorded. Consequently, the approximated absolute uncertainty was 0.21 mm at the Beech site. That would mean a relative uncertainty of 105 %.

4.4.4 Evaluation of Uncertainties in Totals of Canopy Drip and Net Precipitation respectively

The absolute uncertainty of canopy drip P_c and net precipitation P_n respectively was only affected by moistening deficits of devices. In this way, the amount of absolute uncertainty was determined by the number of events, which created measurable P_c. It was found that the number of precipitation events, which caused recorded P_c, was almost identical at both sites, although the total number of events was significant higher at the Spruce site (compare Table 4.1). In that way, the absolute uncertainties of P_c and of P_n respectively were almost identical at both sites; the difference between both sites was only around 1 mm in both periods.

It is recognizable in context to analyses of throughfall P_t, that this procedure causes an underestimation of actual canopy drip P_c and an underestimation of actual uncertainty. So, it was shown in analyses of P_t; that it was between 10 and 15 % of precipitation at both sites. In that way, canopy drip P_c is actually also created by very small events. However, it was not possible to measure these small inputs with available devices.

In relation to the total number of events (see Table 4.1), the number of events is considerable, which were smaller than 1 mm. However, the actual number of events, which did not create measurable canopy drip, was less than 20 at both sites and in both periods. So, the actual uncertainty due to not considered events was maximally 1.5 mm, under the assumption that the average precipitation of such events was 0.5 mm and the percentage of throughfall was 15 %. That means that effects due to not considered events were insignificant for monthly totals or totals of periods of canopy drip. In this way, the restriction to events, which caused measurable canopy drip, was sufficient for the exact quantification of monthly totals as well as uncertainties of monthly totals of canopy drip and net precipitation.

The highest absolute uncertainties of canopy drip and net precipitation were found in months with highest precipitation (August 2006 and May 2007). It was found that these months were not only months with highest precipitation, but also months with the most events of recorded canopy drip. The approximated uncertainties of canopy drip and net precipitation were:

7.4 mm (August 2006) and 5.6 mm (May 2007) at the Beech site and 6.2 mm (August 2006) and 5.8 mm (May 2007) at the Spruce site.

The relative uncertainties of canopy drip P_c and net precipitation P_n were affected significantly by amount of monthly total (total of period) as well as by number of events within a month (within a period). So the relative uncertainty was very different between individual months. At the Beech site, the relative uncertainty of P_c was 11.3 % in average (related to totality of available data). However, it varied between 6.5 % (October 2006) and 25.7 % (October 2007). At the Spruce site, the relative uncertainty was much more variable. It was between 4.2 % (October 2006) and 109 % (July 2007), at which the average was 9.5 %. So, the average of relative uncertainty of P_c was somewhat smaller at the Spruce site than at the Beech site, which was caused by the bigger totals of P_c at the Spruce site. However, the relative uncertainty of net precipitation P_n was smaller at the Beech site than at the Spruce site, because of additional percentage of stem flow. So the average uncertainty of P_n (average related to totality of available data) was 7.5 % at the Beech site and 9.5 % (identical to canopy drip) at the Spruce site.

The amounts of absolute and relative uncertainties showed clearly that measurement uncertainties have significant importance of the quantification of net precipitation and water balance at canopy scale, when time periods of investigation are months or longer periods. It was demonstrated that the uncertainties of monthly totals (or longer periods) are determined due to the superposition of uncertainties of individual events. So, it is not possible to estimate uncertainties on monthly scale from monthly totals of precipitation or net precipitation. The amount of uncertainty is determined due to characteristics of predominant weather. So, the uncertainty is affected by the number of events. That means for the exact quantification of water balance and net precipitation that data are required in a higher temporal resolution than months, even when investigations are related to monthly scale.

4.4.5 Ratio between Net Precipitation and Precipitation

The water balance and the water supply of a canopy respectively are often benchmarked by the ratio between interception and precipitation to evaluate water losses. In context to the intention of this chapter to evaluate the amount of water, which becomes available for plants, adequately the ratio between net precipitation and precipitation was investigated. The percentage of net precipitation related to precipitation (according to meteorological standard) is called p_n in following text and is quantified in percent, when nothing else is denoted.

The error margin and uncertainty of p_n respectively are caused by uncertainties of precipitation and canopy drip. Thus, the associated range of uncertainty is between,

$$p_{n,\min} = \frac{P_s + P_c}{P + \Delta P} \cdot 100\,\% \ , \tag{4.3}$$

and,

$$p_{n,\max} = \frac{P_s + P_c + \Delta P_c}{P} \cdot 100\ \% \ . \qquad (4.4)$$

Here, $p_{n,min}$ denotes the probable minimum and $p_{n,max}$ denotes the probable maximum of p_n. The value, which is calculated directly out of measured data and is calculated without consideration of measurement uncertainties, is used as reference and is called $p_{n,Ref}$. The interrelationship between $p_{n,Ref}$ and precipitation as well as the associated uncertainties of p_n are shown in Figure 4.6 for all investigated months. In addition, the corresponding values are listed for complete periods in Table 4.4.

The effects of measurement uncertainties become especial importance in context to investigations of p_n. Here, the superposition of uncertainties of canopy drip P_c and precipitation P and especially the reinforcing effect of normalization cause significant uncertainties in p_n. The range of uncertainty is visible in Figure 4.6 in terms of differences between $p_{n,max}$ and $p_{n,Ref}$ and $p_{n,min}$ and $p_{n,Ref}$ respectively. The uncertainties are especially important for months with less precipitation like July 2006 or October 2007. However, the uncertainties are also considerable in very rainy months like August 2006 and May 2007.

The comparison of both sites shows, p_n was very variable between individual months at the Spruce site. The range of $p_{n,Ref}$ was between 36 % (July) and 77 % (September) in 2006. The variations of $p_{n,Ref}$ were something smaller in 2007. There, $p_{n,Ref}$ was between 43 % (May) and 66 % (October).

p_n was not so much variable at the Beech site. There, $p_{n,Ref}$ was between 55 % (April) and 71 % (October) in 2006 and between 51 % (May) and 73 % (September) in 2007. The comparison of complete periods (Table 4.4) shows, p_n was fairly similar in both periods. However, p_n was something (around 5 %) higher at the Beech site than at the Spruce site. So, the average (related to totality of available data) was 62.1 % at the Beech site and 56.5 % at the Spruce site. However, this statement must be seen in context to the yearly course of foliation at the Beech site. So, $p_{n,Ref}$ was 61.8 % at the Beech site and 58.1 % at the Spruce site, when the averaging period was delimited to period, when Beech trees were foliated completely (June until September). So, there was not a significant difference between the Beech and Spruce sites in the main growing season.

Further, effects of leaf ageing were identifiable due to the comparison between period of complete foliation and entire period on Beech trees. (Leaf ageing being changes of leaf properties from start of foliation in May up to colouring of leaves in October.) However, these effects were small (< 1%) and were insignificant in relation to measurement uncertainties. Investigations of p_n and also net precipitation P_n indicated the age bracket of leaves is negligible. But, this statement is only related to periods with foliation. It is not transferable to periods without foliation such as winter months.

In context to variations of p_n, but also in context to uncertainty of p_n, the former statement is confirmed: it is not possible to estimate the net precipitation and the percentage of net precipitation p_n on the basis of monthly totals of precipitation. The length, the course and the inten-

sity of individual precipitation events affect the actual value of net precipitation too much. Thus, it is impossible to work with data in temporal resolution of months or longer time periods.

In another context, the analyses of p_n confirm the regression lines of section 4.3.2. Hereby, it is observed that the slopes of regression lines were very similar to estimated averages of p_n. In particular, the values are almost identical at the Beech site. At the Spruce site the slope of regression line was slightly higher than the average of $p_{n,Ref}$. This effect was caused by some minor precipitation events, which did not create canopy drip. However, it is irrelevant and negligible in context to common evaluation, that around two-thirds of precipitation becomes net precipitation at both sites.

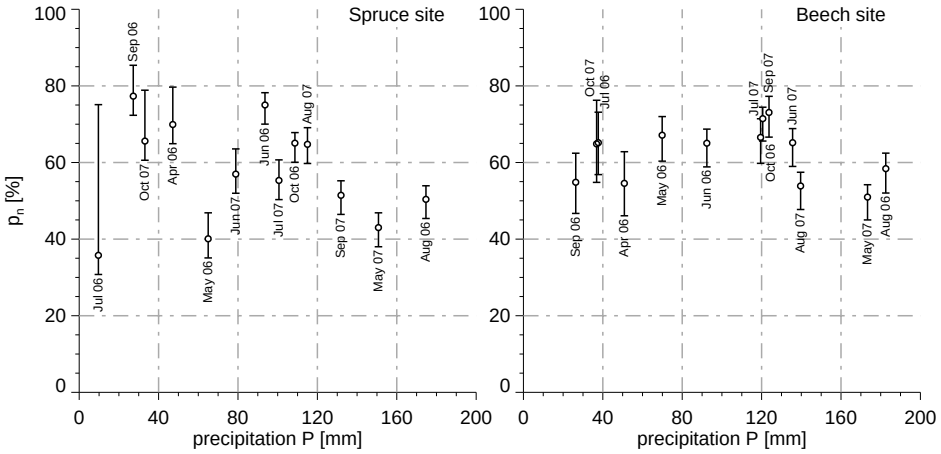

Figure 4.6 Percentage of net precipitation related to precipitation p_n ($p_{n,Ref}$) as well as associated range of uncertainty ($p_{n,min}$, $p_{n,max}$) at the Spruce site (left) and at the Beech site (right); April 2007 is omitted

Table 4.4 Percentage of net precipitation pn related to precipitation at both test sites and in both periods

site (year)	$p_{n,min}$ [%]	$p_{n,Ref}$ [%]	$p_{n,max}$ [%]
Beech (2006)	59.3	63.2	67.8
Spruce (2006)	56.6	59.4	64.7
Beech (2007)	57.3	61.2	65.8
Spruce (2007)	51.4	54.0	59.4

4.5 Concluding Remarks on Net Precipitation

In this chapter the net precipitation (percentage of precipitation which becomes available for plants) was investigated over the period of two growing seasons at a Beech and at a Spruce site. The two seasons were very different and complex concerning precipitation. There were extreme dry months with exclusively convective events of precipitation and there were months with long-lasting events with low precipitation intensities. The investigations are based on the one hand on analyses on the scale of individual precipitation events and on the other hand on analyses on the scale of monthly totals. The investigations clearly showed that it is not possible to approximate net precipitation on the basis of monthly totals of precipitation. The reason is that the net precipitation is affected too much by the characteristic of indi-

vidual events. So, the percentage of precipitation reaching the forest floor varies significantly on a monthly scale; the variations were caused by the length, course and intensity of predominant events of precipitation.

In another context, the investigations showed the significant effects of unavoidable measurement errors in estimations of net precipitation on a monthly scale. The superposition of measurement uncertainties in measured precipitation and measured canopy drip causes significant uncertainties in monthly totals. The effects to the ratio p_n between net precipitation and precipitation were especially important. In the statistical average, p_n was 5 % higher at the Beech site than at the Spruce site. Considering the uncertainties, the amount of water which reaches forest floor was fairly similar at both sites and was on average around two-thirds of precipitation. However, the individual monthly value can differ significantly from the guideline of two-thirds. So, the monthly value depends on the characteristics of predominate events in the specific month. The observed p_n were between 36 and 77 % at the Spruce site and were between 51 and 73 % at the Beech site.

In context of net precipitation, the significant role of stem flow must be emphasized at the Beech site. The percentage of stem flow was around one-third of net precipitation at the investigated Beech stand. However, it was assumed that stem flow is negligible for Spruce trees. So in the growing season, a better water supply is ensured for Beech trees than for Spruce trees in periods with less precipitation because significant percentages of precipitation are directed directly to the roots of Beech trees. Beech trees are therefore quite competitive, because they supply themselves with water. Simultaneously, they cover the understory and competing trees by closed crowns, which reduce canopy drip and radiation.

The investigation of individual events showed similar results to analyses on basis of monthly totals. That means, the statistical average of investigated events confirmed common statements of investigation on a monthly time scale. However, it was possible to analyse running processes in more detail. In another aspect, the investigations were not so much affected by measurements uncertainties because of averaging and compensation effects of random errors. In summary, it was found that net precipitation occurred (or was measured) when the amount of precipitation of an event was more than 1 mm. Further, the statistical analyses showed that the net precipitation was around 60 % of precipitation in the case of events greater than 1 mm at both sites. Here, the results derived from monthly totals were confirmed: the percentage of net precipitation was almost identically at both sites and was around two-thirds of precipitation on average. But, the important role of stem flow in net precipitation at the Beech site also becomes apparent in the analyses on the basis of individual events. It was found that stem flow was typically between 20 and 25 % of precipitation at the Beech site, when events were greater than 1 mm.

The analyses of individual events clearly showed the effects of characteristics of individual events. So, the regression between precipitation and net precipitation and between precipitation and stem flow respectively are only guidelines, which can differ significantly from the actual values of an individual event. The actual amount and the actual percentage of canopy

drip and stem flow are affected by the characteristics of an individual event and eventually also by the previous event. The duration between two events and the degree of drying significantly determine the actual amount and the actual percentage of canopy drip and stem flow. In particular, the amount and percentage of stem flow are determined by the initial wetness of the trunk. Therefore, canopy drip and stem flow decrease in comparison to average behaviour in the case of long lasting events, which are interrupted by many short drying periods. However, canopy drip and stem flow increase in comparison to average behaviour in the case of short events with high intensities of precipitation.

The characteristics of precipitation events and the interval between two events cannot be controlled. However, the percentage of throughfall can be manipulated by typical forestry operations and so has special importance for controlling net precipitation by forest management. The throughfall depends only on the degree of crown cover and crown closure. So, throughfall is controllable by forest operations such as thinning. The estimated percentage of throughfall was 12 % of precipitation at the Spruce site and 14 % at the Beech site based on investigation on the scale of individual events. Those results confirm the order of estimates from sky view factors (15 % at the Spruce site and 12 % at the Beech site). So, the actual percentage of throughfall was between 10 and 15 % at both sites related to precipitation, which means the percentage of throughfall was 15 to 25 % related to the net precipitation. So, controlling throughfall offers some potential to improve the water supply of forests.

A limitation of this study was the restriction to the frost-free season and especially to months when Beech trees were foliated. So, strictly speaking the statement of similar net precipitation holds only for foliated Beech trees. Outside these periods, the net precipitation is significantly higher at the Beech site than at the Spruce site because of significantly higher throughfall in periods without foliation of Beech trees. However, water shortage typically occurs only in summer months and water supply in the summer half-year is typically the critical parameter related to water supply in forest management.

The results of this study are not easily transferred to another canopy without the use of models. It is necessary to consider the specific characteristics of an individual canopy and to adapt a suitable numerical model which has the ability to simulate stem flow, throughfall, canopy drainage and interception separately. Thereby, the simulation of canopy drainage and interception is most critical, i.e. to estimate the interception storage (capacity). Often, the interception storage is approximated by empirical interrelationships to the LAI. However, it is not only the LAI that is important: the structure of leaves also has a significant influence. Using a LAI scaling, the interception loss as percentage of the leaf area was considerable higher on Beech trees than on Spruce trees.

5 Estimation and Comparison of Site Water Budget at a Spruce and at a Beech Canopy – Evapotranspiration

5.1 Role of Evapotranspiration, Transpiration and Seepage in Site Water Budget

Evapotranspiration denotes the total of transpiration, interception and soil evaporation. The percentages of each component as well as the amounts of each component are determined by a multitude of abiotic and biotic parameters and are specific for an individual site and an individual canopy. In forests, transpiration and interception are most important (Dietz et al. 2007). However, the amount of transpiration and interceptions can be very different for different types of forests (Benecke 1984, Weihe 1984, Weihe 1985, Komatsu et al 2007).

Differences in transpiration and interception are mainly caused by characteristics of individual species of trees. So, structure of crowns and development of foliation are especially important for interception (Rutter et al. 1971, Gash 1979). Thereby, the development of foliation and the degree of foliation is a temporally variable parameter typically quantified in terms of LAI (leaf area index). So, the yearly course of foliation and the change of LAI are decisive for differences between deciduous and evergreen forests.

LAI is also an important parameter for transpiration because it correlates with photosynthetic activities, i.e. carbon gain and water loss through stomata. However, transpiration is also determined by the availability of water. In this context, the depth of roots and the distribution of roots in ground are decisive parameters. This means that the characteristic of root system determines the soil layers where water is available for plants. The root system is also important for infiltration, because roots are preferential flow paths (Ebermann 2010). So, the roots and the characteristic of roots affect the soil moisture and the distribution soil water in different soil layers.

In comparison to other types of vegetation, forest evapotranspiration is characterised by the multilayered structure of the forests (Barner 1987). In particular, the segmentation into area of crowns and understory distinguish forests from lower vegetation such as grassland or agricultural stands. In this context, transpiration and interception can be separated into transpiration and interception of crowns and transpiration and interception of understory.

The focus of this chapter is the investigation of evapotranspiration and transpiration at a Beech stand and at a Spruce stand. The same test sites were investigated as in the previous chapter (Chapter 4). However, the focus of Chapter 4 was the interception the net precipitation P_n. Thereby, P_n means the percentage of precipitation which becomes available for plants. The results showed that the interception was very similar at both sites (around one-third of precipitation according to meteorological standard). However, the actual amount and the actual percentage often differed significantly between individual events of precipitation or between individual months. Simplified, it was found that the amount and the percentage of interception decreased in comparison to the statistical average when decisive events of precipi-

tation were predominantly short events with high intensities of precipitation. However, the amount and the percentage increased when decisive events were predominantly long lasting events interrupted by many short drying periods.

In this chapter the same forests and the same test sites were investigated. However, the major focus was evapotranspiration and transpiration on a monthly time scale and on a spatial scale of canopy. The intention was to compare and to specify the behaviour and the characteristics of Beech and of Spruce forests, which are the most important forest types in Germany also economically (Benecke and Ellenberg 1986). The second intention of this study was to compare and to combine different methods of measurement. This means that the focus was to estimate components of evapotranspiration and of water balance which are not directly measurable at forest sites and at a spatial scale of canopy, e.g. these investigations are related to estimations of transpiration of understory, estimations of soil evaporation and estimations of tendencies of seepage.

In the context of combination of different measurements methods, measurements uncertainties and different scales of measurement became fundamentally important in interpretation and evaluation of results. So, special attention is given to investigations of measurement uncertainties at which the primary object is to assess the accuracy of monthly totals. It shows that the superposition of individual errors and reinforcing effects of different scales of measurement cause enormous uncertainties. In this context it is demonstrated that quantitative analyses of indirect estimated variables are often impossible. Thus the investigations are limited to qualitative analyses.

5.2 Material and Methods

5.2.1 Measurements and Investigation Periods

The most important data for this chapter are related to eddy-covariance (EC) measurements, sap flow measurements, measurements of soil moisture and to estimations of interception,. EC data were used for estimation of entire evapotranspiration as well as for approximation of canopy transpiration, which means the totality of transpiration of trees, transpiration of understory and soil evaporation. (The exact estimation of canopy transpiration is explained in Chapter 5.2.5 and Chapter 5.2.6.)

The test sites were identical to Chapter 4. The periods of investigation were defined by the availability of EC data at Beech site and were related to periods between April and October in 2006 and 2007. So, also the periods of investigation were identically to the periods in Chapter 4 which were used there for analyses at monthly scale. However, complete data series were not available before May 2006 at the Beech site.

Both periods represent two different weather scenarios. 2006 was characterized by an extreme hot and dry summer, with potential water shortages possible at the Spruce site in July. In contrast to this, the 2007 was significantly cooler and more humid (plenty of rain) with the exception of April which was characterised by a six-week long drought. However in general, water shortages were excludable for 2007.

Of special importance for evaluation and interpretation of data in this chapter is the winter storm *Kyrill* on January the 18th/19th 2007. This storm caused significant damage on trees at both sites. However, it was assessed that Spruce trees were more affected by the storm because of additional losses of needles. The needle loss is especially important because Spruce trees do not have the ability to renew their needles, whereas Beech trees have the ability to renew their leaves. In this way, it was assumed that the productivity is affected at the Spruce site for several years.

5.2.3 Addendum to Interception

The segmentation of precipitation and net precipitation were the focus of Chapter 4. Interception I was also estimated. However, the interception was secondary because percentage of precipitation available for plants was the main focus. In this chapter the focus is on evapotranspiration. So, the interception is of fundamental importance. It is notes that interception was estimated as the remainder between precipitation P and net precipitation P_n. Thereby, P_n was equal to the canopy drip at the Spruce site. However, P_n was the total of canopy drip and stem flow at the Beech site.

The uncertainties of interception I were determined by the superposition of measurement uncertainties of precipitation ΔP and measurement uncertainties of net precipitation ΔP_n. primarily, the uncertainties were consequences of wind effects or of moistening deficits (Richter 1995). A detailed derivation of the quantification of these uncertainties has already been given in Chapter 4.2.3 and Chapter 4.2.4. In context to this chapter, the range of uncertainties of interception is defined by the range between I_{min} and I_{max}. The probably minimum for interception I_{min} results by,

$$I_{\min} = P - \left(P_n + \Delta P_n\right) . \tag{5.1}$$

However, the probably maximum I_{max} results by,

$$I_{\max} = P + \Delta P - P_n . \tag{5.2}$$

5.2.3 Addendum to Sap Flow Measurements (Quantification of Uncertainties)

Sap flow measurements were used for estimation of transpiration of adult trees T_{SF}. The principle of measurement and the exact configuration of measurement devices have already been explained in Chapter 2.2.5. This chapter is related in particular to quantification of uncertainties in sap flow measurements.

Fundamentally there are three different reasons. One reason is related to actual measurement errors which are device errors and errors of installation. In this context, the correct installation of probes is especially important (Smith and Allen 1996, Köstner et al. 1998). So, significant errors occur when probes are not located correctly in the sapwood. Thereby, the ingrowing of probes is a special problem.

A second reason for uncertainties is caused by assumptions about the cumulative area of sapwood $A_{s,cum}$. In this context, it is noted that every tree and every forest stand is something

individual (Čermák et al. 2004). So, the estimation of cumulative area of sapwood $A_{s,cum}$ due to analyses of stem disks or due to the assignments from other stands causes unquantifiable uncertainties.

However, the major reason of uncertainties is related to the representativeness of sampled trees. There are significant variations in relation to age of tree, diameter of stem, area of crown, vitality and specific locality; the effects of these parameters are specific for each species of tree (Köstner et al. 1998). In context to basic laws of statistic, the representativeness of estimated transpiration T_{SF} increases with increasing number of sampled trees. Additionally, the representativeness is affected by the homogeneity of a forest. So, the representativeness is higher in a homogeneous stand than in a non-homogeneous stand.

According to Čermák et al. (2004), it is assumed that a sample of 20 trees is sufficient in a homogeneous forest (one species, identical age of trees, similar structure, similar habit, homogeneous soil) to reduce the uncertainty below 10 %. In this study, the uncertainty must be significantly higher because the number of sampled trees was only 8 at the Beech site and 9 at the Spruce site. This means that according to Čermák et al. (2004), that the uncertainty due to insufficient representativeness was around 12 % at both sites. However, there must also be other sources of uncertainty. In this way the total uncertainty was assumed by 15 % for sap flow measurements and estimated T_{SF} at both sites.

5.2.4 Estimation of Evapotranspiration and Application of EC Data

The eddy covariance (EC) method was used to measure the turbulence exchange between canopy and atmosphere. In particular, EC measurements were used to estimate the latent heat flux (energy equivalent of evapotranspiration) and the sensible heat flux at both sites. However, the direct measured latent heat flux (covariance between vertical wind speed and gas concentration) often failed in rainy periods or in periods of dewing at the Beech site. The reason was that water droplets or a water film at the open-path-gas analyzer disturbed the measurements of gas concentrations (water vapour and carbon dioxide). It was not possible to close failures in any period. However, the measurements of sensible heat flux (covariance between vertical wind speed and temperature) were widely unaffected by rain or dew. So, the data of sensible heat flux were still available. In this way it was possible to estimate the latent heat flux and the evapotranspiration as remainder of energy balance,

$$LE = R_N - G - H - \Delta S \ . \qquad (5.3)$$

Thereby this means: LE, latent heat flux (as equivalent of evapotranspiration); R_N, net radiation; G, soil heat flux; H, sensible heat flux; and ΔS, total change of energy storage within the canopy.

At the Spruce site, the direct measurements of latent heat flux were widely unaffected by rain or dew because of the closed-path-system used. However, the evapotranspiration was also estimated as remainder of energy balance at the Spruce site to get consistent data sets. The evapotranspiration ET results finally by transformation of latent heat into water equivalent.

The total change of energy storage ΔS within the canopy is the sum of: storage change due to changing air temperature ΔS_h; storage change due to changing air humidity ΔS_l; storage change due to changing biomass temperature ΔS_b; and storage change due to photosynthesis and respiration. However, the storage change due to photosynthesis and respiration can be neglected because of low amounts (Bernhofer et al. 2002). The equations for all considered components of storage change ΔS are:

$$\Delta S_h = \rho_a \, c_P \, z_m \frac{\Delta T_a}{\Delta t} \; ; \tag{5.4}$$

$$\Delta S_l = L \, z_m \frac{\Delta \rho_v}{\Delta t} \; ; \tag{5.5}$$

$$\Delta S_b = m_b \, c_b \frac{\Delta T_c}{\Delta t} \; . \tag{5.6}$$

Thereby: ρ_a, the air density (≈ 1.2 kg m^{-3}); c_p, the specific heat capacity of air (≈ 1005 J kg^{-1} K^{-1}); z_m, the height of measurements; ΔT_a, the change of air temperature in time step Δt; L, the latent heat of evaporation ($\approx 2.5\ 10^6$ J kg^{-1}); $\Delta\rho_v$, the change of absolute humidity in time step Δt; m_b, the biomass related to base area; c_b, the specific heat capacity of biomass; and T_c, the change of biomass temperature in time step Δt. The biomass temperature was not measured, but it can be equalised to measured soil temperature at 2 cm depth. The specific heat capacity of biomass c_b as well as the total amount of biomass m_b was assumed according to Bernhofer et al (2002) by $c_b = 1.7\ 10^3$ J kg^{-1} K^{-1} and by $m_b = 22.1$ kg m^{-2} for the Spruce site and $m_b = 24.7$ kg m^{-2} for the Beech site.

The estimated LE and estimated ET was significantly affected by ΔS on half-hourly time scale. The typical maxima of ΔS were greater than 50 W m^{-2} in some periods. However, the effects of ΔS were insignificant and negligible on daily or monthly time scale because of averaging and compensation effects.

5.2.3 Accuracy of Estimated Evapotranspiration

A critical point is related to the quantification of uncertainties of EC data. EC data are affected by two completely different types of uncertainties. The first type is related to the footprint. The footprint varied permanently due to variations of wind speed, wind direction and atmospheric stratification. There is no serious method to locate the exact footprint of any individual time step within an entire period of investigation. Thus it was not possible to approximate exactly all uncertainties caused by changing footprint. However, the canopies were fairly homogenous in the surrounding area of EC system devices at both sites. So, it was assumed that effects due to changes of footprints were small. However, those effects were not excludable, especially in dry periods when a significant heterogeneity of soil moisture was observed at both sites.

The other type of uncertainties is related to actual uncertainties of measurement. These uncertainties are also not exactly quantifiable. In particular, it is not possible to quantify the uncer-

tainties due to classical error propagations because of too complex algorithms of flux processing (Foken 2006). In Chapter 6, a serious way is shown for the approximation of uncertainties on monthly scale. However, this method requires the direct measured latent heat flux, which was not available at the Beech site. So, a simplified and rougher method was used in this chapter. In principle, the uncertainties were determined by systematic errors of measured net radiation and systematic errors of measured sensible heat flux. However, the systematic uncertainties of storage and soil heat flux were neglected because of low absolute values and of compensation effects on monthly time scale.

The uncertainties of net radiation were specified according to producer information (Kipp & Zonen 2008) for the measurement device used (CNR1) by ± 10 % for daily values. Potential offset errors are noted as they become especially important in monthly totals. For example, an offset of 5 W m^{-2} causes an error of about ± 0.2 mm in daily totals of evapotranspiration, at which uncertainty is added up to ± 5 mm in monthly totals. Thereby, offset errors of about ± 10 W m^{-2} are not untypical.

Exact quantifications of systematic errors in measurements of sensible heat flux H (and also in measurements of latent heat flux LE) are still unsolved problems. According to Mauder et al. (2006) and Foken (2006), an uncertainty of 20 % was assumed for H, at which exactly this uncertainty was related to the complete uncertainty of the term H + G + ΔS. It must be considered that measured fluxes (both H and LE) typically underestimate the actual fluxes because of spectral attenuation (both high frequency and low frequency) and of non-considered advective transport processes. Finally, the uncertainty of evapotranspiration ET was assumed by,

$$ET - \frac{1}{L}\left(0.1\left|R_n\right| + 0.2\left|H\right|\right) < ET < ET + \frac{1}{L}\left(0.1\left|R_n\right|\right). \tag{5.7}$$

5.2.4 Aerodynamic Conductance and Canopy Conductance

Big Leaf Models are widely used approaches for the estimation of transpiration or rather for the estimation of sum of transpiration and soil evaporation. In this study, an inverse solution was used for the estimation of transpiration from EC data. The fundamental of Big Leaf Models is Penman's approach (Penman 1948) for description of distribution of available energy AE into latent heat flux LE and into sensible heat flux H. The derivation of basic equation and the required assumptions were explained in Monteith and Unsworth (1990). The given basic equation was,

$$ET = \frac{1}{L} \cdot \frac{\Delta_e\, AE + g_a\, \rho_a\, c_p\, VPD}{\Delta_e + \gamma\left(1 + \frac{g_a}{g_c}\right)} \tag{5.8}$$

Thereby: VPD, the saturation deficit for water vapour in air; Δ_e, the slope of curve of water vapour saturation; g_a, the aerodynamic conductance; and g_c, the canopy conductance. However, this equation is exact only for low canopies such as grassland and agricultural plants. In

the case of forests, the terms of energy storage ΔS_h (5.4) and ΔS_l (5.5) and ΔS_b (5.6) must be considered additionally. Thereby, ΔS_l was added to LE. However, ΔS_h and ΔS_l were added to available energy AE.

The aerodynamic conductance g_a and its reciprocal (the aerodynamic resistance r_a) are quantities to describe the gas exchange between air within canopy and upper air layers. The calculation of aerodynamic conductance was done by,

$$g_a = \frac{u^{*2}}{u} \quad . \tag{5.9}$$

Where u* means the friction velocity and u means the horizontal wind speed. However, by definition, this aerodynamic conductance is the aerodynamic conductance of momentum flux and is not the aerodynamic conductance of latent heat flux (Monteith and Unsworth 1990). But the difference between aerodynamic conductance of momentum flux and aerodynamic conductance of latent heat flux is small and is negligible in context to unavoidable measurement errors. From another perspective the actual resistance to describe gas exchange between canopy air and atmosphere is the sum of two independent resistances: one to describe turbulent transport and one to describe transport through viscous sublayer (Jensen and Hummelshøj 1995). However, the resistance which characterises the transport through the viscous sublayer is often (also here) neglected and is seen as part of canopy conductance (Monteith and Unsworth 1990).

The canopy conductance g_c is a vegetation specific parameter to describe the plant physiological behaviour. The canopy conductance primarily quantifies the interaction between transpiration and meteorological conditions. Secondly it describes the interaction between transpiration and availability of (soil) water (Granier et al 2000). The estimation of canopy conductance is possible by a rearrangement of the equation (5.8) to,

$$g_c = \frac{g_a}{\frac{\Delta_e}{\gamma L \cdot ET}\left(AE - L \cdot ET + g_a \rho_a c_p VPD\right) - 1} \quad . \tag{5.10}$$

5.2.5 Estimation of Transpiration on the Basis of EC Measurements (T_{EC})

Equation (5.10) was fundamental for separation of periods of transpiration and periods of interception in EC data. In this way, it was fundamental for the estimation of transpiration on the basis of EC measurements T_{EC}. The estimation of T_{EC} had two purposes:

(i) It was possible to estimate the complete transpiration of canopy, which means the sum of transpiration of adult trees and transpiration of understory. In this context, it is noted that actually the soil evaporation was also included. But, the actual soil evaporation in terms of evaporation out of soil matrix was small. However, interception of soil and litter was excluded in T_{EC}.

(ii) T_{EC} was the spatial average of the footprint of the EC system device. Thus T_{EC} was a good quantity for description of total behaviour of canopy; it was possible to average and compensate special effects of smaller scales of measurement.

The algorism for estimation of T_{EC} starts with the separation of periods (half-hourly data sets) when transpiration is categorically excludable. That means night-time and periods with strong interception. So all periods are excluded when photosynthetic active radiation PAR was smaller than 15 µmol m^{-2} s^{-1} and water vapour saturation deficits VPD was smaller than 1 hPa.

Afterwards the canopy conductance g_c is estimated from EC data of remaining periods. It was found that a threshold of g_c = 20 mm s^{-1} is a good separator between periods with predominate transpiration (dry periods) and periods with predominant interception (wet periods). Thereby, the threshold of g_c = 20 mms^{-1} was fixed according to observed maxima of canopy conductance which occurred in dry periods with high solar irradiation and good water supply of canopy. Finally, the monthly total of T_{EC} is the sum of measured ET within all dry periods of month.

5.2.6 Accuracy of Estimated T_{EC}

The described algorithm to separate periods with predominant transpiration (dry periods) and periods with predominant interception (wet periods) failed in individual half hourly data sets. However, these failures were random. So, they were compensated in monthly totals. In that way, the uncertainty of T_{EC} was basically determined by systematic uncertainties of EC measurements and measurements of net radiation R_N. In principle, the range of uncertainty of T_{EC} was defined by the same assumptions like uncertainty of evapotranspiration ET (H ~ 20 %; R_N ~ 10 %).

In the case of ET it was possible to relate the uncertainties directly to monthly totals. But, this proceeding is not possible for T_{EC}, because T_{EC} is only defined in dry periods. Thus it was necessary to estimate the uncertainty of T_{EC} on basis of individual half hourly data sets. It must be considered that the uncertainty of EC data can be enormous in half hourly data sets and can be far away from assumptions (H ~ 20 %; R_N ~ 10 %). However, it is assumed that these quantifications describe the typical uncertainties. So, it is possible to use them for quantification of average uncertainty of half hourly data sets.

The uncertainty of monthly T_{EC} results by superposition of uncertainties of all half hourly data when transpiration is assumed for the specific data set. This means that only dry periods (VPD ≥ 1 hPa, PAR ≥ 15 µmol m^{-2} s^{-1}, g_c < 20 mm s^{-1}) are considered for the approximation of uncertainty of T_{EC}. However, it must also be considered that the uncertainty of ET also affects the separation between wet and dry periods. So the range of uncertainty of ET data must be checked for correct separation on basis of half-hourly data sets.

In detail, the range of uncertainty of T_{EC} is defined due to the range between probable minimum $T_{EC,min}$ and probable maximum $T_{EC,max}$. To estimate $T_{EC,min}$ and $T_{EC,max}$, all periods with VPD ≥ 1 hPa and PAR ≥ 15 µmol m^{-2} s^{-1} are selected. However, all other periods are ex-

cluded because transpiration is excludable categorically and uncertainties of PAR and VPD are negligible.

Afterwards the probable minimum of evapotranspiration ET_{min} and the probable maximum of evapotranspiration ET_{max} are calculated for selected periods. Thereby, an uncertainty of ± 10 % was assumed for R_N and an uncertainty of ± 20 % was assumed for H. It is noted that underestimations as well as overestimations of H are possible at a time scale of half hours; additive as well as subtractive differences of H must be considered. Finally, the potential limits of transpiration T_{pot} must be calculated and checked at which T_{pot} is calculated by usage of equation (5.8) and $g_c = 20$ mm s^{-1}. In this way, $T_{EC,\,min}$ and $T_{EC,\,max}$ are quantifiable by selection of one of three possible cases:

$$T_{pot} < ET_{min} \quad \rightarrow \quad T_{EC,min} = 0\text{mm};\ T_{EC,max} = 0\text{mm} \tag{5.11a}$$

$$ET_{min} \leq T_{pot} < ET_{max} \quad \rightarrow \quad T_{EC,min} = 0\text{mm};\ T_{EC,max} = T_{pot} \tag{5.11b}$$

$$ET_{max} \leq T_{pot} \quad \rightarrow \quad T_{EC,min} = ET_{min};\ T_{EC,max} = ET_{max}\ . \tag{5.11c}$$

The first case (5.11a) means the situation when the lower bound of ET (ET_{min}) was greater than the potential maximum of transpiration T_{pot}. In this case, the restriction for transpiration ($g_c \leq 20$ mm s^{-1}) is injured and the complete range of ET (range between ET_{min} and ET_{max}) is outside of the probable range of transpiration. So, T_{EC}, $T_{EC,min}$ and $T_{EC,max}$ must be set to 0 mm.

In the second case (5.11b), the restriction for transpiration ($g_c \leq 20$ mm s^{-1}) is satisfied by ET_{min}. But the restriction is not satisfied by ET_{max}. So, the minimum $T_{EC,min}$ is set 0 mm, because the upper range of ET injures the restriction for transpiration. Thus, the range of T_{EC} starts with 0 mm to consider the overshooting of ET_{max}. However, ET_{min} is within range of transpiration. So, the upper bound of T_{EC} ($T_{EC,max}$) is represented by T_{pot}.

In the third case (5.11c), T_{pot} is greater than ET_{max}. So, the complete range between ET_{min} and ET_{max} satisfies the restrictions for transpiration. Thus, $T_{EC,min}$ and $T_{EC,max}$ was equalised to ET_{min} and ET_{max}.

5.2.7 Approximation of Soil Evaporation E_S and Estimation of Canopy Transpiration T_C

Besides T_{EC}, the difference between measured evapotranspiration (EC measurements) and estimated interception is a second way to estimate the complete transpiration, which means sum of transpiration of adult trees and transpiration of understory. However, this method does not exclude the interception of understory and litter as opposed to T_{EC}. But, due to integration of sap flow measurements (transpiration of adult trees T_{SF}) it is possible to estimate the evapotranspiration of understory and soil E_S by,

$$E_s = ET - I - T_{SF}\ . \tag{5.12}$$

This method failed in some months because of measurement uncertainties and scaling problems. This means that equation (5.12) caused negative numbers of E_S because the sum of T_{SF}

and I was greater than ET. In those cases, E_S was set to 0 mm to ensure the physical plausibility.

The uncertainty of E_S is caused by uncertainties of EC measurements ΔET, uncertainties of sap flow measurements ΔT_{SF} and uncertainties of precipitation ΔP and net precipitation ΔP_n. So, the range of E_S is defined by the range between upper limit $E_{S,max}$,

$$E_{S,max} = E_S + \Delta ET + \Delta T_{SF} + \Delta P_n \ , \tag{5.13a}$$

and lower limit $E_{S,min}$,

$$E_{S,min} = E_S - \Delta ET - \Delta T_{SF} - \Delta P \ . \tag{5.13b}$$

However, the request for physical plausibility ($E_S \geq 0$ mm) must be ensured in context to $E_{S,min}$.

There are two independent methods for approximation of canopy transpiration T_C. Method 1 means the estimation on basis of EC data with the help of an inverse solution of a Big Leaf Model. However, method 2 means the sum of T_{SF} and E_S. The combination of both methods has the ability to improve the fidelity of estimated canopy transpiration T_C. This means that it is possible to limit the range of uncertainties through combination of both methods. In detail, the actual canopy transpiration must be within the overlap of uncertainties of both methods. In that way it is possible to determine the range between probable minimum of T_C ($T_{C,min}$) and a probable maximum of T_C ($T_{C,max}$). However, it is not possible to define or to declare a central or reference value of T_C.

5.2.8 Estimation of Seepage and Closure of Water Balance

Classical measurements of runoff due to water gauges were not possible at the test sites because surface runoff did not occur. Also, a regionalisation of runoff from ambient catchments was excluded because all available water gauges were too far from test sites. However, regionalisation was also excluded due to the fact that regionalisation would blur the special characteristic of a site. In this context, the change of scale from canopy to catchment would already compensate and average special phenomena. So it was only possible to approximate the runoff as remainder of water balance,

$$R = P_n - T_C - \Delta\Theta \ . \tag{5.14}$$

The input is represented by the net precipitation P_n. Parts of output are represented by canopy transpiration T_C and change of water storage $\Delta\Theta$. The storage term $\Delta\Theta$ became especially important because of the short scale of time (months).

It was only possible to estimate water storage in upper soil layers with available equipment. However, the water storage in deeper layer and especial the storage in lithofacies were not estimable. In this context, the investigations are restricted to upper soil layers. In detail, the storage term is related to the change of measured soil moisture Θ within the upper 50 cm soil, which correspond to the main rooting depth. Thereby, the following conventions were used: a

negative $\Delta\Theta$ means the soil water reservoir is discharged; however, a positive $\Delta\Theta$ means the soil water reservoir is charged.

In this way the effects of geological properties (lithofacies) are excluded. Thus the estimated remainder of water balance is rather the seepage than the actual runoff. However, the estimated seepage holds the availability to compare both sites directly and without effects of geology, averaging, and regionalisation.

A critical point is related to measurements of soil moisture and estimations of $\Delta\Theta$. Thereby, the spatial representativeness is the major problem which causes significant and important uncertainties at canopy scale. It was not possible to quantify these effects. However, it was found that the measured soil moisture was a good indicator for water stress of plant. Thus it was possible to use the estimated soil water storage for qualitative (not for quantitative) evaluations of water supply. Furthermore, in context to seepage, it means quantitative analyses are excluded because of missing spatial representativeness. However, qualitative evaluations and approximation of tendencies of seepage are still possible.

5.3 Results and Discussion

5.3.1 Evapotranspiration

Evapotranspiration ET as sum of transpiration, interception and soil evaporation was measured with the EC method. Rather, the complete atmospheric exchange of water vapour was measured by using the EC method. So, the atmospheric inputs of water vapour were also included and considered in estimated ET by EC method. However, the atmospheric inputs (predominantly dew) were small and were negligible in the water balance. In particular, the inputs were insignificant in context to potential uncertainties of measurements.

The measured evapotranspiration ET as well as the associated ranges of uncertainty are shown in Figure 5.1 for 2006 and in Figure 5.2 for 2007. The approximated uncertainty of monthly ET was maximally around one-third of estimated reference as a consequence of superposition of uncertainties of H and R_N. Furthermore, Figure 5.1 and Figure 5.2 show: the transpiration, which was measured via sap flow measurements T_{SF}, and the estimated interception I as stapled bars with associated uncertainties for comparison with ET. Thereby, it is noted that the shown uncertainty is related to the totality of $I + T_{SF}$.

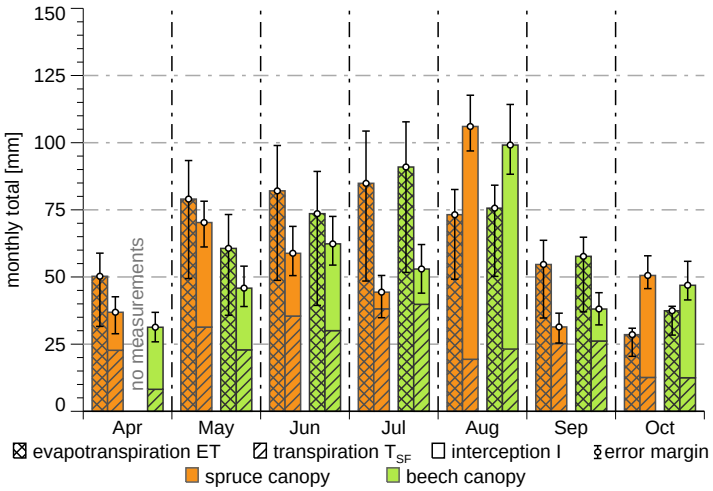

Figure 5.1 Monthly sums of evapotranspiration *ET*, transpiration T_{SF} (sap flow measurements) and interception *I* in 2006 (In April no EC-data available)

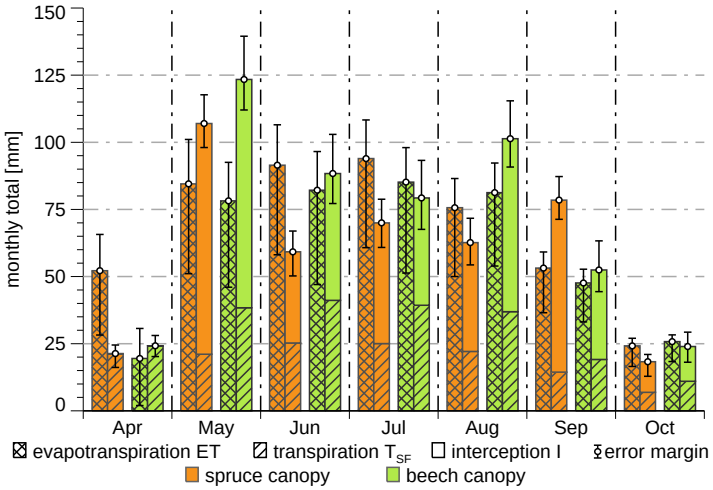

Figure 5.2 Monthly sums of evapotranspiration *ET*, transpiration T_{SF} (sap flow measurements) and interception *I* in 2007

The estimated monthly sums of ET were very similar at both sites. Significant differences were only in May 2006 and April 2007, when ET was lower at the Beech site than at the Spruce site. However, these differences were only caused by the later start of the growing season and so by incomplete foliation of Beech trees in spring. But, the differences of monthly ET were small between both sites related to the general behaviour. Thereby, typical yearly courses of ET were observable which were correlated to incoming solar radiation. In this way, ET started with low values in spring. It had the maxima in early summer and it decreased in autumn. The highest monthly values of ET occurred in June and July at both sites and in both periods.

The periods when complete foliation was assumable for Beech (June until September), were especially interesting because it was possible to compare both sites directly. The sums of ET for periods June until September were almost identical at both sites. But also the sums of both years were very similar. So, the sums of ET for period June until September were 295 mm at the Spruce site and 298 mm at the Beech site in 2006, and were 314 mm at the Spruce site and

296 mm at the Beech site in 2007. That means the difference between the Beech site and the Spruce site was only 3 mm in 2006 and was 18 mm in 2007. Related to the average of both sites, it means the difference was around 1 % in 2006 and around 6 % in 2007.

5.3.2 Transpiration of Adult Trees

The transpiration of adult trees T_{SF} (sap flow measurements) had a different characteristic than ET. So, T_{SF} was fairly similar at the Beech site and the Spruce site in 2006 with the exception of April. T_{SF} was significantly lower at the Beech site than at the Spruce site in April 2006 because growing season had not started at the Beech site. (The start of foliation was April the 23rd and foliation was almost completed by May the 3rd in 2006.) However, in contrast to 2006, T_{SF} was significantly higher at the Beech site than at the Spruce site in the complete period 2007. This was especially interesting related to April 2007. There, T_{SF} was higher at the Beech site than at the Spruce site. However, Beech trees were not yet foliated at beginning of April. (The start of foliation was April the 13th and full foliation was reached approximately by April the 20th.)

The comparison of periods showed that the monthly totals of T_{SF} were nearly equal at the Beech site in both periods or were only insignificant higher in 2007 than in 2006, with the exception of April and May. (Differences in April and May were caused by the later start of growing season and later start of foliation in 2006.) The sums of the period when complete foliation was assumed for Beech trees (June until September) were 119 mm in 2006 and 136 mm in 2007. However, the comparison of periods showed other results at the Spruce site. Here, the monthly totals of T_{SF} were significant higher in 2006 than in 2007. It is noted that these effects were also related to months when water shortage was assumed at the Spruce site (July 2006 and September 2006). The sums of the period (June until September) were 118 mm in 2006, but only 87 mm in 2007. That means T_{SF} of Spruces was always higher in 2006 than in 2007, although the soil moisture was higher and so the water supply was better in 2007.

5.3.3 Evaluation of Differences between the Beech and the Spruce Sites Related ET and T_{SF}

The different characteristic of T_{SF} between Beech and Spruce site in 2006 and 2007 had probably two reasons. One reason (i) was the winter storm *Kyrill*, which damaged and affected the trees significantly at both sites. Thereby, the injuries of bark and the losses of twigs were comparable at both sites. However, the losses of needles were an additional heavy damage exclusively on coniferous trees; therefore the coniferous trees at the Spruce site were more affected by the storm than the deciduous trees at the Beech site. Another point is related to injuries of roots, sap wood and vessels. Also in this context, it is assumed that Spruce trees were more affected than Beech trees. It is assumable, Spruce trees were more swayed because of a larger area of attack than skinny Beech trees. So, the heavy injuries of Spruce trees were probably the main reason for the reduction of transpiration T_{SF} at the Spruce site in 2007.

The other reason (ii) is related to soil moisture Θ and water supply of canopies. So, Θ was significant higher in 2007 than 2006. Furthermore Θ was higher at the Beech site than at the Spruce site. That means, the water supply was better in period 2007 than in period 2006, and was better at the Beech site than at the Spruce site. In this context, damage to Beech trees was not as severe as to Spruce trees. So, effects of storm damage at the Beech site were compensated by a better water supply. However, the storm damage was too heavy than compensable by better water supply at the Spruce site. Additionally, the water supply was worse at the Spruce site than at the Beech site.

It was conspicuous that the differences were observable between both sites and both periods in data estimated via sap flow T_{SF}. But, differences were not observable in EC data. This circumstance pointed to different spatial scales between EC measurements and sap flow measurements. However, different scales between EC measurements and measurements of interception were less important because important parameters such as height, age, leaf area index (LAI) and degree of crown closure (and sky view coefficient) were widely similar within the footprint. But, a potential heterogeneity of interception within the footprint of EC system device would also never explain the differences. In this context, systematic differences were not found in data of inception either related to sites or related to periods.

However, differences of transpiration are quite possible within the footprint. So, significant differences of soil moisture were found within the footprint (manual measurements). This means that the water supply was very heterogenic for different parts of canopy. In this way, it is assumed that differences between sap flow measurements and EC measurements are caused by heterogenic canopy water supply. In another context, it was also found (visual evaluation) that the effects of winter storm *Kyrill* were different within the footprint at the Spruce site. So, it is possible that the footprint of EC measurements included areas at the Spruce site which were less affected by storm damage.

Another aspect is related to principles of measurements. So, the transpiration of adult trees was only measured with sap flow measurements. But, the transpiration of understory and in particular the transpiration of the young growth Beech trees at the Spruce site were not measured. However, EC measurement included both transpiration of adult trees and transpiration of understory. So, there was also another reason for the different characteristics between sap flow measurements and EC measurements at the Spruce site. The transpiration of understory and, in particular, the transpiration of young growth Beech was a significant component of evapotranspiration ET at the Spruce site. After the storm, the understory and the young growth Beech received more radiation because of damage and needle loss on adult trees. In this way, the transpiration of understory increased. This means that the decreased transpiration of adult trees was compensated by a higher transpiration of understory at the Spruce site in 2007. So, ET was similar because of compensation effects in 2006 and in 2007.

5.3.4 Estimation of Soil Evaporation E_S

A major point was the estimation of water balance components which were not directly measureable due to the combination of different measurement methods. The combination of measured evapotranspiration ET (eddy covariance), measured transpiration of trees T_{SF} (sap flow) and estimated interception I was used to close the evaporation balance and was used to approximate soil evaporation E_S by,

$$E_S = ET - T - I \quad . \tag{5.15}$$

However, E_S means exactly the totally of soil evaporation, transpiration of understory, and interception of understory and interception of litter.

It was visible in Figure 5.1 and Figure 5.2 that there were often significant gaps between measured ET and estimated sum of I and T_{SF}. These gaps were not explainable completely by soil evaporation or by interception of understory. However, these gaps were also not satisfactorily explainable only by uncertainties of measurement. In particular, situations were not interpretable when the measured evapotranspiration ET was smaller than the sum of transpiration T_{SF} and interception I. These negative gaps occurred at both sites in August 2006, October 2006, May 2007 and September 2007 and occurred only at the Beech site in June 2007 and in August 2007.

The big positive gaps in July 2006 and September 2006 were difficult to understand at the Beech site. Transpiration of understory was ignorable at the Beech site because an understory was not present. In this way, the only reasons for gaps between ET and sum of T_{SF} and I were actual soil evaporation and interception of litter. But the gaps were almost identical between the Beech site and the Spruce site. However, an understory was present at the Spruce site, which was responsible for a high evapotranspiration of understory. In another context, the gaps (July 2006, September 2006) were in dry periods with less precipitation and less net precipitation. So, it was assessed that interception of soil and litter was small. The only component of evapotranspiration was actual soil evaporation, which remained for gaps (July 2006, September 2006). However, actual soil evaporation is too small to be responsible for these gaps.

A logical explication was given by different scales of measurement between EC measurements and measurements of sap flow and interception. The thesis was that EC data included or included partly signals from areas which were better supplied with water than the area which was investigated by sap flow measurements. So, the observed gaps in evaporation balance (5.15) were caused by spatial heterogeneity of water supply of canopies. This means that the gaps are related to potential scaling problems between EC measurements and sap flow measurements.

Consequently, the primary problem is related to different scales between EC measurements and sap flow measurements. Secondly, the large uncertainties of ET and T_{SF} cause another major problem. However, effects of different scales between interception and EC data are less

important. Also, effects of measurement uncertainties of interception are ignorable. A special approach for minimizing scaling effects is given in Chapter 5.3.8. In this context, a method is also given for minimizing effects due to measurement uncertainties.

5.3.5 Investigations of Aerodynamic Conductance and Canopy Conductance

The estimation of aerodynamic conductance g_a and canopy conductance g_c was a necessary precondition for the inverse solution of Big Leave Model and for the estimation of canopy transpiration T_{EC}. The estimated aerodynamic conductance g_a is shown in Figure 5.3. It shows the arithmetic average as well as the standard deviation of all available data.

The estimated aerodynamic conductance g_a was always higher at the Spruce site than at the Beech site with the exception of the spring months. So, the gas exchange between canopy and atmosphere was stronger at the Spruce site than at the Beech site in months when Beech trees were foliated. However, the gas exchange between canopy and atmosphere were stronger at Beech canopy when Beech trees were defoliated. In another aspect, g_a depends on predominant wind conditions within a period. In this way, higher wind speeds increased the aerodynamic conductance and so the gas exchange between canopy and atmosphere.

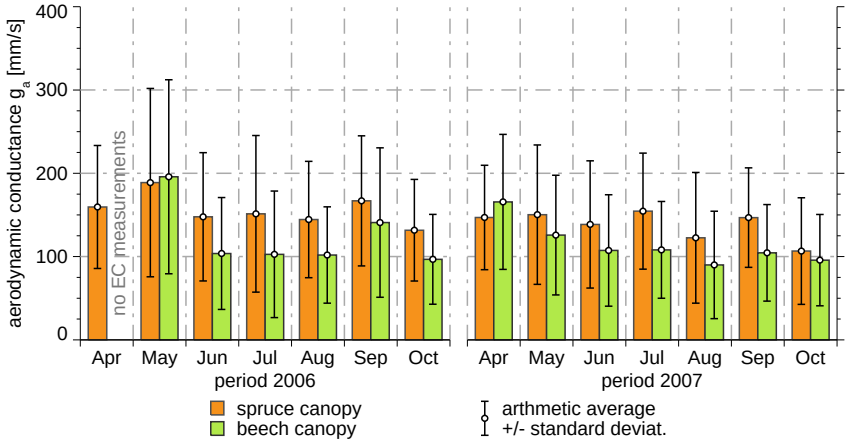

Figure 5.3 Arithmetic mean and standard derivation of aerodynamic conductance g_a derived from EC-measurements (left 2006, right 2007)

The estimated canopy conductance g_c is shown in Figure 5.4 for both sites. Analogous to aerodynamic conductance, it shows the arithmetic average and standard deviation. However, the data were limited to periods when evapotranspiration was dominated by transpiration (dry conditions). Further, the shown g_c were derived from EC data. In this way, the estimated g_c are related to the superposition of transpiration of adult trees, transpiration of understory and actual evaporation of soil.

The monthly values and the characteristic of g_c were very similar between both canopies with the exception of spring months, when Beech trees were not foliated completely. However, typical seasonal cycles were only observable at the Beech site in 2007. There g_c was low at the beginning of the growing season because of missing or incomplete foliation. Later, g_c increased and was maximally in June and July. In autumn, g_c decreased because of autumn colouring and fall of leaves. However, such a distinct seasonal cycle was not observable in 2006

and was never observed at the Spruce site. But, Spruce trees also lost old needles in autumn, which typically caused a decrease of g_c in autumn. Thereby, this characteristic was observable by comparison of months September and October.

The comparison of both periods showed that the canopy conductance g_c was in general lower in 2006 than in 2007 with the exceptions of August 2006 and May 2006. But, the exception of May 2006 was only relevant for the Spruce site, where g_c was significantly the lower in 2007 than in 2006. This effect was the direct consequence of low soil moisture at the Spruce site because of the previous drought in April 2007. However, this effect was also reinforced by effects of storm damage. At the Beech site, analogous effects were not observable because the drought in April did not affect the transpiration at the Beech site due to the later start of the growing season. Additional, the effect was blurred due to different starts of growing seasons between 2006 and 2007.

The general behaviour of g_c (with the exception of August) was a direct consequence of water supply. So, the low soil moisture forced trees to reduce transpiration in 2006 (especially in June and July), which was represented by a reduction of canopy conductance g_c. August 2006 was an interesting exception of general behaviour of periods. In this month, the soil moisture Θ increased rapidly due to above average precipitation; Θ was nearly on the same level as in 2007 (compare Figure 2.6). So, there was no need to reduce transpiration and g_c increased to almost the same level as 2007.

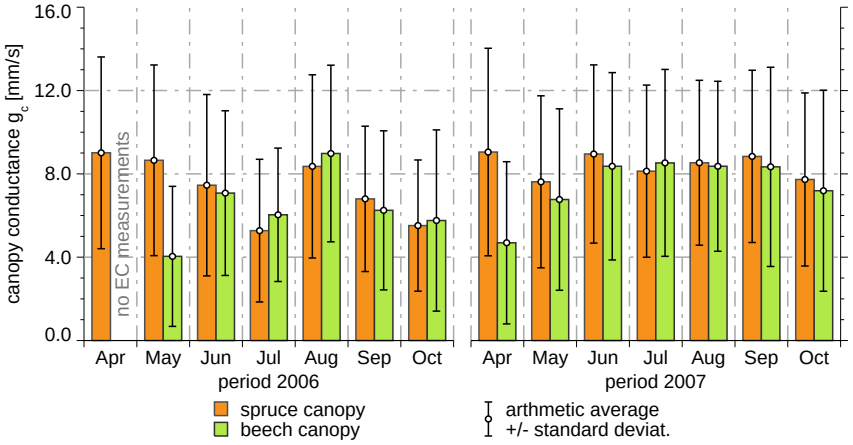

Figure 5.4 Arithmetic mean and standard derivation of canopy conductance g_c derived from EC-measurements (left site: 2006, right site 2007)

5.3.6 Comparison between T_{EC} and T_{SF}

The transpiration derived from EC measurements T_{EC} and the associated range of uncertainties are shown in Figure 5.5 (2006) and in Figure 5.6 (2007). Additionally, it shows the transpiration estimated by sap flow measurements T_{SF} and the soil evaporation E_S, which was estimated as the remainder of evaporation balance (5.15) for comparison. Thereby, the uncertainty shown is related to the sum of T_{SF} and E_S. The comparison between T_{EC} and sum of T_{SF} and E_S showed that both methods caused often very different results. However, the ranges of uncertainties of both methods overlap in any case. In this way, it was possible to locate the

probable range for canopy transpiration T_C, which is shown as red arrows in Figure 5.5 and Figure 5.6. Thereby, T_C means the total of transpiration (understory and adult trees) and actual soil evaporation. (A detailed discussion of T_C follows in chapter 5.3.8).

The estimated T_{EC} was mostly slightly higher at the Beech site than at the Spruce site in both periods of with exception of months when Beeches were not completely foliated. The higher T_{EC} at the Beech site was in conflict to T_{SF} in period 2006, when T_{SF} was almost similar at both sites. In detail, the conflict resulted from the following: T_{SF} was the represented transpiration of trees. But, T_{EC} was representative for the totality of transpiration of trees, transpiration of understory and actual soil evaporation. However, an understory did not exist at the Beech site. Further, it was assumed that the amount of actual soil evaporation was small and was negligible in comparison to transpiration of trees and transpiration of understory. In this way, T_{EC} should be almost identical to T_{SF} at the Beech site or should be only marginally different.

In contrast to the Beech site, an understory was distinct at the Spruce site. So, the transpiration of understory should be a significant part of canopy transpiration and in this way a significant part of T_{EC} at the Spruce site. A new conflict was caused between T_{EC} and T_{SF} related to the agreement of T_{SF} at both sites in 2006. In this context, T_{EC} should be higher at the Spruce site than at the Beech site because of additional transpiration of understory. However, the measurements results disagreed to this thesis and indicated a possible scaling problem between sap flow measurements and EC measurements.

In this context, the disagreements between T_{EC} and T_{SF} were especially conspicuous at the Beech site in July 2006. Here, the maximal difference occurred between T_{EC} and T_{SF}, which was 48.9 mm. This large difference is difficult to explain only by measurement uncertainties. Methodical uncertainties were excludable for T_{EC} in this month, because July 2006 was very dry. The measured precipitation was 37.7 mm at the Beech site, of which the net precipitation was 24.6 mm. The estimated interception was between 10 and 16 mm in relation to potential measurement uncertainties. So, the estimated T_{EC} of 87 mm and measured evapotranspiration ET of 93 mm were in close agreement in relation to estimated interception and in relation to typical uncertainties of measurement. However, the large amount of E_S was conspicuous in context to low net precipitation in July 2006. Hence, the former thesis was affirmed EC data included or included partly signals from areas which were better supplied with water than the area which was investigated by sap flow measurements. Further, different scales of measurements were more significant in dry than in more humid months.

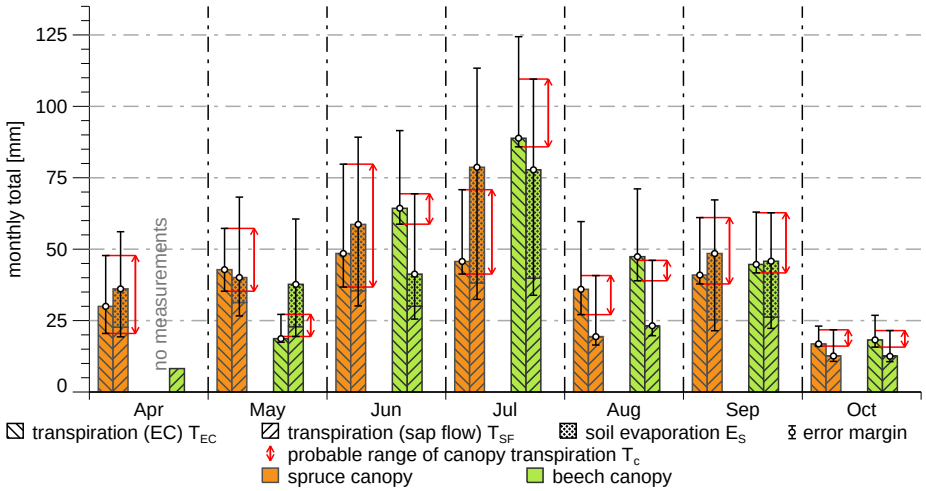

Figure 5.5 Transpiration estimated out of EC data T_{EC} and associated range of uncertainty; transpiration measured via sap flow measurements T_{SF} and approximated soil evaporation E_S (associated range of uncertainty is related to sum of T_{SF} and E_s); range of probable canopy transpiration T_C (period 2006)

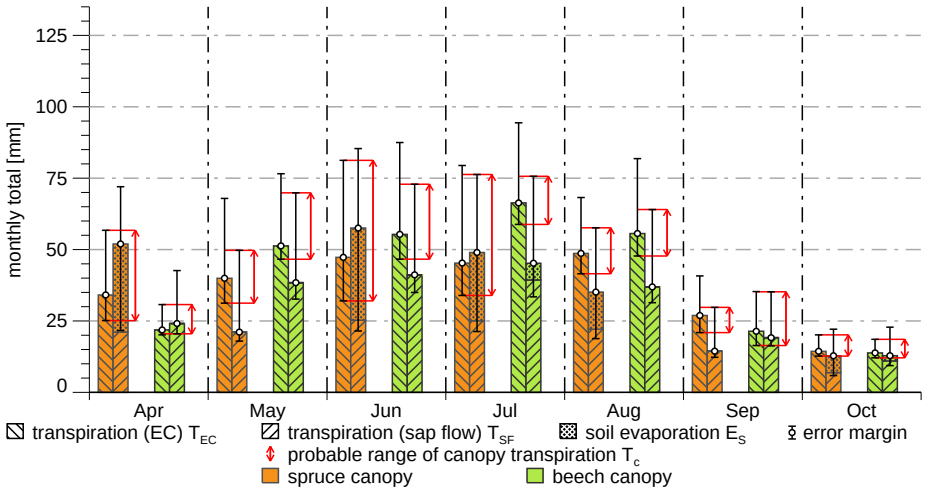

Figure 5.6 Transpiration estimated out of EC data T_{EC} and associated range of uncertainty; transpiration measured via sap flow measurements T_{SF} and approximated soil evaporation E_S (associated range of uncertainty is related to sum of T_{SF} and E_s); range of probable canopy transpiration T_C (period 2006)

5.3.7 Evaluation of Differences between T_{SF} and T_{EC}

Different scales of measurements made it difficult to compare both sites directly. In particular, quantitative analyses and evaluations were only possible in a restricted way. However, it was possible to characterise the general behaviour of both canopies. So, the difference between T_{EC} and T_{SF} clearly showed the effects of transpiration of understory and soil evaporation, which were visible in Figure 5.5 and Figure 5.6 as difference between both bars. (Please note: this statement is related to actual difference between T_{EC} and T_{SF} and is not related to shown bars of E_S.) So, the comparison between 2006 and 2007 showed an increase in understory transpiration at the Spruce site. This effect affirmed the former thesis: transpiration of understory (particularly transpiration of young growth Beech trees) increased due to more solar radiation in 2007, at which the increase of solar radiation was related to storm damage on

adult trees. However, there was no increase observable at the Beech site as opposed to the Spruce site.

The gaps between T_{SF} and T_{EC} were not explainable by transpiration of understory at the Beech site because an understory did not exist. However, the soil was covered by a thick litter layer. The litter (including the upper layer of humus) was a significant storage of net precipitation, which dispenses the water slowly via evaporation and seepage. So, the differences between T_{SF} and T_{EC} were explainable partly by the evaporation of litter. This means that the evaporation of litter had nearly the same role at the Beech site as the transpiration of understory at the Spruce site. In particular, the agreement between T_{SF} and T_{EC} in April 2007 confirmed this thesis. Here, the litter was desiccated because of the six week drought; the evaporation of litter was negligible in April 2007. Another good example was September 2006; this month was also characterised by very dry conditions. So, the measured precipitation was 26.4 mm, of which the net precipitation was 14.7 mm with an uncertainty of 2.2 mm. In that way, the estimated gap between T_{EC} and T_{SF} of about 18.5 was completely explainable by evaporation of net precipitation, which was infiltrated in the litter.

The maximal gap between T_{EC} and T_{SF} at the Beech site in July 2006 was not explainable by evaporation of litter, although it was a very dry month (the lowest soil moisture of investigation periods was measured this month). The difference between T_{EC} and T_{SF} was 48.9 mm. In that way, it was larger than estimated net precipitation (24.6 mm) and was even larger than measured precipitation (37.7 mm). This circumstance affirmed the thesis of different scales of measurement between sap flow measurements and EC measurements. However, the small gap between T_{EC} and T_{SF} at the Spruce site in July 2006 was simple to explain by decreased transpiration of understory due to low soil moisture. In particular, the upper layers of soil (up to depths of 10 cm) were extremely dry. So, the measured soil water content was below 4.5 % in these layers. In this way, the predominant grass did not have the availability to reach water and desiccated. This circumstance almost caused identical values of T_{EC} and T_{SF} at the Spruce site in July 2006.

5.3.8 Estimation of Canopy Transpiration T_C

The agreement between T_{EC} and sum of T_{SF} and E_S was very variable in individual months. However, there was an overlap between uncertainties of both methods in any month. Furthermore, the ranges of uncertainty of both methods were of the same magnitude. In this way, there were two almost independent and equivalent methods for the approximation canopy transpiration T_C. Thereby, T_C means the totally of transpiration of adult trees, transpiration of understory and soil evaporation. It was possible to improve fidelity of T_C due to the assumption that the actual T_C must to be within the range of overlap of both uncertainties. In that way, it was possible to approximate the probable range of canopy transpiration T_C. The probable minimum $T_{C,min}$ and probable maximum $T_{C,max}$ are marked by red arrows in Figure 5.5 and Figure 5.6.

The ranges of T_C (range between $T_{C,min}$ and $T_{C,max}$) were typically of the same magnitude at the Beech and the Spruce sites. Significant differences of T_C were only in months when Beech

trees were not foliated completely and in July 2006. So, the canopy transpiration T_C as sum of transpiration of adult trees, transpiration of understory and soil evaporation was similar at both sites under typical weather conditions in primary growing season (June until September).

However, T_C showed significant differences between the Beech site and the Spruce site under very dry and hot conditions like July 2006. It was not possible to clearly estimate the reason for these differences in July 2006 because T_{SF} and ET were almost identical at both sites in this month. In this context, the close agreement between T_{EC} and T_{SF} is conspicuous at the Spruce site, which seems to be plausible in context to reduced transpiration of understory and reduced soil evaporation under dry conditions. However, the differences between T_{EC} and T_{SF} are critical. In this way, an overestimation of measured ET and thereby an overestimation of approximated E_S seems to be the most plausible reason. In this context, the range of uncertainty of EC measurements is noted, which is visible in Figure 5.1 and Figure 5.2.

5.3.9 Closure of Water Balance at Spatial Scale of Canopy

The seepage R was estimated as the remainder of water balance (5.14). All estimated variables are shown in Figure 5.7 (2006) and Figure 5.8 (2007), at which inputs and outputs of water balance are confronted. The input was given by net precipitation P_n and discharge of soil water storage (negative number of $\Delta\Theta$). Thereby, it was observed that P_n was the predominant component of input with the exception of dry months (July 2006, September 2006 and April 2007). The measured components of output were the canopy transpiration T_C and the charge of soil water storage (positive number of $\Delta\Theta$). In this way, the change of soil water storage $\Delta\Theta$ was an input when the soil moisture Θ decreased, and was an output when soil moisture increased Θ.

The remaining gap between input and output was an approximation for seepage R. However, it was not possible to close the water balance and to estimate a plausible seepage in any month because of measurement uncertainties and scaling problems. So, the closure of water balance failed especially in dry months like July 2006, September 2006 and April 2007. It was assumed that the heterogeneity of soil moisture and so the heterogeneity of transpiration within the footprint of the EC system device were the major reasons.

However, the closure of water balance and approximated seepage were plausible in rainy months. The approximated minimums of seepage R_{min} are marked by solid rectangles in Figure 5.7 and Figure 5.8. In this context, R_{min} means the amount of seepage, which was probably not undershot within the footprint. The maxima of seepage R_{max} were marked by grey arrows. It is visible that uncertainties of measurement or different scales of measurement prevented a successful approximation of R_{min} in some months. In these months R_{min} was set to 0 mm. It was possible to approximate R_{max} in most months with exception of dry months (July 2006, September 2006 and April 2007).

The estimated values of R were affected by a high uncertainty. So, quantitative analyses of R were not possible. However, it was possible to approximate common tendencies. It was found that R_{max} was in the same magnitude at both sites in rainy months. However, R_{min} was only

plausible when the totality of input terms was higher than the totality of output terms. Thereby, it was conspicuous that R_{min} was almost identically between both sites in August 2006 and October 2006. However, an agreement of R_{min} was not found in 2007 because the net precipitation P_n was typically slightly higher at the Beech site than at the Spruce site in 2007.

The characteristic of R was completely different under dry conditions. So, the calculated seepage (predominately R_{min}) was negative and was set to 0 mm. In this context, it was assumed that the measured soil moisture did not represent the typical soil water storage and the typical change of soil water storage $\Delta\Theta$. The heterogeneity of soil moisture was more important for R under dry conditions than under wet conditions. However, the net precipitation P_n and the canopy transpiration T_C were similar at both sites and were also similar in months when estimated seepage and estimated $\Delta\Theta$ were different.

In this way, the characteristic of water balance and the amount of seepage were determined predominately by soil properties. Thereby, the heterogeneity of soil water storage and the restricted representativeness of soil moisture measurements were responsible for estimated variations of seepage. However, the composition of species was subordinate for estimated seepage under typical weather conditions. Significant differences occurred only in abnormal dry situations like July 2006. This means that the composition of trees affected the seepage only in extreme dry situations. However, this statement is related only to the growing season. It is assumed that the seepage is significant higher in winter months, when Beech tree are not foliated. Additionally, it is noted that this statement does not include any argument if the respective species of tree can grow on the respective site.

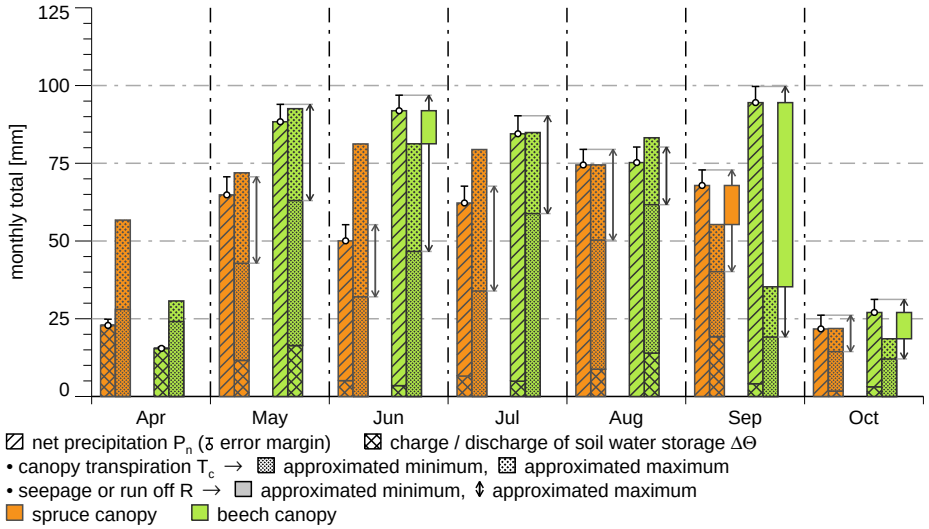

Figure 5.7 Confrontation of inputs and outputs of water balance and approximations of seepage (2006)

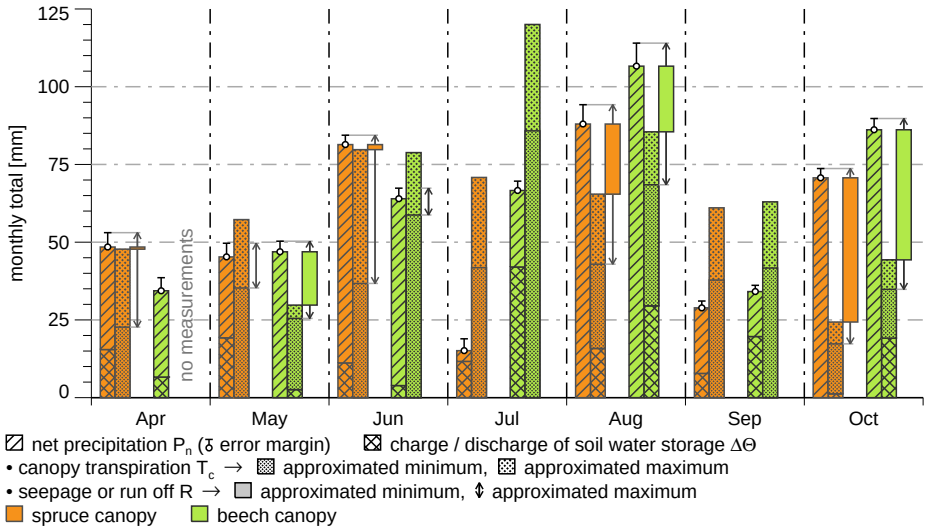

Figure 5.8 Confrontation of input and output of water balance and approximations of seepage (2007)

5.4 Concluding Remarks on Site Water Budget of Investigated Spruce and Beech Stand

The characteristic of evapotranspiration and transpiration were investigated at two different sites (a Beech canopy and a Spruce canopy) in two growing seasons. Complete data series were available from periods April until October of 2006 and of 2007. The weather conditions were very different in both periods; 2006 was characterized by an extreme hot and dry summer while, in contrast to this, 2007 was significantly cooler and wetter. A special event between the two investigation periods was the winter storm *Kyrill* on January the 18th/19th 2007. Although no trees were broken in the immediate surroundings, the stands were damaged heavily. It was found that the effects of *Kyrill* were more significant at the Spruce site than at the Beech site. However, effects were only found in transpiration of adult Spruce trees. But, effects were not detectable in data of interception and net precipitation (compare Chapter 4). It was assumed that the massive losses of needles were a major reason. But also injuries of roots, sap wood and vessels were potential reasons, which cause long lasting effects in water balance components.

The investigations were based on different micrometeorological methods for measuring of components of evapotranspiration. Sap flow measurements were used for the estimation of transpiration of adult trees; eddy covariance (EC) measurements were used to estimate complete evapotranspiration; and the interception was estimated as remainder between gross rain and net precipitation. Further, the canopy transpiration as totality of transpiration of trees and transpiration of understory was estimated by two almost independent methods. One method was an inverse solution of Big Leaf Model, whereas, the second method was based on balance closure between evapotranspiration, interception and transpiration of trees. It was possible to improve fidelity of canopy transpiration through the combination of both methods. Rather, it was possible to locate the probable range of canopy transpiration. Besides the estimation of components of evapotranspiration, the estimation of soil water storage was important and was approximated due to TDR-measurements.

The results of measurement showed that the transpiration of adult Spruce trees and the transpiration of adult Beech trees were almost identical in the growing season 2006. Differences were only in periods when Beech trees were not foliated completely. Thereby, significant differences were not even found in the extreme dry period like July 2006. However, the transpiration of Spruce trees decreased significantly after the winter storm *Kyrill*. So, the transpiration of adult trees was significant lower at the Spruce site than at the Beech site in 2007. In contrast to transpiration of adult trees, the complete canopy transpiration was almost identical in both investigation periods (including 2007) and was still similar at both sites. In this way, it was possible to detect an increase of transpiration of understory at the Spruce site in 2007. This means that the canopy transpiration stayed equal. However, the composition of canopy transpiration was changed. In this context, it was also found that the soil evaporation in terms of evaporation out of litter had nearly the same importance at the Beech site as transpiration of understory at the Spruce site.

From another perspective, the investigations dealt with measurement uncertainties and problems of scaling between different measurement methods. The measurements of soil moisture were related to single point. But also, sap flow measurements as well as estimations of interception were rather at a point scale than at an area in comparison to EC measurements. It was found that different scales of measurements became especially important in dry periods but they were less important in wet periods. So, the heterogeneity of soil properties caused a high variability of soil moisture particularly in dry periods, which reduced the representativeness of approximated change of soil water storage. But also, the representativeness of sap flow measurements was limited in dry periods because the heterogeneity of soil moisture affected the canopy water supply and consequently the transpiration of adult tree. However, water was not the limiting parameter in wet periods. In this way, the heterogeneity of soil moisture was unimportant for transpiration. This means that the transpiration was controlled by radiation in wet conditions.

Different scales of measurement and the superposition of measurement errors caused big problems in quantitative analyses. However, it was possible to estimate the common behaviour of water balance. So, it was possible to evaluate tendencies of seepage. It was found that there were not significant differences between both canopies under typical weather conditions within the growing season. Significant differences were only found between both canopies under extreme dry conditions (July 2006). So, the seepage was determined predominately by amount of net precipitation. However, the effects of vegetation were small and were only significant in droughts.

In summarization, the water balance and the individual components of water balance components were very similar at both sites. This means that it was not possible to find significant differences clearly caused by differences of vegetation. Thereby, major problems were unavoidable in uncertainties of measurement, the superposition of measurement uncertainties, the restricted spatial representativeness of measurements and different scales of measurement. These problems were often neglected in other studies, which predicted significant differences between Beech and Spruce stands. In this study, it was found that the differences between

Beech and Spruce were marginal within the growing season. In particular, the differences were insignificant in relation to typical tasks of water resources management. So, the small differences which were found between both sites were primary caused by different soil properties.

6 Influences of Measurement Uncertainties and Effects of Model Complexity on Results of Water Balance Simulations

6.1 Numerical Water Balance Simulations: Objectives, Methods and Uncertainties

In the former chapters, estimations and measurements of water balance components were the primary focus. But, exact measurements are typically not available for most sites. However, the exact knowledge of individual water balance components is a necessary precondition for successful and sustainable water resources management, farming and forestry. This knowledge is especially important in context of ongoing and future climate change in parts of Central Europe, with lower precipitation sums in summer months, more rainfall extremes, shorter periods with snow cover and a changing growing season (Niemand et al. 2005; Franke et al. 2006a; Franke et al. 2006b; Franke and Köstner 2007; IPCC, 2007).

Typically, the water balance and individual components of water balance are estimated with the help of numerical models. At present there are many different models for the simulation and estimation of water balance components. The models are quite different concerning concept, structure and complexity. On the one hand there are very complex models, which address all kinds of processes (e.g. interception, transpiration, snowmelt and soil water movement) separately and as exact as possible. On the other hand there are much simpler conceptual models or Black Box Models.

The focus of this chapter is the simulation and estimation of annual evapotranspiration ET_a and annual seepage R_a on sites in the low mountain range of the *Erzgebirge* (Ore Mountains, Germany). The test sites are three different stands: coniferous forest (Norway Spruce, *Picea abies*), grassland and agricultural land. These land uses are typically for the landscape of the *Erzgebirge*. In context to the water balance, ET_a is the component which is most controlled by climatic conditions and by the vegetation. So, ET_a is determined significantly by effects of vegetation in terms of growing season, depth of roots and interception storage capacity.

R_a defines the percentage of precipitation P, which percolates through the soils and runs off. In context to this study, R_a is related to water partitioning below to the rooting zone. So the storage term of the water balance equation is only related to the upper soil layers, which is negligible on the annual time scale. However, effects due to geological properties and storage in lithofacies can be excluded. Furthermore, surface runoff and other lateral components of runoff are also widely negligible at test sites because of flat terrain and high infiltration rates. In this way R_a can be equalized directly to annual the groundwater recharge and seepage.

A robust method for the approximation of ET_a and R_a are the hydro-pedotransfer functions (HPTFs) according to Wessolek et al. (2008), which are Black Box Models for the description of typical interrelationships between climate, soil, vegetation and expected annual evapotranspiration ET_a and annual seepage R_a respectively. The typical application of HPTFs is

founded in land planning and geography, where annual values are often needed for overview and categorization. In this context, the Hydrological Atlas of Germany (*Hydrologischer Atlas von Deutschland*) (Bundesanstalt für Gewässerkunde 2003), which is often used as a guideline for such applications, based on HPTFs. Hereby HPTFs bridge the scales from soil column (used for parameterization) to landscape (estimated ET_a and R_a) (Wessolek et al. 2008, Lin 2003).

This study investigates if (i) HPTFs are useable for the estimation of ET_a and R_a at canopy scale. That means, the area of investigation is less than 0.75 km² and is represented by the footprint of an eddy covariance system device, which provides the reference data. So, the reference for validation and evaluation is the measured evapotranspiration instead of runoff, which is typically used as a reference in hydrological investigations. Through the limitation to this small spatial scale, the effects of regionalization and generalization are minimized. Furthermore, effects due to hydrogeologic properties of lithofacies are also excluded, because the investigations are related only to the upper soil layers, which are involved in plant atmosphere interaction by root water uptake and soil evaporation.

Another point of investigation is related to the required input data and the parameterization of HPTFs. The HPTFs operate on an annual time scale. However, input data are necessary in a higher temporal resolution for the calculation of required FAO grass reference evapotranspiration ET_0 (Allen et al. 2006). Thereby, the required input data are typically available in daily resolution for most sites in Germany. The parameterization of HPTFs is very simple: Only the knowledge about vegetation and some soil properties are necessary. In contrast to this simple parameterization, the effort of parameterization is much higher for complex models. However, it is possible to reduce the effort of parameterization through applying guidelines and standard values in most cases. That means that the effort of parameterization can be reduced to the level of HPTFs. In this context, the question is posed: why not use a more complex model, when required input data are available and effort of parameterization is the same? This is expanded to the second question: (ii) Do more complex models deliver more exact results than HPTFs, when the parameterization is simplified to the level of HPTFs?

Representative for other complex models BROOK90 (Federer 2002) was chosen because the required input data are equal to HPTFs and the effort for parameterization can be equalized to HPTFs by simplification to standard and default parameters. So the account for identical parameterization is satisfied and it is possible to test, if BROOK90 as complex model delivers more exact results than HPTFs. In particular a test is made if the detailed description of running hydrological processes improves the accuracy of results on an annual time scale.

The third question (iii) which is posed deals with effects of measurements errors. Uncertainties resulting from regionalization and generalization cause well known problems. Also uncertainties resulting from vague parameters are well known. In this context, in particular the parameterization of soil causes often significant uncertainties because of high heterogeneity of soil properties. However, the investigated sites are widely homogenous. So, it is assumed for the investigated spatial scale (< 0.75 km²), that effects due to heterogeneity of soil (also vege-

tation) are negligible. Furthermore, effects of regionalization and generalization can also be ignored for meteorological input data.

In contrast to uncertainties of parameterization or uncertainties in data due to regionalization and generalization, the uncertainties caused by actual measurement errors are often neglected. Here, it is demonstrated that also the superposition of seemingly small uncertainties in measurements cause significant uncertainties in estimated ET_a and R_a. The simple but unavoidable measurement errors can cause significant uncertainties in model results. So, measurement errors have for investigation on canopy scale (spatial scale < 0.75 km²) the same importance as uncertainties due to regionalization and generalization in investigations on bigger spatial scales such as catchments.

6.2 Applied Models

6.2.1 Hydro-Pedotransfer Functions (HPTFs)

The simulations of annual evapotranspiration ET_a and annual seepage R_a were done with two different complex models. The simple descriptions (Black Box Model) are HPTFs according to Wessolek et al. (2008). The concept of HPTFs is based on the description of the typical statistical interrelationship between precipitation P, FAO grass reference evapotranspiration ET_0, capillary rise and occurred ET_a and R_a respectively. The published interrelationships were estimated for typical sites in Germany dependent on land use, soils and distance between soil surface and groundwater table, which determines capillary rise.

The HPTFs used for this study are listed in Table 6.1. Wessolek's original functions include an additional term for the description of capillary rise. However, it was possible to eliminate this term, because the distance to groundwater was far and effects due to capillary rise were excluded. Furthermore, the original functions included some approaches for the description of surface flow in context to hang slope and sealing. However, these terms were also negligible because the terrain was flat and the surface featured good properties of infiltration at all sites.

The required input data of HPTFs were: the yearly sum of precipitation P_a (corrected in according to Richter, 1995), the sum of precipitation in summer months P_s (summer denotes period April to September) and the yearly sum of potential evapotranspiration ET_0, which is represented by the FAO grass reference evapotranspiration (Allen et al. 2006). For the application of HPTFs, it was considered that HPTFs had different algorithms for dry and wet conditions, at which the separation between dry and wet conditions was done by a land use specific threshold for the sum of $W_a + P_s$. Thereby, W_a is the plant available soil water within the root zone.

The parameters of HPTFs were only the type of land use and the plant available water within the root zone W_a. However, land use was fixed by the site characteristic. In that way, the sole variable parameter was W_a. For the following analyses, two scenarios (H1 and H2) were created. In scenario H1, W_a was set to its lowest value, which was observed or assumed at the specific site. However, W_a was set to the observed or assumed maximum in H2 scenario. Thus the analyses also implicitly included a sensitivity analysis of HPFTs.

Table 6.1 HPTFs used for approximation of seepage R_a

Land use	threshold wet/dry; HPTFs (algorithms)
Crop	dry condition: $W_a + P_s \le 650\,mm$ $R_a = P_a - E_0\left(1.45\log\left(W_a + P_s\right) - 3.08\right)\left(0.685\log\left(\frac{1}{E_0}\right) + 2.865\right)$
	wet condition: $W_a + P_s > 650\,mm$ $R_a = P_a - 1.05\,E_0\left(0.685\log\left(\frac{1}{E_0}\right) + 2.865\right)$
Grass	dry condition: $W_a + P_s \le 650\,mm$ $R_a = P_a - E_0\left(1.79\log\left(W_a + P_s\right) - 3.89\right)\left(0.53\log\left(\frac{1}{E_0}\right) + 2.43\right)$
	wet condition: $W_a + P_s > 650\,mm$ $R_a = P_a - 1.2\,E_0\left(0.53\log\left(\frac{1}{E_0}\right) + 2.43\right)$
Coniferous forest	dry condition: $W_a + P_s \le 700\,mm$ $R_a = P_a - E_0\left(1.68\log\left(W_a + P_s\right) - 3.53\right)\left(0.865\log\left(\frac{1}{E_0}\right) + 3.36\right)$
	wet condition: $W_a + P_s > 700\,mm$ $R_a = P_a - 1.3\,E_0\left(0.865\log\left(\frac{1}{E_0}\right) + 3.36\right)$
Deciduous forest	dry condition: $W_a + P_s \le 700\,mm$ $R_a = P_a - 0.90\,E_0\left(1.68\log\left(W_a + P_s\right) - 3.53\right)\left(0.865\log\left(\frac{1}{E_0}\right) + 3.36\right)$
	wet condition: $W_a + P_s > 700\,mm$ $R_a = P_a - 1.17\,E_0\left(0.865\log\left(\frac{1}{E_0}\right) + 3.36\right)$

6.2.2 BROOK90

The complex water balance model BROOK90 version 4.4e (Federer 2002) was representatively chosen for other complex water balance models. However, the source code was slightly modified for creating of a version which has the ability to run in batch mode. BROOK90 is a complex one-dimensional column model, which consists of several approaches for calculation of interception, transpiration, snow melt, infiltration, soil water movement, exfiltration and runoff. Thereby, transpiration, snow melt and soil water movement are described by physical based approaches. However, interception and all descriptions of runoff behaviour are conceptual approaches.

The required input data of BROOK90 are identical to the actual required input of HPTFs and are the daily values of: precipitation P, global radiation R_G, wind speed u, maximum and minimum of air temperature T_{max}/ T_{min} and vapour pressure e. It is noted, that R_G, e, u, T_{max} and T_{min} are only necessary for the calculation of FAO grass reference evapotranspiration ET_0 in HPTFs. So, data in a lower temporal resolution are also useable for HPTFs in principle.

However, the same data sets (and the same temporal resolution) were used for both HPTFs and BROOK90 to ensure comparability of model results.

The parameterization of BROOK90 is much more complex than parameterization of HPTFs. BROOK90 includes almost 100 parameters, arranged in five groups: (i) description of localization (8 parameters), (ii) behaviour of infiltration and run off (12 parameters), (iii) vegetation and canopy (19 parameters), (iv) characterization of soil (8 parameters per soil layer) and (v) fixed parameters (42 parameters). Thereby, the parameterization or calibration of fixed parameters is normally not necessary. So, parameters of group (v) can be seen as constants.

The large amount of parameters in BROOK90 allows the creation of multifarious scenarios. Here, two scenarios were created for the investigation of effects due to complexity and for the investigation of effects due to parameterization to accuracy of simulated ET_a and R_a. The first scenario B1 is a simple parameterization. There, BROOK90 was simplified as much as possible. This means that only standard (default) values were used and the effort of parameterization was limited to adjustments of soil and vegetation. So, the parameterization is adequate and comparable to adjustments in HPTFs.

The second scenario B2 is a well fitted model, which is adapted to local specifics. In the case of the Spruce site, Monte Carlo Simulations were used to optimize the parameterization. However, such extensive optimization was not possible at the Grass and Agricultural site because of limited data series. So, an advanced parameterization was used at these sites, which includes information normally not available for engineering applications. In detail B2 is distinguished from B1 by more exact parameterization of soil and vegetation. So, the layering of soil, the distribution of roots, the times of cutting and harvest, the yearly course of vegetation height and the yearly course of LAI were considered as exact as possible.

6.2.3 Effects due to Complexity of Models and Parameterization of Models

The analyses are based in principle on three different complex models: a simple Black Box Description (HPTFs), a complex model with a simple parameterization (B1) and a complex model with an extensive parameterization (B2). Thereby, the effort of parameterization was similar between HPTFs and B1. However, the complexity of models is quite different between HPTFs and B1. In contrast to HPTFs, the complexity of model is identical between the B1 scenario and the B2 scenario. However, the parameterization was improved in B2 scenario.

The comparison of HPTFs with B1 has the ability to approximate effects of complexity to simulation results of ET_a and R_a. That means that the comparison shows the potential of exact descriptions of interception, transpiration, snow melt, soil water movement and soil water storage to the quality of model results against simple Black Box Descriptions, at which the effort of parameterization was the same. However, the comparison between B1 and B2 shows the effects of parameterization. In particular, the potential of high quality parameterization is shown on the one hand and the limitations due to suboptimal parameterization on the other hand.

6.3 Input and Reference Data: Measurement and Quantification of Uncertainties

6.3.1 Test sites and Measurements

The test sites are the three sites of FLUXNET/ EUROFLUX programme within *Tharandter Wald* (CarboEurope-IP 2008a, FLUXNET 2007). In detail, the investigations are related to measurements at the Spruce, Grass and Agricultural site, at which eddy-covariance (EC) measurements and meteorological standard measurements (global radiation R_G, minimum and maximum of air temperature T_{min}/T_{max}, air humidity, wind speed u and precipitation P) are most important. The investigations were restricted due to the availability of EC data at individual sites. In this way, the periods of investigation are: 1997 to 2008 at the Spruce site, 2004 to 2009 at the Grass site and 2005 to 2009 at the Agricultural site (periods starting on April 1st and finishing on March 31st).

6.3.2 Uncertainties in Input Data

The data of R_G, e, u, T_{max}/ T_{min} and P were measured directly at individual test sites. In this way, effects due to regionalization were excluded. However, relative humidity RH was measured instead of vapour pressure e, which was converted according to Allen et al. (2006). One intention was to quantify effects of measurement errors to model results. However, it is more correct to handle measurement errors as uncertainties of measurement than as actual errors. So, the term measurement uncertainty is used instead of measurement error in the following text.

A quantification of effects due to measurement uncertainties on results of HPTFs and BROOK90 was not possible with a classical error approach because of too complex model structures and because of non-monotone or inconsistent algorithms. The applied approach is based on a special term of Monte-Carlo-Simulation called uncertainty model. In detail, this approach was used on 50000 artificial data series, which were generated by the superposition of original data with artificial errors (both systematic and stochastic errors). The data series were created for all three sites and were used for simulations of ET_a und R_a. In this way, a band of model results was created instead of one deterministic output. Finally, the error margin and the confidence interval respectively were derived from variations between individual data series and from variations between individual model runs. The range between empirical 5% and 95% quantile was used for quantifications.

6.3.3 The Uncertainty Model

The uncertainty model was in principle a random generator for creation of data series with artificial measurement uncertainties. This means that the original data series were superposed by artificial systematic errors and by artificial stochastic errors. Systematic errors were described by one random value for each individual artificial data series. However, the stochastic errors were described by random values, which were created individually for each day and were even created individually for each individual data series.

The characteristics of random values were different between systematic and stochastic errors. In the case of systematic errors, the actual value was unknown. However, it was within the range of approximated error margin. Because of the missing knowledge about the actual error, it was assumed that every number inside error margin could be potentially the actual value. It was assumed that the probability was equal for each number inside the error margin. So, uniformly distributed random numbers were chosen for the description of systematic errors.

For stochastic errors, it was assumed that stochastic errors were compensated in the statistical average. Secondary, it was assumed that stochastic errors are typically Gaussian-distributed. So, a normally distributed random number was chosen for the description of stochastical variations. The borders of error margin were scaled to the 5σ-level of a normally distributed random number (σ denotes the standard derivation). Potentially also other σ level between 3σ and 10σ are possible. However, in the case of an σ-level < 5σ, the created random values were often outside the error margin. So, the range of artificial errors was overshot and extensive additionally reworking was required. In the case of an σ-level > 5σ, the variations between random values were too low and the distribution of uncertainty seemed to be implausible. In that context, the 5σ-level was a good compromise to generate a plausible range for stochastic error.

The actual quantification of error values (used for simulation of artificial systematic and stochastic errors) was based on simplifications of actual error characteristic. It was assumed that both errors (systematic and random errors) are represented by errors of slope and errors of offset. However, it was assumed that all other species of errors (like hysteresis or linearity) were insignificant and negligible. In this way, the characteristic of errors was describable by a slope term A and an offset term B. In practice, two random numbers (RN_A and RN_B) were generated and scaled to the range of A and B of each individual variable. That means that there are actually 4 different random values for description of uncertainties of input variables. There were two uniformly distributed random numbers to describe A and B of systematic errors, and there were two normally distributed random numbers to describe A and B of stochastic errors. In this context, it is repeated that for systematic error one specific A and one specific B were generated for whole data series. However, for stochastic errors A and B were generated individually for each day.

For application of the uncertainty model to data series of temperature and precipitation the proceeding was somewhat modified. In the case of temperature (T_{max} and T_{min}), the error description was reduced to offset term B. Furthermore, the same error values for description of systematic errors were used for T_{max} and T_{min}, because these variables were typically measured with the same devices at test sites (VAISALA HMP 35 at the Spruce site; VAISALA HMP 45 at the Grass and Agricultural site). However, the stochastic errors were generated separately for T_{max} and T_{min}. In the case of T_{max}, a second stochastic error was introduced for description of potential radiation effects. In contrast to temperature and all other variables, the error description of precipitation data was something more complex and is explained separately in Section 6.3.5.

6.3.4 Quantification of Uncertainties in Meteorological Input Data

The actual quantification of uncertainties (i.e. the parameterization of A and B) is based on the one hand on specifications and datasheets of measurements devices and on the other hand on parallel measurements with different devices. The manuals and datasheets gave a guideline for the range of potential total uncertainty. However, it was not possible or it was uncertain to derive a useful separation into systematic and random uncertainties. In this context parallel measurements with different measurement devices (done on stations themselves or in context to other experiments) gave more reliable clues. In this way, it was also possible to approximate effects, which were caused by different arrangements and different installations of devices. Such effects were observed at every site. Although measurements were done with greatest care and were done according to meteorological standards and guidelines (WMO). The approximated and used parameterizations of uncertainty model are listed in Table 6.2 for variables: R_G, T_{max}, T_{min}, RH and u.

Table 6.2 Derived quantifications of systematic and random errors in meteorological input data based on producer information and on parallel measurements

Variable	Systematic Error (uniformly distributed)	Random Error (normally distributed)
Measurement of global radiation R_G	Slope: 0.95 – 1.05 Offset: ± 0.4 MJ m^{-2} d^{-1}	Slope: 0.90 – 1.10 Offset: ± 0.6 MJ m^{-2} d^{-1}
Measurement of temperature	Offset: ± 0.1 K * random number was used for both T_{max} and T_{min}	Offset: ± 0.5 K * separate random numbers for T_{max} and T_{min} # random number was tested against $T_{min} < T_{max}$
Errors in T_{max} caused by radiation ($R_{G,pot}$… potential global radiation)	a in range: 0.7 – 1.0 ("a" denotes start criterion for simulation of radiation effects)	Offset: 0 – 2.5 K * absolute value of quantile was used # algorithm was applied when: $R_G > a\ R_{G,pot}$
Measurements of wind speed u	Slope: 0.98 – 1.02 Offset: ± 0.2 m s^{-1} * random number was tested against $u \geq 0$ m s^{-1}	Slope: 0.98 – 1.02 Offset: ± 0.2 m s^{-1} (however $u \geq 0$ m s^{-1}) * random number was tested against $u \geq 0$ m s^{-1}
Measurements of relative humidity RH	Slope: 0.97 – 1.03 Offset: ± 2.5 % * random number was tested against $0 \leq RH \leq 100$ %	Slope: 0.97 – 1.03 Offset: ± 5.0 % * random number was tested against $0 \leq RH \leq 100$ %

Beside uncertainties of measurement, there are uncertainties in conversion of measured values into data usable for HPTFs and BROOK90. In detail, this means the uncertainty of some parameters that are necessary: (i) for the conversion of measured wind speed into wind speed in 2 m above ground on a grassy place and (ii) for calculation of potential global radiation $R_{G,pot}$. The quantification of uncertainties of these parameters is listed in Table 6.3. The effects of uncertainties of conversion parameters were low und insignificant against uncertainties of measurement. However, they were systematic and had to be considered adequately.

Table 6.3 Quantification of uncertainties in parameters necessary for calculation of ET_0

Variable	Description of error
Canopy height h_C * necessary for conversion of measured wind speed into wind speed in 2 m	Offset: ± 6 % of reference (normally distributed)
Zero plan displacement z_D $z_D = A\ h_C$ * necessary for conversion of measured wind speed measured into wind speed in 2 m	Slope: 0.5 h_C to 0.7 h_C (uniformly distributed)
Roughness height z_0 $z_0 = A\ h_C$ * necessary for conversion of measured wind speed measured into wind speed in 2 m	Slope: 0.08 h_C to 0.12 h_C (uniformly distributed)
Height of internal boundary layer * necessary for conversion of measured wind speed measured into wind speed in 2 m	Offset: ± 4 m (normally distributed)
Latitude * necessary for calculation of potential global radiation $R_{G,pot}$	Offset: ± 1° (normally distributed)
Attitude of gauging station * necessary for calculation of potential global radiation $R_{G,pot}$	Offset: ± 15 m (normally distributed)

6.3.5 Description of Uncertainty in Precipitation Data

The description of uncertainty in precipitation data is different to all other input variables because measured precipitation is always an underestimation of actual precipitation. Thereby, underestimations are caused by:

(i) Precipitation which drifts past the rain gauge due to wind induced turbulence, which are created at the measurement device (Nešpor and Sevruk 1999). This error is called wind error and has the strongest effect to uncertainties of precipitation data. Typically, it is higher with increasing wind speed and when precipitation is snow or sleet.

(ii) A second underestimation is caused by losses at the beginning of precipitation events and is called moistening loss (moistening error). It means the amount of water (typically ~ 0.1 mm) which is necessary to create runoff into a storage tank. Effects of moistening losses on uncertainties of precipitation data increase in the case of long lasting precipitation events, which are often interrupted by drying periods. However, moistening losses are insignificant for heavy storm events.

(iii) The third error is caused by loses due to evaporation out of the storage vessel and is called evaporation error. This error is significantly lower than wind errors or moistening errors. However, it must be regarded for rain gauges with low temporal resolutions such as totalizators or rain gauges according to Hellmann. However, evaporation errors are excluded for weighing rain gauges such as PLUVIO (OTT). In the case of bucked rain gauges, evaporation errors occur when the precipitation event ends before the compensator pan is filled completely and it follows a longer period of drying. However, the created underestimation is typically lower than 0.1 mm for most types of bucked rain gauges.

In practice it is difficult to regard every error of precipitation measurement separately and it is not possible to quantify errors of every individual precipitation event. The common way to

estimate and to correct the systematic underestimation is given by Richter's correction algorithm (Richter 1995),

$$\Delta P = b\, P^{\varepsilon} \quad . \tag{6.1}$$

The parameters b and ε depend on the level of protection of the station and on the phase of precipitation. The level of protection of the station is derived from the angle of horizon line and is classified into four levels: (0) exposed, angle of horizon line is below 3°, (1) slightly protected, angle of horizon line is below 7°, (2) moderately protected, angle of horizon line is below 12° and (4) very protected, angle of horizon line is above 12°. The assessment of precipitation phase depends on limits in daily average of air temperature. Typically, the limit between rain and sleet is 3.2 °C and the limit between sleet and snow is 0.0 °C. Furthermore, the typical precipitation behaviour of rain is separated between summer and winter to regard the typical precipitation behaviour. Thereby, it is assumed for the region of *Tharandter Wald*, the summer period starts on April 1st and ends on October 31st. In context to the intention to regard and to describe potential uncertainties, there are three sources for systematic errors in Richter's algorithm:

(i) The temperature thresholds for the separation rain-sleet and sleet-snow are only guidelines and can differ at the specific locality.

(ii) Similar to the former point, the separation into summer and winter precipitation is also only guideline and only a rough approximation for the separation between convective and stratiform precipitation. So, the precipitation characteristic can be very different for individual precipitation events.

(iii) The assessed level of protection does not agree with actual protection. The angle of horizon line can be different for different wind directions. Furthermore turbulences caused on edges of forests around the stations can blur the accurate interrelationship between angle of horizon line and level of protection.

Our approach for description and correction of systematic uncertainties is based on Richter's correction algorithm. However, the algorithm was superposed by artificial uncertainties. In detail, normally distributed random numbers were used to attend uncertainties, which were explained in points (i), (ii) and (iii).

It was possible to quantify the uncertainties of points (i) and (ii) due to empirical observations. A range of about ± 1 K for the thresholds of separation rain-sleet and sleet-snow are reliable assumptions for variations. For the separation of summer and winter (as guidelines for separation of predominately convective and stratiform precipitation) a variation about ± 30 days was assumed.

The quantification of uncertainties in the level of protection (iii) was more complex. The error in ΔP (caused by wrong assumptions of the level of protection) varied depending on amount and phase of precipitation. In the statistical average, the differences between ΔP of two neighbouring classes of the level of protection were between 10 and 15 % in the case of rain

and between 40 and 60 % in the case of snow for predominately daily sums of precipitation. It was necessary to consider that Richter's algorithm describes only the underestimation on average. This means that the actual underestimation can be different to underestimation, which was approximated by Richter's correction algorithm. In consequence, not only an uncertainty in the level of protection must be considered, but also an uncertainty which describes the statistical variations of the correction function. In that way, the complexity of uncertainty model would increase even more, at which it would be critical to parameterize the model.

It is assumed that related to the derivation of Richter's correction algorithm (Richter 1995), a simplified description with normally distributed random number is sufficient to regard the uncertainty due to point (iii). Thus it was possible to quantify the uncertainty of ΔP by approximately ± 50%, which was scaled to 5σ-level of the normally distributed random number. In this way, it was possible to create typical systematic uncertainties, which were between 2 and 5 % for rain and were between 4 and 8 % for snow related to the corrected precipitation.

Besides systematic errors artificial stochastic errors were also included in precipitation data. The model for description of stochastic errors in precipitation data worked similarly to models for all other climate variables, which were based on a separation into a slope term A and an offset term B. The quantification of A and B was based on parallel measurements with different devices. A range was approximated for A between 0.8 and 1.2 and for B a range of ± 0.2 mm. However, the model for description of errors was limited to days when precipitation was measured. So, an uncertainty still remained due to non-recorded precipitation events. However, such situations occurred only in the case of very small precipitation events and were insignificant for monthly or yearly totals.

6.3.6 Reference Data

The reference data were primary the evapotranspiration ET, which was measured with closed-path eddy-covariance (EC) system devices in terms of latent heat flux LE at all three sites. At the same time, the sensible heat flux H was also measured with the EC system device. Furthermore, the net radiation R_N and the soil heat flux G were also measured at all sites. So, besides ET, all components of energy balance were measured and were available as additional reference. It is to note, all used data are included in Carbo Europe database (CarboEurope-IP 2008b). Furthermore, processing of EC data was done according to acknowledged standard methods (Aubinet et al. 2000, Foken 2006, Grünwald and Bernhofer 2007, Lee et al. 2004, Schotanus et al. 1983, Spank and Bernhofer 2008, Wilczak et al. 2001). The applied algorithm is included in the appendix A1.

A rough method for the approximation of accuracy of EC data was given due to the comparison of LE, measured directly with the EC system device LE_{EC}, and LE, which was estimated as residual of the energy balance LE_{EB},

$$LE_{EB} = R_n - G - H \; . \tag{6.2}$$

The measured turbulent fluxes (H and LE_{EC}) typically underestimate the actual fluxes of LE and H (Foken 2006, Foken et al. 2006). So, there is typically a gap in energy balance between available energy AE (means $R_N - G$) and turbulent exchange (means H + LE). Furthermore the gap causes a difference between LE_{EB} and LE_{EC}. The gap in energy balance is related to long time observations and is not caused by temporal effects of energy storage. At test sites, the estimated gaps were between 20 and 40 % on an annual time scale.

The error margin of evapotranspiration ΔET can be approximated on the basis of difference between LE_{EB} and LE_{EC}. Thereby, the lower limit of evapotranspiration ET_L was assumed by LE_{EC}. However, the upper limit of evapotranspiration ET_U was assumed by LE_{EB}. To find a value which matches the actual value of ET as best as possible (ET_R), the gap in energy balance is divided into percents added to LE_{EC} and percents added H on basis of Bowen ratio. Finally, the probable range of ET (ΔET) is bordered by ET_L as lower limit, ET_R as probably most representative value and ET_U as upper limit.

However, ET_R and ET_U are affected besides uncertainties of EC measurements also by uncertainties of measured net radiation ΔR_N and measured soil heat flux ΔG, which were summarized as uncertainty of available energy ΔAE. Primary, ΔAE was handled like uncertainties of input data. However, the analyses showed that it is possible to integrate them in ΔET without an explicit error simulation. A detailed explanation therefore is given in Section 6.4.2.

Additional to annual evapotranspiration, the investigations are also related for annual seepage R_a. In this context, it is necessary to estimate a reference of R_a. The applied approach is based on the assumption that the storage term of water balance is negligible, because investigations are focused to annual time scale. In another context, the investigations are restricted to the rooting zone. In this way, the storage term is only affected by soil moisture. Furthermore, the start of investigations was arranged for April 1st. At this time, the soil moisture is typically near field capacity. So differences of soil moisture are small between individual periods and potential effects of storage are ignorable. Consequently R_a is estimable by,

$$R_a = P_a - ET_a \,. \tag{6.3}$$

The uncertainty of R_a is determined predominately by uncertainties of ET_a. However, R_a was also affected by uncertainties of P_a. But, uncertainties of P_a are small in comparison to ΔET (Further details see Section 6.4.2.). Additional, there still remains an uncertainty due to negligence of storage term in equation (6.3).

6.4 Evaluation of Uncertainties in Input and Reference Data

6.4.1 Uncertainties of Meteorological Data, Characterization of Weather Conditions

The uncertainties of input data as well as their effects on annual totals were estimated on the basis of the empirical 5 % and 95 % quantile of artificial data series. In context to primary objects of investigation, the uncertainties of precipitation P and the effects of measurement uncertainties to grass reference evapotranspiration E_0 are most important. Thereby, it can be assumed, that E_0 was affected by uncertainties of all meteorological input variables (R_G, e, u,

T_{max} and T_{min}). So, the error margin of E_0 (ΔE_0) is representative values for the aggregation of uncertainties of meteorological variables.

Furthermore, ΔE_0 gives a guideline for potential uncertainties of simulated evapotranspiration, which are caused by uncertainties of measurements. But ET_0 describes only the theoretical (potential) evapotranspiration of an idealized grassland site. Furthermore, BROOK90 uses a two-layer transpiration model (Shuttleworth and Wallace 1985) instead of Penman's approach (Monteith and Unsworth 1990, Allen et al. 2006), which is used for calculation of ET_0. So, the actual simulated evapotranspiration is different to ET_0. However, the uncertainty of simulated evapotranspiration should be in the same magnitude as ΔE_0.

The yearly sums of ET_0, the yearly sums of precipitation P_a, as well as the sums of precipitation in summer months P_s are shown in Figure 6.1 for the Spruce site; they also represent all the other sites. It shows the median (It is used as reference in the following), the 5 % and the 95 % quantile, and the maximum and minimum of generated artificial data series. Figure 6.1 characterizes the averaged climatic conditions for 1997 to 2008. In comparison to the average, two outliers are conspicuous: 2002 and 2003.

2002 was characterized by above average P_a and P_s, which were caused by an extreme rainfall in August. At the Spruce site, precipitation of 264.3 mm was measured from August 11th to August 13th. This extreme rainfall meant that P_s was one and a half times higher than the long-term average in 2002. In contrast to 2002, 2003 was extremely dry (significant drier than 2006 related to Chapter 5). The measured precipitation in summer month was only 262.7 mm. Additional, 2003 was characterized by extremely high temperatures and by an above average high number of sunny days. In consequence, ET_0 increased extremely and exceed even the annual precipitation P_a (664.8 mm) in 2003. However, 2003 was an absolute anomaly of climate, whose probability of appearance was approximated at less than once per 100 years (Franke 2009).

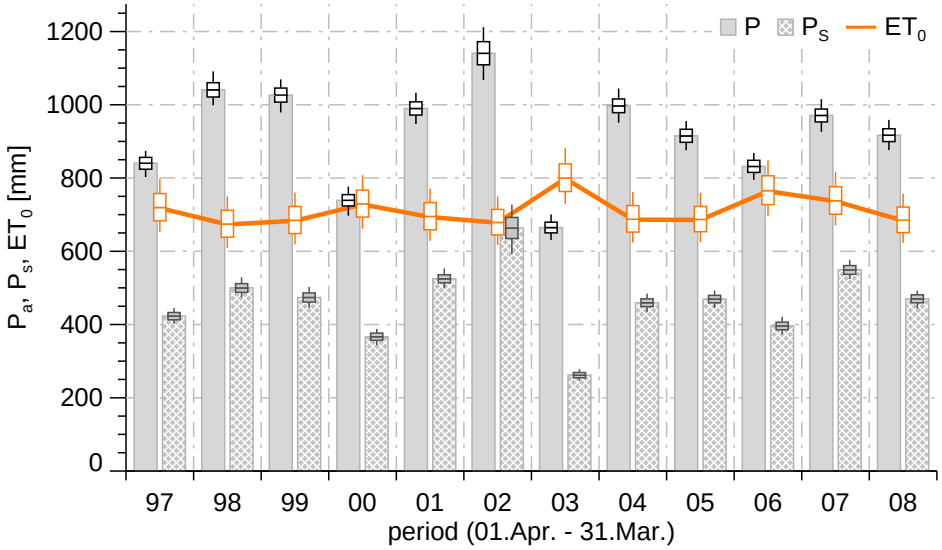

Figure 6.1 Annual precipitation, precipitation in summer months and annual grass reference evapotranspiration measured at the Spruce site with associated ranges of uncertainties (shown: minimum, maximum, median, 5 % und 95 % quantile)

6.4.2 Evaluation of Uncertainties in Precipitation Data

The interrelation between annual precipitation P_a and associated uncertainty ΔP_a as well as the interrelation between precipitation in summer month P_s and associated uncertainty ΔP_s are shown in Figure 6.2. Thereby, the uncertainties are shown as absolute values [mm] and in relation to the reference [%]. All values are related to precipitation that was corrected according to Richter (1995). The absolute uncertainties of P_a and of P_s showed an almost linear interrelationship to references of P_a and P_s respectively. This behaviour explains the constancy of relative uncertainties of P_a. However, the relative uncertainties varied significantly in the case of P_s. Furthermore, a significant derivation to common behaviour of P_a and P_s was observed for 2002. This derivation was a direct consequence of enormous absolute uncertainty of extreme precipitation in August, which even affected the annual values.

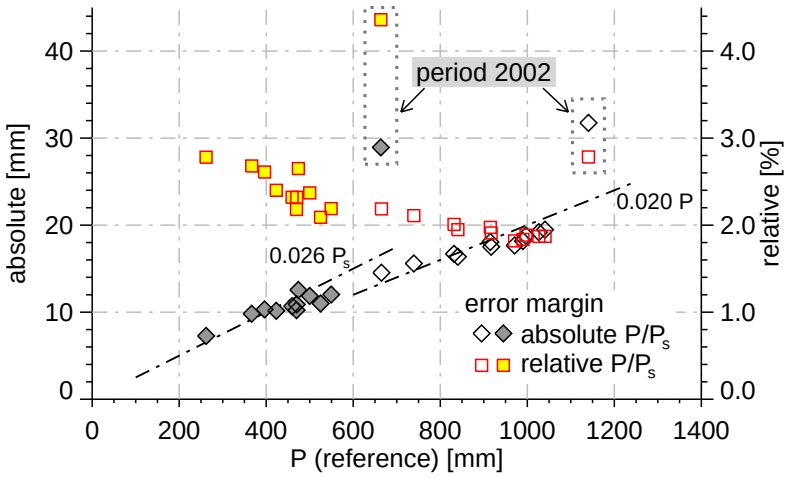

Figure 6.2 Absolute and relative uncertainties of P_a and P_s in dependence to measured P_a and measured P_s (Spruce site)

The uncertainty of P_a was about ± 2 % on average and so was between ± 15 and ± 20 mm in typical years. The uncertainty of P_s was slightly higher and was ± 2.6 % on average, at which the absolute uncertainty was typically ± 10 up to ± 12 mm. However, the uncertainty was significantly higher when the specific year was affected by extreme rainfall. So, the uncertainty of P_a was ± 2.8 % (± 31.6 mm) and the uncertainty of P_s was even ± 4.4 % (± 29.1 mm) in 2002. The absolute uncertainty of P_a and P_s did not differ significantly in 2002. So, the uncertainty of P_a was significantly affected by uncertainties of the extreme event in August. In contrast to 2002, the uncertainties of P_a and P_s were significant lower in the extremely dry year of 2003. Then, the uncertainty of P_a was ± 2.2 % (± 14.5 mm) and the uncertainty of P_a was ± 2.8 % (7.3 mm). It is conspicuous that the uncertainties were higher than averagely in 2003 because the year was extreme dry and the number of days with precipitation was significant lower than average.

In this way, the characteristic of uncertainty of corrected precipitation becomes understandable. The absolute amount of uncertainty is determined by the superposition of uncertainties of daily totals. Thereby, the absolute uncertainty of daily totals increases with an increasing amount of measured precipitation. Additionally, the uncertainty increases when the phase of precipitation is sleet or snow. However, the uncertainty of daily totals is composed of stochastic uncertainties and systematic uncertainties. Systematic uncertainties of daily totals are summed up by estimation of annual totals. However, stochastic uncertainties of daily totals are averaged. This means that the effects of stochastic uncertainties in annual totals of precipitation decrease with an increasing number of days with precipitation.

So the uncertainties of P_a and P_s were higher when predominate events of precipitation were convective rather than stratiform, because the number of days with precipitation were typically lower in the case of predominate convective precipitation Furthermore, extreme events can even affect the uncertainty of annual totals of precipitation.

6.4.3 Evaluation of Uncertainties in FAO Grass Reference Evapotranspiration ET_0

The FAO Grass Reference Evapotranspiration ET_0 is affected by the interaction of all meteorological variables (R_G, e, u, T_{max} and T_{min}). But predominately it is defined by global radiation R_G. The interrelationship between annual ET_0 and annual R_G is shown in Figure 6.3, at which R_G is converted to water equivalent. The classical regression (dashed line) has a coefficient of determination $\Re^2 = 0.71$. However, the offset of – 99.7 mm is not interpretable by physical means. But also the regression line through the origin (dotted line) fits ET_0 very well ($\Re^2 = 0.70$) and reveals ET_0 is on average 46 % of R_G. This simple linear interrelation between R_G and ET_0 explains 73 % of variance in ET_0. So, it is derived that all other meteorological variables (e, u , T_{max} and T_{min}) have only subdominant influence on variance of ET_0.

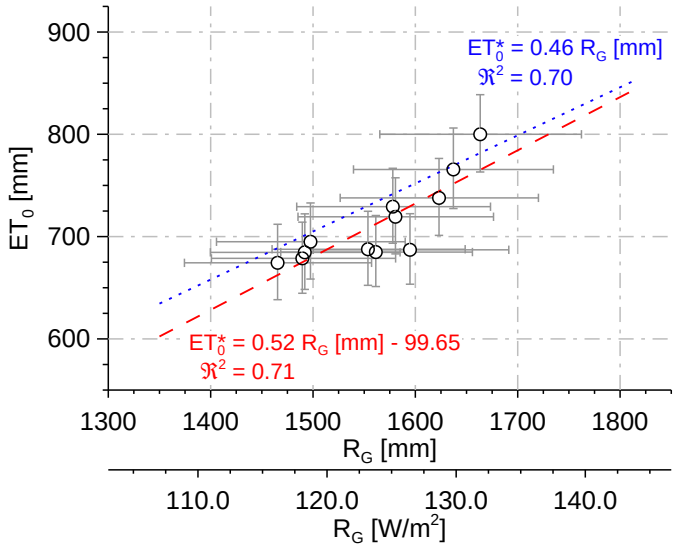

Figure 6.3 Interrelationship between annual R_G and annual ET_0 at the Spruce site (regression lines base on medians of artificial data series, estimated error margin base on 5% and 95 quantiles)

The error margin of ET_0 is determined predominately by uncertainties of R_G because of the predominant role of R_G. However, the uncertainties of other meteorological variables are subordinated. The relative uncertainty in annual R_G was 6.1 % ± 0.2 %. This means that the absolute uncertainty was between ± 91.1 mm (≈ 228 MJ) and ± 98.9 mm (≈ 247 MJ) within the investigation periods, in which the average was ± 95.0 mm (≈ 238 MJ). In this way, an uncertainty of ± 100 mm (≈ 250 MJ) must be assumed for annual R_G.

Although R_G controls ET_0, the uncertainty of ET_0 is significant lower than uncertainty of R_G. The estimated uncertainty of ET_0 was between 4.8 % and 5.6 %, with the average at 5.1 %. This means that ET_0 as well as the uncertainty of ET_0 reacted damped to uncertainty of R_G. However, the uncertainty of R_G is still significant for uncertainty of ET_0. The absolute uncertainty of ET_0 was ± 35.3 mm up to ± 40.5 mm and was ± 37.3 mm on average. Thereby, the uncertainty of ET_0 increases in the case of sunny summer months with high impacts of global radiation. So, the maximal uncertainty occurred in 2006, which was characterized by an extremely sunny and dry June and July.

6.4.4 Evaluation of Uncertainties in Reference Data of Evapotranspiration

The approach for the evaluation of uncertainties in EC data and hence for the evaluation of uncertainties in reference values of ET (ΔET) depends firstly on the closure of energy balance. This means that the uncertainty ΔET is determined primarily by differences between available energy AE and sum of turbulent fluxes (H + LE). Thereby, ΔET is divided into the differences between ET_U and ET_R as well as between ET_R and ET_L (compare Section 6.3.6). Secondly, ΔET is overlaid by uncertainties of AE (ΔAE), which are affected predominantly by uncertainties of net radiation R_N. In this context, it is possible to neglect the uncertainties of soil heat flux G because of small values and compensation effects.

ΔAE affects only ET_R and ET_U. However, it does not affect ET_L, because ET_L is defined by the direct measured evapotranspiration, which is not affected by measurements of energy balance. Furthermore, ΔAE affects the uncertainty of ET_U more than the uncertainty of ET_R, because ΔAE is added completely to uncertainty of ET_U; however ΔAE is divided between sensible heat flux and latent heat flux in the case of ET_R. So, the uncertainty of ET_U is higher than the uncertainty of ET_R.

The actual quantification of uncertainties is explained with the help of Figure 6.4 at the example of the Spruce site. In Figure 6.4 the reference of ET (ET_R) is shown as a grey column. Furthermore, the approximated limits of ET (ET_L and ET_U) are marked by additional orange columns, and the additional uncertainty of ΔAE is marked by a yellow column. The finally approximated range of uncertainty ΔET is shown as grey band in the background.

Between 1997 and 2005 the difference between ET_L, ET_R and ET_U was relatively small, with the exception of 2002. However, the differences increase significantly after 2006. The reason for this increase is not completely clear. However, the exchange of device components of EC system (exchange of sonic anemometer in May 2006 and exchange of gas analyzer in November 2006) can be excluded as a reason, because parallel measurements (done with both system configurations) gave similar results.

The most favoured thesis explains increasing differences between ET_L, ET_R and ET_U by meteorological conditions, at which interactions between meteorological conditions and accuracy of EC-measurements are very complex and are not unique in all cases. Primarily the accuracy of measured fluxes depends on atmospheric stratification and wind speed (Kaimal and Finnigan 1994). Thereby, the following guidelines are applicable: The accuracy decreases in the case of stable atmospheric stratification, because of significant attenuation effects in EC raw-data (Foken and Wichura 1996, Spank and Bernhofer 2008). In the same way, the accuracy is affected by wind. Here, the accuracy decreases because of missing turbulence with very weak wind ($< 1\ m\ s^{-1}$) and because of attenuation effects with strong wind ($> 5\ m\ s^{-1}$). Another point is related to failures which are caused by falling droplets or water films on the sensors. So, the accuracy is affected by the duration and frequency of rain events.

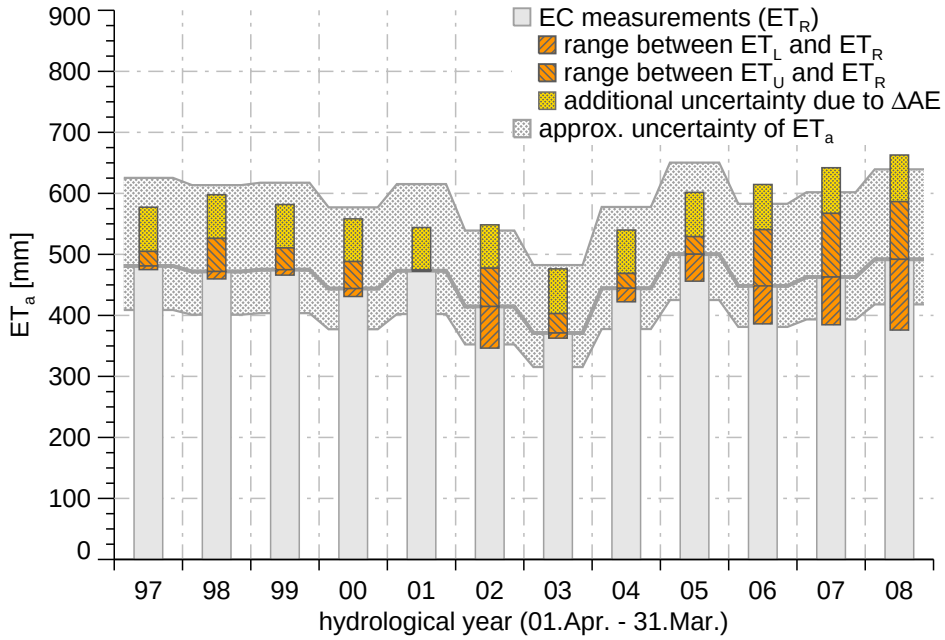

Figure 6.4 Estimated reference of annual evapotranspiration ET_R; estimated upper limit ET_U and estimated lower limit ET_L of eddy covariance measurements; additional uncertainty due to uncertainties of available energy ΔAE; and average range of uncertainty of evapotranspiration ET (further detail see text)

Based on actual measurements (without additional uncertainty of ΔAE), the differences between upper boundary (ET_U) and lower boundary (ET_L) were between 1.7 mm (2001) and 210.5 mm (2008), with an average of 86.5 mm. Thereby, the differences between ET_L and ET_R (reference) were between 0.4 mm (2001) and 115.9 mm (2007). However, the differences between ET_U and ET_R were between 1.3 mm (2001) and 104.3 mm (2008). So, the perceptual differences (related to ET_R) were between ET_L and ET_R 0.1 % up to 23.6 % (average 8.0 %) and between ET_U and ET_R 0.3 % up to 22.5 % (average 11.0 %). The maxima and the average were higher for differences between ET_L and ET_R than for differences between ET_R and ET_L. However, related to individual years, the differences between ET_R and ET_L were higher than differences between ET_L and ET_R in most cases.

The uncertainty of available energy ΔAE was relatively constant in individual years. It was between 69.6 mm (2001) and 76.5 mm (2008), with an average of 72.4 mm. That means a perceptual uncertainty (related to ET_R) of 14.5 % up to 19.7 % (average 15.9 %), which must be considered as additional uncertainty in ΔET. In this way, the differences between ET_U and ET_R were increased by about 70 mm. The actual difference between ET_U and ET_R was 71.0 mm (2001) up to 179.2 mm (2007), and was 122.2 mm on average. Related to ET_R, the differences were 15.0 % up to 38.7 % (average 26.9 %). So, the differences were significantly higher between ET_U and ET_R than between ET_R and ET_L.

The differences between ET_R and ET_L as well as between ET_U and ET_L were significantly higher at the Grass and Agricultural site than at the Spruce site. This circumstance is related to differences of individual periods as well as to the average. However, it is to note in context of the average, that data series were shorter and included periods when the differences were also

untypically high at the Spruce site. The average differences (related to ET_R) were between ET_R and ET_L 44.0 % at the Grass site and 28.8 % at the Agricultural site. The differences between ET_U and ET_R were 28.3 % at the Grass site and 35.7 % at the Agricultural site.

The average difference between ET_R and ET_L was higher than the average difference between ET_U and ET_R at the Grass site, although ET_U already included the additional uncertainty ΔAE. The reason for this behaviour (and also for the enormous difference between ET_U and ET_L) was that this site was often affected by stable atmospheric stratifications which disturbed the EC measurements significantly by attenuation effects in EC raw-data. So, the estimated ET_L and the estimated ET_U mismatch the actual ET more at the Grass site than at the other sites.

ET_L and ET_U never represent the typical boundaries of error margin. Rather, ET_L and ET_U are the worst cases of accuracy, at which the extreme case was explained with the example of the Grass site. However, the effects of raw-data processing were excluded completely up to now. The quality and the accuracy of EC data, are significantly affected and to a large magnitude by the application, the negligence or the exchange of individual processing steps (see Appendix A1) (Aubinet et al. 2000, Foken 2006, Walter 2007, Spank and Bernhofer 2008). Complete analyses of the effects of raw-data processing were not possible in this study. However, it is assumed that effects of processing are less significant than general method for estimation ET_a, (i.e. ET_U, ET_R or ET_L) when standard roles and guidelines (Aubinet et al. 2000, Foken 2006, Lee et al. 2004) are considered

For the practical application, it was necessary to simplify and to generalize the description of uncertainties in reference data. The applied approach for simplification is based primary on observations at the Spruce site and guidelines given by Foken (2006). The observations at other sites are also considered. This means that the measured ET_R is used for reference and standard. However, a tolerance of + 30 % is used for the upper limit instead of ET_U, at which + 30 % is a good approximation for observed difference between ET_U and ET_R and uncertainty ΔAE. Additionally, the tolerance of + 30 % has some reserve for unconsidered uncertainties of flux processing. The tolerance of + 30% means the typical uncertainty; but it does not mean the theoretical maximum. In that way, the applied tolerance of + 30 % was greater than ET_U in most periods. However, it was lower in the case of untypically big differences between ET_U and ET_R.

For the lower limit it is to consider that the measured latent heat flux LE is always an underestimation of actual LE, because of non turbulent fluxes (advection, Moderow et al. 2007) and because of attenuation effects. So, ET_U is inevitably lower than the actual lower limit of uncertainty. However, it is necessary to consider a tolerance for additional (unknown) uncertainty of flux processing. The difference between ET_R and ET_U were very variable between individual periods and were also very variable between different sites. Basing on the intention to simplify and to generalize the description of uncertainties, a tolerance of – 15 % is assumed for the lower limit. In that way, the complete uncertainty of ET is arranged by,

$$0.85\,ET_R \le ET_R \le 1.30\,ET_R\,. \tag{6.4}$$

6.4.5 Evaluation of Uncertainties in Seepage Reference Data

The annual seepage R_a is estimated as the reminder of water balance (6.3). In that way, the uncertainty of seepage ΔR_a is caused by the superposition of uncertainties of ET_a and uncertainties of P_a. However, it is necessary to include some additional (although unknown) uncertainty, which is caused by different charge of soil water storages at the beginning of the investigation periods. It was assumed for a simplified and generalized description of uncertainties in seepage an uncertainty of ± 3% for effects of precipitation P_a and storage change. So, in the context of uncertainties of ET_a, the complete uncertainty of R_a is assumed by,

$$0.67\,R_a \le R_a \le 1.18\,R_a\,. \tag{6.5}$$

The approximated reference of annual seepage R_a, as well as the associated range of uncertainty, is shown in Figure 6.5. Additionally, it is shown for comparison the approximated reference of annual evapotranspiration ET_a (including associated uncertainty).

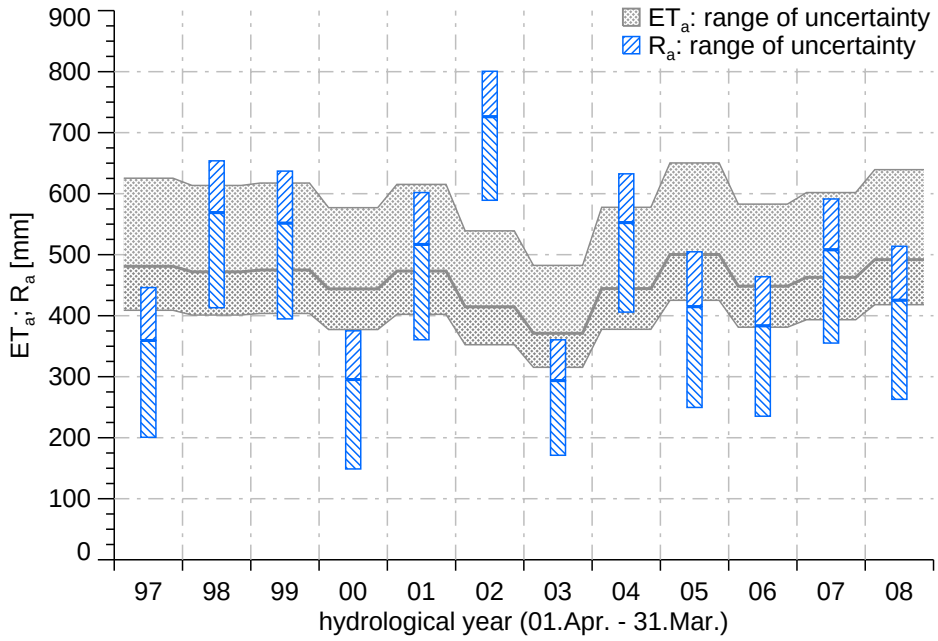

Figure 6.5 Estimated reference of annual seepage R_a and annual evapotranspiration ET_a as well as associated range of uncertainty

6.5 Evaluation of Model Results

6.5.1 Sensitivity Analyses of HPTFs

A necessary precondition for successful application of models and for evaluations of model results respectively is a sensitivity analysis of model parameters. In the case of BROOK90, it was possible to access the analyses of Eishold (2002) and Spank (2003), where the sensitivity and the complex interaction of parameters were investigated and analyzed in detail. However, such intensive analyses were not available for HPTFs.

HPTFs have two adjustable parameters: the type of land use and the plant available water within the root zone W_a. However, the type of land use is typically fixed due to the character-

istic of site. So, W_a is the sole variable parameter. The influence of W_a to simulated seepage R_a is shown in dependence to different meteorological variables in Figure 6.6 a, b and d. Additionally, the influence of land use to simulated R_a is shown in Figure 6.6 c. In context to meteorological variables, the typical climatic conditions within investigation periods were characterized. So, average values and typical variations were used for the meteorological input.

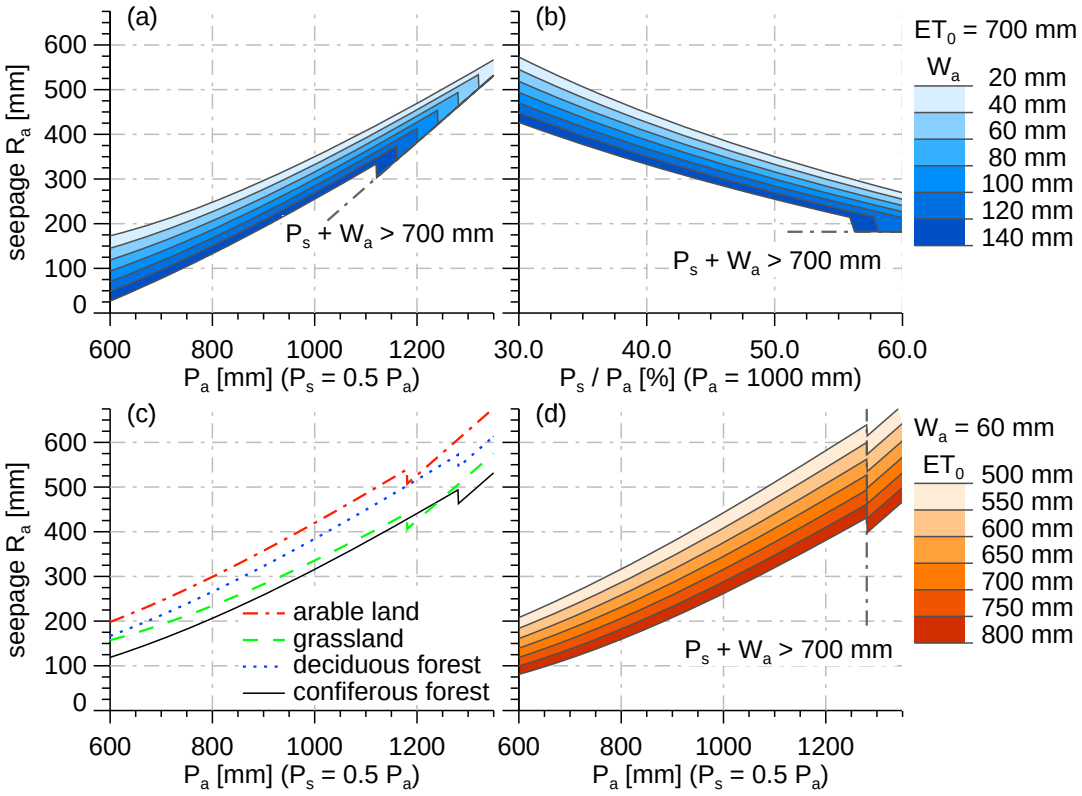

Figure 6.6 Sensitivity of HPTFs related to: (a) P_a; (b) percentage of P_s related P_a; (c) land use; and (d) ET_0 (if nothing else given: land use = coniferous forest; P_a = 1000 mm; P_s = 0.5 P_a; ET_0 = 700 mm; W_a = 60 mm)

In the context of the description of typical meteorological conditions, the change of HPTFs from dry to wet conditions (compare Table 6.1) was secondary, because the threshold $P_s + W_a > 700$ mm (forests) and $P_s + W_a > 650$ mm (grassland and agricultural) was seldom exceeded and was exceeded only under untypical weather conditions. However, the exceeding of threshold is marked in Figure 6.6 a, b and d by a bold grey dash-dot line and it is visible by steps in the curve courses in Figure 6.6 c. The change from dry to wet conditions caused an inconsistence in model algorithm and caused implausible curve courses in the nearer range of threshold.

The reason for change of model algorithm is given by Wessolek's assumption (Wessolek et al. 2008): ET_a is only determined by meteorological conditions when sufficient water is available (expressed as threshold $P_s + W_a$). However soil properties are insignificant. In that way, ET_a is only controlled by grass reference evapotranspiration ET_0 and so by global radiation R_G. However, Wessolek's assumption should be treated with respect, because the threshold

does not consider the distribution of precipitation within a period. In particular, predominant durations and intensities of precipitation events are ignored.

Figure 6.6 a shows the increase of R_a in relation to increasing annual precipitation P_a for different levels of W_a. Thereby, the model was parameterised with coniferous forest as land use, 700 mm for ET_0 and 50 % of corresponding P_a for sum of precipitation in summer months P_s. An increase of W_a cause a reduction of R_a, which means an increase of ET_a at the same time. The sensitivity of R_a to W_a is relatively constant in relation to R_a under dry conditions. However, the effect of W_a decreases with increasing P_a. In contrast to dry conditions, the simulated R_a is independent from W_a under wet conditions. So, R_a is only determined by P_a, ET_0 and land use, when the threshold for wet conditions is exceeded. Thereby, the downward step in curve courses at the change point from wet to dry conditions is conspicuous and is caused by the change of model algorithm.

The analyses of ratio between P_s and P_a are shown in Figure 6.6 b, at which land use and ET_0 were identical to analyses of Figure 6.6 a. However, P_a was fixed at 900 mm, which is the accepted guideline for annual precipitation P_a in *Tharandter Wald*. It is observed under dry conditions that more precipitation in summer P_s decreases R_a. This means that HPTFs assume an increase of ET_a as consequence of higher amounts of available water. However, this assumption causes significant uncertainties in the case of heavy storms, when significant parts of precipitation becomes run off and are not stored as plant available water. Analyses of Figure 6.6 b confirm analysis of Figure 6.6 a. So, an increase of W_a causes a decrease of R_a (and an increase of ET_a respectively). Furthermore, the former statement related to inconsistent curve courses is also confirmed.

Figure 6.6 c shows the influence of land use to simulated R_a in relation to P_a. Here, ET_a is 700 mm, W_a is 60 mm and P_s is 50 % of corresponding P_a. The differences between curve curses are low between grassland and coniferous forest (evergreen vegetation). Furthermore, the differences are also low between agricultural land and deciduous forest (deciduous vegetation). However, there are significant differences between evergreen vegetation (grassland and coniferous forest) and deciduous vegetation (agricultural land and deciduous forest). This means that R_a is significantly higher (and so ET_a significantly lower) for deciduous vegetation (where the growing seasons is limited by phenological phases) than for evergreen vegetation. However, the height or the LAI (leaf area index) of vegetation are less important. Additionally, inconsistent model algorithms concern all land uses.

The influence of ET_0 on simulated R_a is shown in Figure 6.6 d in relation to P_a. Thereby, W_a is fixed at 60 mm. But, all other parameters are quantified as in Figure 6.6 a. Increasing ET_0 caused a decrease of R_a (and hence an increase of ET_a). In the context of correlation between global radiation R_G and ET_0, Figure 6.6 d also illustrates the effects of global radiation R_G to R_a, at which an increase of R_G causes a decrease of R_a (and an increase of ET_a). Further, Figure 6.6 d points to the (already explained) inconsistence of HPTFs, which cause significant downward steps in curve courses at $P_a = 1280$ mm, which correspond to the threshold $P_s + W_a = 700$ mm for coniferous forests, and by the quantifications $W_a = 60$ mm and $P_s = 0.5\ P_a$.

6.5.2 Common Overview about Measured and Simulated Evapotranspiration and Measured and Simulated Seepage

The simulated values of annual evapotranspiration ET_a and annual seepage R_a as well as the associated uncertainties caused by uncertainties of input data are shown in Figure 6.7 and Figure 6.8 respectively. They show the results of HPTFs by usage of lower limit for plant available water H1 and by usage of the upper limit for plant available water H2, and there are shown the results of BROOK90 in the case of a simple parameterization B1 and in the case of an advanced parameterization (calibration) B2. Furthermore, they show the reference values of ET_a and R_a respectively associated uncertainty as a grey area in the background.

R_a varied significantly between individual years, for which variations in precipitation were the main reason. However, ET_a was relatively constant, especially at the Spruce site. Variations of ET_a were also small on other sites in comparison to R_a. However, ET_a was significant more variable at the Grass and Agricultural site than on the Spruce site. Thereby, effects of agricultural management were the major reason. But, also effects of growing seasons were important, especially in relation to the Agricultural site. However, variations of meteorological variables were less important, which was demonstrated in context to grass reference evapotranspiration (Section 6.4.1, Figure 6.1).

ET_a was significant lower at the Agricultural site than at both other sites. The reason for low ET_a was the short growing season of agricultural plants. So, vegetation cover was only present for few months. In other times, the crop was empty and bare soil represents the surface. In that way, the most important components of evapotranspiration (transpiration and interception) did not exist or were significantly reduced in many months. This means that the evapotranspiration was created only by soil evaporation outside of the growing season, at which the soil evaporation is significant lower than transpiration and interception. In this context, the very short growing season of Maize is noted, which caused the particular low ET_a at the Agricultural site in 2007.

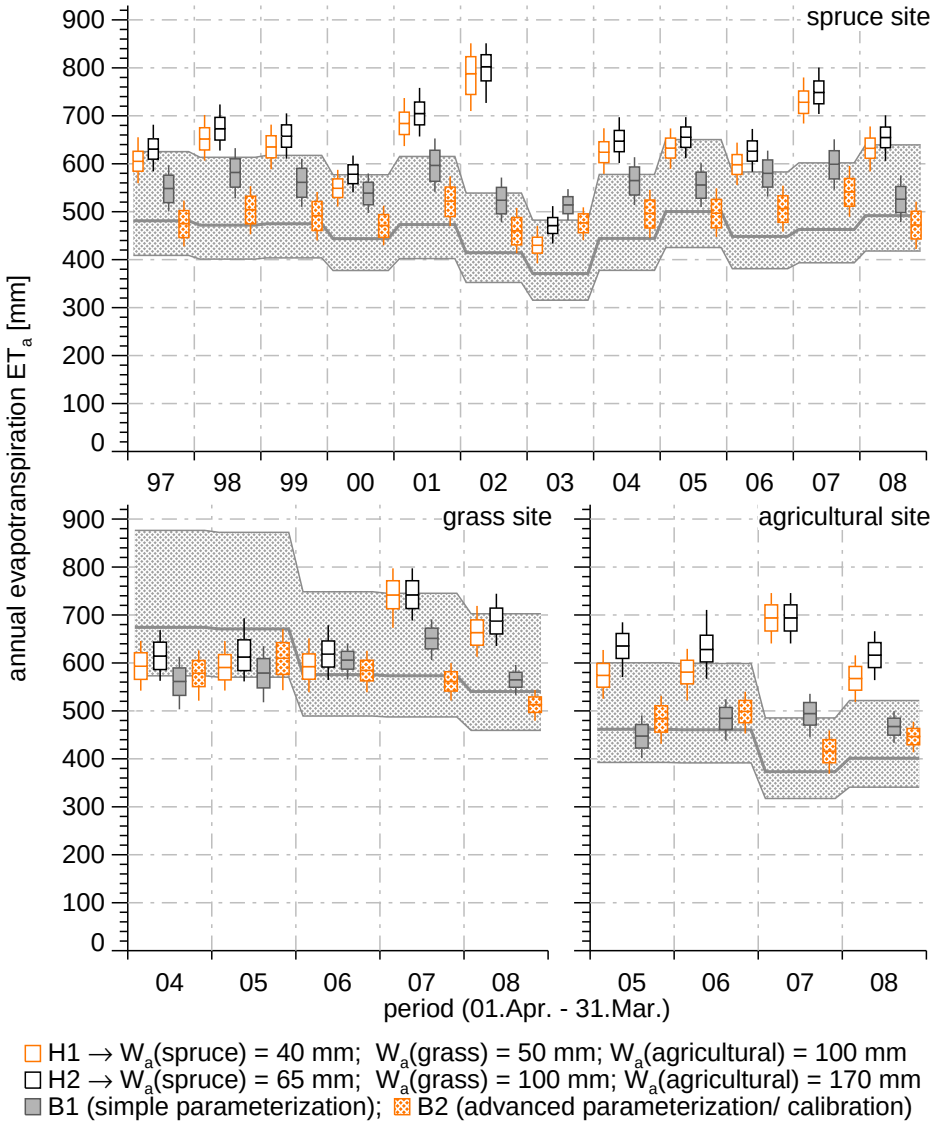

Figure 6.7 Measured and simulated annual evapotranspiration ET_a as well as associated ranges of uncertainty

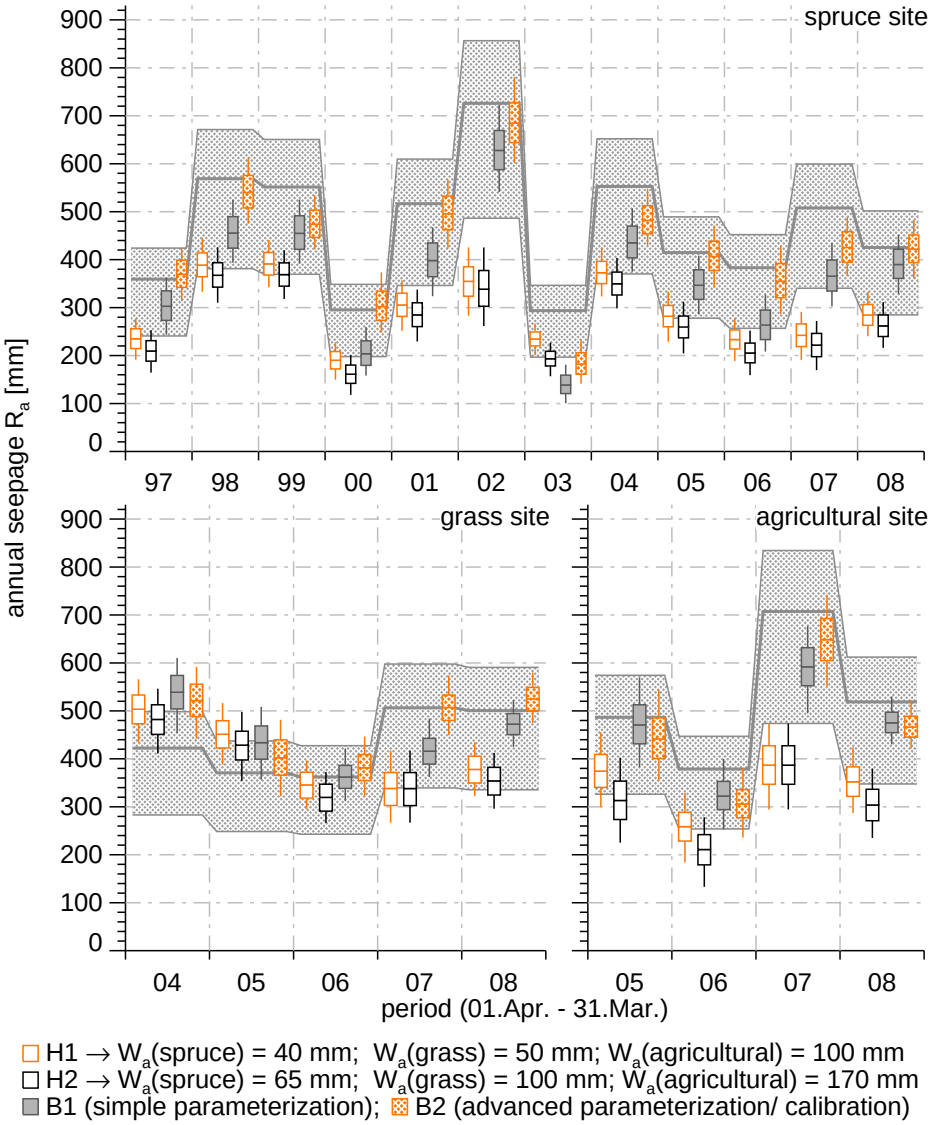

Figure 6.8 Measured and simulated annual evapotranspiration R_a as well as associated ranges of uncertainty

6.5.3 Evaluation of Simulation Results in Relation to Parameterization and Complexity of Model

Figure 6.7 and Figure 6.8 already illustrated that well parameterized (calibrated) complex models (B2) have the ability to simulate and to prognosticate annual evapotranspiration ET_a and annual seepage R_a in high accuracy. The results of B2 simulations match the reference of ET_a and R_a at all three sites and in all periods, with exception of 2004 (at the Grass site) and 2003 (at the Spruce site). However, the discrepancy at the Grass site in 2004 was caused only by a suboptimal parameterization, which was caused by insufficient information about yearly course of vegetation height and yearly course of LAI in this year. That means, the discrepancy in 2004 is a problem of insufficient information, but is not a problem of the model concept.

Another situation is the discrepancy at the Spruce site in 2003. As already noted, 2003 was an extremely hot and dry year. The reason for the discrepancy in 2003 is not completely clear (Schwärzel et al 2009a). One possible reason is that several parameters in BROOK90 are not

measureable. This means that they were approximated or estimated inversely by calibration. In that context, some parameters are insensitive under normal conditions. But, these parameters are sensitive in extreme situations. Furthermore, some parameters change in dependence to environmental conditions (such as the distribution of fine roots).

This means that it would be necessary to create several parameters sets, which are adapted to different environmental or climatic scenarios. However, this option is very restricted because of missing information and insufficient data for calibration in extreme situations. Besides a suboptimal parameterization, it is not excludable that internal algorithms of BROOK90 are insufficient to simulate correct evapotranspiration and seepage respectively in extreme droughts. However, B2 (as a replacement for other complex models) demonstrates in general, that well parameterized/ calibrated models have the ability to simulate and to predict ET_a and R_a in sufficient accuracy, especially under typical climatic conditions.

The simulation results of complex model with simplified parameterization (B1) are less accurate in comparison to B2. So, the results of B1 (range of simulated ET_a and R_a) are often cross the reference (range of uncertainty). So the uncertainty caused by uncertainties of input data decides if the simulation passes or fails. That means, the uncertainty of input data is a decisive parameter for accuracy of simulation; the uncertainty of input data is more important for applicability in the case of the simplified parameterization B1 than in the case of the advanced parameterization B2. However, also in case of simplified parameterization B1 the median of model results was only outside of reference in two periods for R_a (2004 at the Grass site, 2003 at the Spruce site) and three periods for ET_a (2004 at the Grass site, 2003 at the Spruce site, 2007 at Agricultural site).

On the basis of the results shown it can be concluded that an extensive parameterization (B2) is necessary when exact quantifications of ET_a and R_a are required. However, it is sufficient to work with a simplified parameterization (B1), when the common behaviour or tendencies are the focus. In particular, it is possible to simplify the yearly course of vegetation height and the yearly course of LAI by standard assumptions for these applications. But it is suggested to use courses which are typical for the specific land use. As an example, the standard assumption (used in B1) caused a significant overestimation of ET_a in 2007, when Maize was planted at the Agricultural site, which has a significant shorter growing season than other crops.

In contrast to complex models (B1 and B2), HPTFs do not have the ability to simulate and to prognosticate ET_a and R_a in sufficient accuracy at the test sites. Both scenarios (H1 and H2) failed the range of reference in many periods. The reason for insufficient simulation results is the generalized description of ET_a and R_a, which is independent from special characteristics of a site. This means that HPTFs were developed to describe the typical interrelationship between soil and climate, and resulting ET_a and R_a respectively in Germany (Wessolek 2008). However, HPTFs were not developed and adapted for special conditions in the *Erzgebirge* and in *Tharandter Wald*.

In context to test sites, the characteristic of predominate precipitation events is not regarded sufficiently. So, the influence of interception to ET_a is assessed wrongly by HPTFs, which

causes a significant overestimation of ET_a especially at the Spruce site. This means that the generalized and summarized description used for the approximation of evapotranspiration in HPTFs is insufficient when interception is a sensitive component of simulated evapotranspiration. In these situations, only complex models which can simulate the interception separately have the ability to calculate useful results. Furthermore, the low values of W_a caused by the high rock content, are another major source for discrepancy between reference and simulations. High rock contents cause significantly higher infiltration rates than soils with lower rock contents. The high infiltration caused by the high rock content, acts like a preferential flow. However, HPTFs (but also B1) are not able to manage preferential flow, which causes an underestimation of R_a.

In this context, it is pointed to the maximal difference between HPTFs and reference in 2002 that was caused by the precipitation extremes in August. The precipitation extremes affected the difference in two ways: firstly, the infiltration was underestimated and so the soil water storage was overestimated, and secondly, HPTFs do not have ability to regard the distribution of precipitation within a period. So, the precipitation amount of the extreme events was assumed as uniformly distributed over the whole summer period. In that way, the evapotranspiration (especially in context to interception) was misinterpreted and caused significant differences to actual ET_a and actual R_a. But, also in the case of less extreme storms, the Black Box Description of HPTFs was not able to calculate correct values of ET_a and R_a, which is visible in the example of 2007 at the Spruce and at Agricultural site.

It is interesting that HPTFs match references of ET_a and R_a very well in the dry year of 2003. In particular it is remarkable that simulations with HPTFs match the reference even better than simulations with complex models (B1 and B2). In this context, the former statements are confirmed, which are related to effects of interception and infiltration. Interception and infiltration were low in 2003 because of low precipitation. Thus their influence to the water balance was also small and acceptable results were created with H1 in 2003.

For the general application of HPTFs, it is derived that HPTFs are not useable for sites that are similar to the Spruce and Agricultural site. So it is assumable, HPTFs are inappropriate for the most sites in the mountain and low mountain range. HPTFs mismatch the actual values of ET_a and of R_a significantly at sites where high infiltration rates and preferential flow respectively occur. Furthermore HPTFs are inappropriate, when correct estimations of interception are necessary for correct estimations of evapotranspiration. However, HPTFs create widely acceptable results at sites where interception is less important and infiltration rates are moderate such as at the investigated Grass site.

There are two reasons for the better results at the Grass site (in comparison to the other sites). Firstly, the soil at the Grass site has a significantly lower rock content than soils at other sites. Consequently the infiltration rate is significant lower and the soil water storage is higher than at the other sites. Secondly, interception and its percentage related to the evapotranspiration is significant lower for grass than for other land uses (especially for forests). That means that the Grass site is less affected by special characteristics of precipitation in context to duration, in-

tensity and frequency. Thus, the characteristics of the Grass site are more similar to characteristics of typical sites in Germany that caused a decrease of discrepancies between HPTFs and reference. However, it must be additionally supplemented that phenological phases are also less important for grass. So, generalized assumptions are sufficient for grass in contrast to crops.

In general and in the context of practical applications, the former analyses show that it is necessary for simulations of ET_a and R_a to use models with explicit descriptions of interception and soil water movement at sites in the mountains and low mountain range. Only in this way is it possible to simulate useable results of ET_a and R_a. A complex model with standard parameterization (B1) gives better results than Black Box Descriptions (HPTFs). The effort of parameterization was the same for B1 and for HPTFs (H1 and H2). A complex model with a simplified parameterization has the ability to regard effects of interception and soil water movement sufficiently. Thus a higher quality of simulation results can be attained without a higher effort for parameterization and without an increase of required input data.

Finally, it is noted that complex models with simplified parameterizations are useable for calculations of tendencies and guidelines. However, these simplified parameterizations are insufficient when exact quantifications of ET_a and R_a are needed. For these applications an extensive parameterization or calibration is required even when the focus is on an annual time scale. Thus an optimal reproduction of running processes is indispensable for exact quantifications.

6.5.4 Evaluation of Uncertainty in Model Results Caused by Uncertainty of Input Data

The effects of uncertainties in input data on simulation results were already suggested in the former analyses. It was visible in Figures 6.7 and Figure 6.8 that the uncertainties of input data caused a range of simulated values of ET_a and R_a. This range is called *simulation uncertainty* in the following text. It was observed that the simulation uncertainty sometimes crosses the borders of reference and is important for the decision if the simulation passes or fails the references. The focus of the following analyses does not concern the accuracy and applicability of models. Moreover, the simulation uncertainty is on focus. This means that the analyses are focused to the internal variations of simulation results caused by uncertainties in input data.

The variations of simulation results (and so the simulation uncertainty) were estimated on the basis of distance between 5 % and 95 % quantile respectively and the median. In that way, the typical range of simulation uncertainty was estimable and the typical influence of measurement uncertainties to simulation results was derivable. However, the quantification on basis of 5 % and 95 % quantile means that 10 % of simulations exceed the approximated range of simulation uncertainty. So, the maximal influence of measurement uncertainties is potentially higher. However, the focus was to describe the typical influence. In that context, the arrangement to the 5 % and 95 % quantile is a good assumption, especially for well supported measuring sites.

The estimated averages and the maxima of simulation uncertainties of ET_a and R_a are listed in Table 6.4 for all sites and all models. Additionally, the uncertainties of grass reference evapotranspiration ET_0 are listed as reference and for comparison. Thereby, the averages and the maxima of simulation uncertainties are shown in each case as absolute value [mm] and as relative value related to the median [%].

Table 6.4 Uncertainty of simulation results caused by uncertainties of input data (absolute values in mm)

variable	model	Spruce site		Grass site		Agricultural site	
		average	max	average	max	average	max
ET_0	-	36.6 (5.1%)	40.5 (5.6%)	33.4 (5.4%)	36.0 (5.9%)	40.7 (5.9%)	43.3 (6.1%)
ET_a	H1	22.8 (3.6%)	43.2 (5.5%)	27.2 (4.3%)	29.6 (4.7%)	25.3 (4.2%)	27.4 (4.4%)
ET_a	H2	22.1 (3.4%)	29.6 (3.7%)	28.8 (4.4%)	35.8 (5.8%)	26.8 (4.2%)	29.6 (4.7%)
ET_a	B1	27.6 (4.9%)	33.3 (5.6%)	23.0 (3.8%)	31.2 (5.4%)	22.2 (4.6%)	25.1 (5.6%)
ET_a	B2	27.8 (5.6%)	32.3 (6.4%)	23.7 (4.0%)	34.0 (5.6%)	22.9 (4.9%)	28.3 (5.8%)
R_a	H1	22.3 (7.7%)	31.1 (9.8%)	29.5 (7.4%)	35.4 (10.5%)	33.8 (9.9%)	40.5 (11.7%)
R_a	H2	23.5 (8.9%)	39.0 (11.8%)	30.4 (8.0%)	35.6 (10.5%)	36.1 (12.1%)	40.5 (15.1%)
R_a	B1	31.5 (9.1%)	41.6 (14.8%)	28.5 (6.3%)	35.0 (8.0%)	32.8 (7.0%)	42.0 (9.4%)
R_a	B2	31.4 (7.6%)	42.1 (12.9%)	29.7 (6.3%)	37.4 (9.3%)	34.3 (7.3%)	44.1 (9.9%)

It can be seen that the effect of measurement uncertainties on results of simulation is very similar for all sites and for all models. The uncertainty of input data typically causes a simulation uncertainty of 22.1 up to 28.8 mm in ET_a. However, the maximal simulation uncertainty of ET_a was extremely higher than the average for simulations with HPTFs (H1 and H2) in individual periods. The highest observed simulation uncertainty of ET_a was 43.2 mm in 2002 (H1). The reason for this untypical high simulation uncertainty was the extreme precipitation in August that caused an enormous uncertainty in precipitation data.

The high amount of precipitation as well as the high uncertainty of precipitation data caused that the model algorithm changed between the algorithm for wet conditions and the algorithm for dry conditions in relation to effective uncertainties in precipitation data (changeover effect). Thus the simulation uncertainty increases rapidly because of the inconsistent algorithms in HPTFs. The same effect also occurred in H2 simulations. However, the H2 simulations are more shifted to wet conditions because of higher W_a. Changeover effects (wet/dry) also occurred at the Grass and Agricultural site in 2007. However, the effects of changeover were less significant in 2007 than in 2002 because precipitation (and hence the uncertainty of precipitation) was lower in 2007. At the Spruce site no changeover effects were observed in 2007 because W_a was too low and so the threshold (wet/dry) was too high for a changeover from wet to wet conditions.

Changeover effects were not observed in the case of BROOK90 (B1 and B2) because of more consistent algorithms. However, the maximum of simulation uncertainties were also significantly higher than the average of simulation uncertainty. The observed maximum was 34.0 mm in the case of ET_a and occurred at the Grass site in the B2 scenario in 2005. It is derived in context to the occurrence of the highest simulation uncertainties that the simulation uncertainty depends significantly on total of precipitation. However, the simulation uncer-

tainty of BROOK90 is a complex interaction of uncertainties in different meteorological variables, in which many variables are not independent from another. In particular, uncertainties of global radiation R_G and the distribution of precipitation in yearly course are important for the characteristic of simulation uncertainty.

The comparison between simulation uncertainty of ET_a and R_a shows the simulation uncertainty of R_a is in the case of average values around 5 mm higher than the simulation uncertainty of ET_a. For the maximal values, the simulation uncertainty of R_a is even 7.1 mm on average higher than the simulation uncertainty of ET_a, at which the maximum was 17.0 mm. This means that the influence of uncertainties in meteorological input data is more important for R_a than for ET_a because the uncertainties of precipitation data affect the simulation uncertainty of R_a directly. However, they affect the simulation uncertainty of ET_a indirectly.

So, the uncertainty of ET_a is determined primarily by uncertainties of R_G and secondarily by uncertainties in precipitation data. However, R_a is directly affected by uncertainties in precipitation data and is directly as well as indirectly affected by uncertainties of R_G. The superposition of uncertainties in precipitation data and in data of R_G causes a significantly higher simulation uncertainty of R_a than of ET_a in most periods. However, the maximal values of simulation uncertainty were lower for R_a than for ET_a in some H1 and H2 simulations. But, these effects were caused only by already described changeover effects and were the result of complex interactions of uncertainties in input data. These effects do not represent the typical behaviour of model uncertainty.

The comparison of simulation uncertainties between ET_0 and ET_a show that the uncertainties of meteorological input data affects ET_0 stronger than ET_a. The uncertainties of ET_0 are predominately caused by uncertainties of measured R_G. So, uncertainties of R_G are also a major source of uncertainties for ET_a. However, the uncertainties in ET_a are also significantly affected by other meteorological variables, at which the inaction of variables and uncertainties is very complex. The inaction of variables typically causes a decrease of simulation uncertainties through damping and compensation effects. An exception is the maximum value of simulation uncertainty of ET_a for the H1 scenario at the Spruce site. However, it was caused only by untypical heavy changeover effects.

In general, the comparison of simulation uncertainties between ET_0 and ET_a clarifies that the complex inaction of variables avoids prognoses of uncertainties in simulation results by a simple superposition of individual measurement uncertainties. Furthermore, the inaction of variables and, particularly the interdependence of meteorological variables, produce unpredictable uncertainties in simulation results. In that context, the Monte-Carlo-Simulations are an applicable way to approximate a reliable range for simulation results and give the possibility to derive the uncertainties of simulations.

The analyses of relative values of simulation uncertainties are less meaningful than absolute values of uncertainty because the relative uncertainty depends on absolute values of ET_a and R_a. However, they are a good guideline for common evaluations. It can be assumed for practical applications that uncertainties of measurements cause uncertainties of around 5 % in simu-

lated ET_a and of around 10 % in simulated R_a. However it is noted that the given guidelines refer to actual measurement uncertainties and do not include uncertainties caused by generalization and regionalization of variables.

6.6 Concluding Remarks on Water Balance Simulations

The annual evapotranspiration ET_a and the annual seepage R_a were investigated at three sites (Spruce forest, Grassland, Agricultural land) in the low mountain range of the *Erzgebirge*. The investigations were related to the canopy scale (spatial scale < 0.75 km²). It was possible to ignore effects due to regionalization and generalization in data and parameters because of this small spatial scale. Furthermore, the investigations were focused primarily on the plant-atmosphere-interaction, for which eddy covariance data were used as reference. So, only the upper soil layers (affected by root water uptake and soil evaporation) needed to be considered in the investigations. The properties of deeper layers as well as processes in deeper layers (such as groundwater flow and groundwater storage) were negligible.

ET_a and R_a were simulated with two models of different complexity. Thereby the effects of complexity were investigated in relation to the accuracy of simulation. For a simple (Black Box) model, the HPTFs according to Wessolek et al. (2008) were chosen because this model is widely used in Germany in the context of the Hydrological Atlas of Germany (*Hydrologischer Atlas von Deutschland*). For a complex model BROOK90 was chosen to represent other complex models because the required input data were identical to HPTFs and it was possible to equalize the parameterization by some simplifications to parameterization of HPTFs.

The application of HPTFs showed the usage of HPTFs was insufficient at test sites. In this context, it is assumed that HPTFs are inappropriate in general for most sites in the mountain and low-mountain range. The observed difference between simulations and references were enormous at the Spruce and at the Agricultural site. Only at the Grass site were the discrepancies moderate and acceptable. The reasons for the discrepancies were:

(i) HPTFs do not have the ability to consider the special climatic conditions of site. Site specifics are major sources for discrepancies, which affect the evapotranspiration directly and especially in term of interception. Consequently, the non-observance of characteristic of predominate precipitation characteristic and the non-observance of seasonal distribution of precipitation causes significant discrepancies when interception is a major component of evapotranspiration such as in forest sites.

(ii) It is assumed, that the statistical interrelationships that are used in HPTFs are not applicable when the plant available water content W_a is extreme low or when preferential flow is not excludable at a site. In these cases, the role of fast infiltrating water is underestimated by HPTFs and causes significant underestimations of R_a and overestimations of ET_a. However, limitations of W_a (because of high rock content) or preferential flow because of root channels) are typical for sites in the mountain and low mountain range.

(iii) In the context of the Agricultural site, it was shown that the generalized assumption for growing season can also create significant discrepancies. Thereby, differences of growing season can be caused on the one hand by characteristics of individual plant species and on the other hand as a consequence of other climate conditions.

The application of a complex model with a simple parameterization (identical to HPTFs) improves the accuracy of model results significantly and improves the accuracy without additional expenses for parameterization and data. The improvements were caused primary by the consideration of the precipitation curve course and so by better reproduction of interception. Secondarily, the accuracy is improved by the explicit description of soil water movement and so by more realistic approximations of infiltration and soil water storage. However, it is not possible with this simple parameterization to regard effects of preferential flow and specifics of growing season. Thus, simple parameterizations are sufficient to describe the general behaviour of water balance at a site. However, the application of simple parameterized can cause unexpected uncertainties that are critical for quantifications or for the application at unmonitored sites.

Advanced parameterization or calibration improves the simulation results of complex models. So, in addition to a description of general behaviour of water balance it was possible to give exact quantification of water balance components under typical weather conditions. In particular, better results were realized in comparison to a simplified parameterization when the course of growing seasons or curve courses of vegetation height and LAI were sensitive parameters. However, the improvements do not create an impeccable model. So, well fitted models (like all other models) also showed important differences to reference data in the case of untypical weather conditions (such as extreme storms or extreme droughts). The reasons of these discrepancies were either restrictions of internal algorithms or variations of parameters in relation to climatic conditions.

The influence of measurement uncertainties to model results was also investigated. Thereby, Monte-Carlo-Simulations (called uncertainty model) were used to approximate the range of uncertainty which was caused by uncertainties in input data. It was shown that the applied uncertainty model was a practical and reliable method for the simulation and approximation of uncertainties. In particular, it was possible to quantify the uncertainties in the case of complex models and complex algorithms (which prevented the application of classical error approximations). Furthermore, the uncertainty model also implicitly regarded the complex interactions of meteorological input variables. So it gave more realistic results than classical error approximations.

The application of the uncertainty model showed that effects of measurement uncertainties were widely identical for the simple Black Box model (HPTFs) and for the complex water balance model (BROOK90). The uncertainty of simulated ET_a (caused by measurement uncertainties) was ca. 25 mm on average and 43.2 mm maximally. This means that an uncertainty about 5 % must be assumed for simulated ET_a, which is caused by measurement uncertainties. For R_a the uncertainty is slightly higher and was about 30 mm on average, for which

the maximum was 44.1 mm. So, an uncertainty of about 10 % must be assumed as guideline for R_a.

The main reasons for the uncertainties are predominately uncertainties in data of precipitation and global radiation. However, the effects of uncertainties in other meteorological input data were less important. In the context to precipitation data, uncertainties are not related to actual uncertainties of measurement, rather to uncertainties and vulnerabilities of precipitation correction. But even these uncertainties are major sources for uncertainties in simulation results. On another perspective, it was assessed that uncertainties in individual input data have less effect on the uncertainties of ET_a and R_a. That means, uncertainties of ET_a and R_a are lower than expected by the superposition of uncertainties of individual variables because of compensation effects and complex interactions of input variables. However, the analyses demonstrated in any case that uncertainties of measurement cause significant uncertainties in simulation results, which must be considered in investigations and evaluations of water balances.

7 Summary and Conclusions

7.1 General Objectives

The water balance and the soil-vegetation-atmosphere interaction were investigated at a spatial scale of canopy and primary at temporal scales of months and years. Thereby, the scale of canopy was defined by the footprint of an eddy-covariance (EC) system device and meant an area of around 0.75 km². The investigated sites were located in the eastern part of the *Erzgebirge* (Germany) and more precisely in the immediate vicinity of *Tharandter Wald*. The individual test sites were a Spruce (*Picea abies*), a Beech (*Fagus sylvatica*), a Grass and an Agricultural site. Thus the sites differ in vegetation cover. However, all sites were similar related to climate conditions, relief and soil. So it was possible to compare the sites directly and it was possible to evaluate effects of vegetation.

The investigations were based on different methods for measuring and estimation of water balance components. The following were used: sap flow measurements for estimation of transpiration, eddy covariance (EC-) measurements predominantly for estimation of total evapotranspiration, measurements of soil moisture for estimation of storage change and measurements of precipitation, canopy drip and stem flow for estimation of interception. Furthermore, meteorological standard measurements (temperature, wind speed, wind direction) and measurements of radiation and radiation balance were fundamental for this study.

The objective of this study was to investigate the effects of different vegetation on the water balance. To do this, the combination of different measurement methods was necessary to derive components of water balance, which were not measurable directly. In this way it was possible to estimate tendencies of seepage and to estimate the magnitude of soil evaporation. Another main object of investigation was the assessment of accuracies and uncertainties of measured and derived values. An additional object was to analyze effects of measurement uncertainties to results of water balance simulations. That means that the effects of uncertainties in input data as well as the uncertainties of reference data were investigated. In general, this study was focused on analyses of effects of uncertainties on the evaluations of water balance and water balance components.

7.2 Provision of Reference Data of Evapotranspiration

Chapter 3 was dedicated to the provision of reference data of evapotranspiration. Here, the processing of EC raw-data was of main concern with focus on the correction of the spectral attenuation (spectral correction). The spectral correction is an important step in raw data processing especially for closed-path EC system devices. Four different methods for estimation and correction of spectral attenuation in EC raw data were tested and compared. Although estimated correction coefficients differed significantly between individual methods, the effects were small for absolute values of individual half-hourly data sets. However, the choice of methods has significant influence on monthly totals of estimated evapotranspiration (and carbon dioxide exchange).

The maximal differences between individual methods concerning monthly totals were up to 20 mm (30 %) in relation to the correction according to Moore (1986), which was used as reference. However, the average differences were smaller and were typically lower than 10 mm (less than 20 %) related to the monthly total of reference. In this context, results showed that the differences between individual methods depend on predominant weather conditions. Differences increased in the case of stable atmospheric stratification. Furthermore, differences increased also in the case of high wind speeds, which were typically related to a neutral stratification. However, the differences were small in the case of unstable stratification and low wind speed.

7.3 Measuring, Estimation and Evaluation of Water Balance Components at Canopy Scale

7.3.1 Input Terms of Water Balance

The general objectives of Chapter 4 and Chapter 5 were the assessment of the water balance and its components by a combination of different measurement methods. The main objective was to evaluate and to compare the water balance and individual components of the water balance in a Spruce and a Beech stand. The input of water balance (the net precipitation) was the main object of investigation in Chapter 4. However, the analysis of individual outputs of water balance (evapotranspiration, transpiration, soil evaporation and seepage) was focused on in Chapter 5. Thereby, the investigations were related to two main growing seasons (April to October). One of them (growing season 2006) was dry and unusually warm, and the other (growing season 2007) was cooler and more humid compared to the first one. The growing season of 2007 was also influences by effects of the storm *Kyrill* in January 2007.

It was shown in Chapter 4 that the net precipitation (percentage of precipitation that becomes available for plants) and interception was almost identical in both stands in the growing season. So, the net precipitation was around two-thirds and the interception one-third of precipitation in the statistical average at each site. However, the actual values of net precipitation and of interception, (related to specific events of precipitation or to specific months) differed significantly from average. Thereby, the variations were larger at the Spruce site than at the Beech site. In this context, the net precipitation consisted of one-third of stem flow at the Beech site. That means that 20 to 25 % of precipitation reached the forest floor as stem flow at the Beech site. However, stem flow was negligible at the Spruce site.

Other objects of investigation were the estimation of (direct) throughfall and canopy storage capacity. At both sites, the canopy storage capacity was very similar. The canopy storage capacity of the Spruce site was typical for coniferous forests whereas the canopy storage capacity of the Beech site was higher than typical for broadleaf forests. Related to the LAI (leaf area index), the storage capacity per leaf area was significantly higher at the Beech site than at the Spruce site. Thus the structure of leaves and the form of tree crowns were additional important parameters, which must be considered in interception models besides LAI.

The direct throughfall is an important component of net precipitation, because it is the only variable which is directly controllable by forest operations. The estimated percentages of direct throughfall were 12 % at the Spruce site and 14 % at the Beech site related to precipitation measured according to meteorological standards. These results corresponded very well with estimates based on sky view coefficients. Therefore, it can be assumed that forest operations such as thinning can increase the percentage of throughfall and can affect the input of water balance significantly.

7.3.1 Output Terms of Water Balance

The outputs of water balance were in the focus of Chapter 5. Thereby, the same test sites as well as the same periods of investigations were used as in Chapter 4. Most analyses were related to investigations and evaluations of individual components of evapotranspiration; but the soil water storage and seepage were also analysed. The interpretation of measurements results was very complex. The reasons were, on the one hand, uncertainties of measurement, superposition of uncertainties and different scales of measurement; and on the other hand, the complexity of interpretation was reinforced due to effects of the winter storm *Kyrill*.

The evapotranspiration as well as the canopy transpiration (transpiration derived from EC measurements) were very similar at both sites and in both investigated periods. However, the transpiration characteristic of adult trees showed significant differences between the period before and after *Kyrill*. It can be assumed that the storm caused long-lasting damage especially at the Spruce site. The transpiration of adult trees decreased at the Spruce site in the period after *Kyrill*. However, the decrease of transpiration of adult trees was compensated by an increase of transpiration from the understory.

Interception was not affected by the storm at both sites. More precisely, effects of the storm were not detected in interception data. Furthermore, storm effects were also not found in data of transpiration of adult trees at the Beech site. It was assumed that the damage were not so heavy at the Beech site compared to the Spruce site. The storm damages due to *Kyrill* were compensated by better water supply in the following growing season. In another context it was possible to identify the importance of evaporation of litter at the Beech site. The evaporation of litter had nearly the same magnitude as transpiration of understory at the Spruce site.

The interpretation of derived seepage and soil water storage was massively affected by measurement uncertainties and especially by different scales of measurements. Therefore, it was not possible to find representative estimates of soil water storage because of significant heterogeneity of soil properties at the test sites. The heterogeneity of soil properties affects the representativeness of measured soil moisture more under dry conditions than under wet conditions. In context to heterogeneity of soil properties and to enormous measurement uncertainties, quantitative analyses of seepage were excluded. However, it was possible to compare and to evaluate the general behaviour of seepage at both sites.

Differences of seepage between both sites were primarily caused by different soil properties. However, effects of vegetation were unimportant under typical weather conditions. Effects

were identifiable only under extremely dry conditions. These effects were caused by different transpiration due to different water supply. Therefore, in general and with regard to the enormous uncertainties it could be stated the water balance and its components were very similar at both sites for the two investigated growing seasons. In particular, differences of vegetation were insignificant in the context of measurement uncertainties and the heterogeneity of soil properties.

7.4 Influence of Measurement Uncertainties and of Model Complexity on Results of Water Balance Simulations

7.4.1 Effects of Measurement Uncertainties

The investigation of measurement uncertainties was also the focus of Chapter 6. Here, the effects of uncertainties on simulations of evapotranspiration and seepage were investigated for three sites (Spruce, Grass and Agricultural site). At first the effects caused by measurement uncertainties in input data were investigated by Monte-Carlo-Simulations. The term *uncertainty* was related to actual uncertainties of measurement. However, effects of regionalization and generalization were excluded. Uncertainties in input data of precipitation and global radiation caused significant uncertainties in simulated evapotranspiration and simulated seepage. However, the effects of measurement uncertainties in other input data (such as temperature, wind speed and air humidity) were negligible. In general it was derived that uncertainties of measurements caused an uncertainty on simulated annual evapotranspiration of around 25 mm (5 %) on average. However, the uncertainty of simulated annual seepage was higher and was around 30 mm (10 %) on average.

It was demonstrated that Monte-Carlo-Simulations (called uncertainty model) are a practical and reliable method for the estimation of effects due to measurement uncertainties in water balance simulations. In particular the method holds the ability to quantify the effects of uncertainties in case of complex models and in case of complex algorithms, which do not allow the application of classical error approximations. Furthermore, the uncertainty model regards implicitly also the complex interactions of meteorological input variables. Thus the uncertainty model generates more realistic results than a classical error approximation.

The uncertainties in reference data of evapotranspiration and seepage were analyzed and evaluated in Chapter 6. Data of evapotranspiration based on measured latent heat flux (EC method) were taken as reference data. To account for an unclosed energy balance the available energy was partitioned into sensible and latent heat flux according to the Bowen ratio. Based on the uncertainty analysis the actual value of annual evapotranspiration should be within the range between 85 % and 130 % of estimated reference. The uncertainty of seepage was defined predominately by uncertainties of evapotranspiration. However, additional uncertainties (predominately uncertainties of precipitation data) caused an increase of uncertainty. In case of seepage the results indicate that the actual values of annual seepage should be in between 67 % and 118 % of the here used reference data.

7.4.2 Effects of Model Complexity

The effects of model complexity on simulation results were analyzed by comparison of two water balance models of different complexity. These models were: a simple Black Box Model (HPTFs) and a complex water balance model (BROOK90). In case of the complex model two scenarios of parameterization were used. The first scenario was a simplified parameterization where the effort of parameterization was similar to that of HPTFs and the second scenario was extensively parameterized and well calibrated.

The HPTFs did not have the ability to simulate the annual evapotranspiration and seepage in sufficient accuracy. The reason was that the HPTFs did not regard the special characteristics of climate and soil at the test sites. The model did not have the ability to consider actual values of interception and infiltration. Therefore, the model failed on sites where preferential flow and interception were relevant processes.

In contrast to HPTFs, BROOK90 had the ability to simulate the annual evapotranspiration and seepage in sufficient accuracy. Already with the simplified parameterization option, it was possible to derive tendencies and to evaluate the behaviour of water balance at a specific site. However, quantitative analyses were only possible with extensively parameterized and calibrated models. However, complex models also failed in some cases even when they were extensively parameterized and calibrated. Significant differences to references occurred under untypical weather conditions. In particular, significant differences were found when the specific period was affected by droughts or extreme precipitation events. Thereby, the reasons for mismatches were either restrictions of internal algorithms or variations of parameters in dependence to climatic conditions.

7.5 Final Conclusions

The estimation and quantification of uncertainties was a core point of the present study. It was shown in all chapters that effects of uncertainties have fundamental importance for the estimation, the simulation and the evaluation of water balance components (even at canopy scale). The term *uncertainty* was related to actual uncertainties of measurement, superposition of measurement uncertainties, uncertainties due to different scales of measurements and uncertainties of models. It was demonstrated that uncertainties have the ability to blur differences in the water balance between sites. That means that special characteristics of water balance components (caused by vegetation and soil) were overlain by uncertainties. In this context, it was difficult to find special effects of vegetation and soil. In particular, it was found that these effects were only relevant under untypical weather condition. However, they were ignorable under typical weather conditions.

The results of this study are in contrast to the results of many former studies (Benecke 1984, Weihe 1984, Weihe 1985, Tužinský 2000, Komatsu et al. 2007, FVA 2010), which report significant differences between deciduous and evergreen forests concerning their water balances. It has to be kept in mind that (i) this study concerns the vegetation period only and (ii) a site water budget is determined by many site-specific parameters and by the complex inter-

action of parameters. The estimation and the evaluation of a site water budget is always a case study due to different site characteristics. Therefore, comparison of sites is limited as they are affected by uncertainties due to different conditions. The influence of vegetation on the water balance at a catchment scale should be interpreted carefully and should only be transferred to other sites with caution. Furthermore, effects of measurement uncertainties were often ignored or were only considered insufficiently in former studies and the results should be revisited carefully in relation to measurement uncertainties. The study indicates that effects of uncertainties increase at larger spatial scales because of additional uncertainties due to regionalization, generalization and spatial averaging.

Appendix

A1 Correction Algorithm applied to obtain Energy and Mass Fluxes

(1) De-spiking: De-spiking identifies the removal of outliers in the raw data: first, the measured data were tested against their physical plausibility. Second, all values outside $\bar{x} \pm \sigma_x^2$ were marked in an iterative process. Here $\bar{x}$ is the arithmetic mean and σ_x^2 the standard deviation of the dataset in the corresponding iteration loop. The located errors or outliers were replaced by an interpolation between the next valid data points. Please note, for spectral investigations (Chapter 3; but not for flux or balance calculations) only datasets with less than 50 invalid data points, were used.

(2) Tilt Correction: The tilt correction (also called rotation) is a coordinate transformation that is used to eliminate the horizontal components in the measured vertical wind speed w. Here, a double rotation is used as described in Foken (2006).

(3) Time Lag Removal: In case of closed-path EC system devices (Spruce site, Gras site, Agricultural site), the transport of air through the intake tube introduces a time delay between the eddy signals from the ultrasonic anemometer and from the gas analyser. The size of this time lag depends on the actual flow rate, which is strongly influenced by the condition of the particle filter. The time delay was estimated for individual half-hourly datasets by the determination of peak in cross-covariance (correlation between fluctuation of vertical wind speed w' and fluctuation of gas concentration c'). But also open-path EC system devices can be affected by a time delay between measured vertical wind speed w and measured gas concentration c. However, it depends only on hardware internal data processing routines and is constant for every data set. The time delay in data of the open-path EC system at Beech site was -0.1 s.

(4) Calculations of Raw Fluxes: In the forth step the covariances and accordingly the raw fluxes as well as the spectra and the cospecta were calculated. At first the linear trend was eliminated by using a half-hour block average. Additionally a Hamming-window was applied (Kaimal and Kristensen 1991) for spectra and cospectra calculations. The linear de-trending and the half-hourly block average was a compromise between the necessary stationary conditions on the one hand and avoiding of low frequency attenuation on the other hand. Other high-pass filters were also tested: different splines and running means with different averaging periods. However, the influence to the calculated fluxes and correction coefficients (Chapter 3) was negligible.

(5) Spectral correction: The correction of spectral attenuation is main topic of Chapter 3. There four different methods for estimation and correction of hardware caused attenuations effects are tested. Primary it was used the correcting algorithm according to Moore (1986). However, this algorism was insufficient for the EC system device at Spruce site (Grünwald 2002). So, the algorithm of Bernhofer et al. (2003) was used at Spruce site, which is described in detail in Chapter 3.

(6) Sonic temperature (Schotanus) correction: As with most EC systems the sensible heat flux is determined by using the sonic's accoustic temperature. In consequence, the sonic temperature's dependence from air density changes due to moisture changes and from momentum flux has to be considered. Here, the standard correction according to Schotanus et al. (1983) was used.

(7) WPL (Density) correction: The gas concentration measured by the open-path-gasanalyzer (Beech site) depends on the actual air density. Accordingly the estimated water vapour and carbon dioxide fluxes are depending on the air density. For correction the algorithm according to Webb et al (1980) was used. In the case of closed-path systems (Spruce site, Gras site, Agricultural site) an adequate correction is not necessary. The long intake tube damps temperature fluctuations as well as the related density fluctuations. So, a density correction is dispensable (Rannik 1997)

(8) Quality check: Completing the flux processing several quality checks were done. For this study, it was concentrated on the stationary tests as described by Foken and Wichura (1996). For spectral investigations of Chapter 3 only datasets with stationary classes of 3 or better (9 being poor and 1 perfect) were used.

(9) Gap filling: The last point is not related to actual flux processing. It means the closure of data series in case of failures of EC system device. Small gap with a maximal length of 1 hour were closed by an interpolation between the next valid data. But larger gaps were closed by mean diurnal courses of 7 days (Grünwald and Bernhofer 2007).

A2 Technical Details about EC System Devices at Test Sites

instrument or component	Spruce site	Gras site	Agricultural site	Beech site
type of EC system device	closed-path	closed-path	closed-path	open-path
ultra sonic anemometer	Solent Gill R2 (Gill Instruments); since May 2006: Solent Gill R3 (Gill Instruments)	Solent Gill R3(Gill Instruments)	Solent Gill R3(Gill Instruments)	Campbell CSAT3 (Campbell Sientific)
gas analyser	LI 6262 (LI-COR Biosciences); since Nov. 2006: LI 7000 (LI-COR Biosciences)	LI 7000 (LI-COR Biosciences)	LI 7000 (LI-COR Biosciences)	LI 7500 (LI-COR Biosciences)
sensor distance	~ 20 cm (distance between sonic and tube inlet)	6 cm (distance between sonic and tube inlet)	7 cm (distance between sonic and tube inlet)	~ 25 cm (distance between sonic and gas analyzer)
primary tube tube length internal diameter flow rate	 59 m 10.7 mm ~ 50 L min^{-1}	 3.8 m 4 mm ~ 3 L min^{-1}	 7.8 m 4 mm ~ 5 L min^{-1}	---
secondary tube tube length internal diameter flow rate	 4 m 4 mm ~ 4 - 6 L min^{-1}	---	---	---
particle filter	Gelman ACRO50 PTFE, Ann Arbor, MI, USA; pore width ≤ 1 µm	Gelman ACRO50 PTFE, Ann Arbor, MI, USA; pore width ≤ 1 µm	Gelman ACRO50 PTFE, Ann Arbor, MI, USA; pore width ≤ 1 µm	---
data recording	PC, ~ 20 s^{-1}, Binary files (30 min data sets)	PC, ~ 20 s^{-1}, Binary files (30 min data sets)	PC, ~ 20 s^{-1}, Binary files (30 min data sets)	Logger: Campbell CR5000 (Campbell Sientific), 10 s^{-1}, ring buffer (5 - 10 days), however 30 min data sets (ASCII files) used for flux processing

A3 Attenuation terms and equations of the component specific or process specific sub-transfer-functions

affected device component and reference	equation*
sensor separation (Moore 1986)	$T_s(f) = \exp\left(-9.9\left(\frac{f\ s}{u}\right)^{1.5}\right)$
path averaging at anemometer (Moore 1986)	$T_w(f) = \frac{2}{\pi\ f_P}\left(1+\frac{1}{2}\exp(-2\pi\ f_P) - 3\frac{1-\exp(-2\pi\ f_P)}{4\pi\ f_P}\right);\ f_P = \frac{f\ p_1}{u}$
path averaging at gas analyzer (Moore 1986)	$T_x(f) = \frac{1}{2\pi\ f_P}\left(3+\exp(-2\pi\ f_P) - 4\frac{1-\exp(-2\pi\ f_P)}{2\pi\ f_P}\right);\ f_p = \frac{f\ p_2}{\mathrm{v}_P}$
sensor inertia (Moore 1986)	$T_g(f) = \frac{1}{\sqrt{1+(2\pi\ \tau\ f)^2}}$
sensor response mismatch (Moore 1986)	$T_m(f) = \frac{1+(2\pi\ f)^2\ \tau_1\ \tau_2}{\sqrt{1+(2\pi\ f\ \tau_1)^2}\ \sqrt{1+(2\pi f\ \tau_2)^2}}$
aliasing effects (Moore 1986)	$T_a(f) = \begin{cases} 1+\left(\frac{f}{f_M - f}\right)^b & f \le f_{Ny} \\ 0 & f > f_{Ny} \end{cases}$
high pass filter: linear detrending (Aubinet et al. 2000)	$T_h(f) = 1 - \frac{\sin^2(\pi\ f\ t_{ds})}{(\pi\ f\ t_{ds})^2} - 3\left(\frac{\frac{\sin(\pi\ f\ t_{ds})}{\pi\ f\ t_{ds}} - \cos(\pi\ f\ t_{ds})}{\pi\ f\ t_{ds}}\right)^2$
tube attenuation (Aubinet et al. 2000)	$T_t(f) = \exp\left(-40\ l_t\ d_t\ \mathrm{Re}^{-\frac{1}{8}}\left(\frac{f}{\mathrm{v}_t}\right)^2\right);\ \mathrm{Re} = \frac{d_t\ \mathrm{v}_t}{\upsilon_{kin}}$ Note: turbulent flow is assumed; l_t is approximated by the total tube length (sum of primary and secondary tube); v_t is approximated as quotient between l_t and the time delay TL
resulting whole transfer function (Moore 1986)	$T(f) = T_s\ T_g(\tau_1)\ T_g(\tau_2)\ T_m\ \sqrt{T_w}\ \sqrt{T_x}\ T_t\ T_a\ T_h$

* List of all not already identified symbols

b: dimensionless parameter
d_t: tube internal diameter
f_M: measurement frequency
f_{Ny}: Nyquist-frequency
l_t: total tube length
p: path length of measurement
Re: Reynolds-number
s: separation of sensors
t_{ds}: averaging time
TL: time delay between sonic and gas analyzer
u: wind speed
v_p: flow velocity through the measurement chamber of the gas analyzer
v_t: flow velocity in the tube
ν_{kin}: kinematic viscosity
τ: sensor inertia

Abbreviations, Figures, Tables

Most common Abbreviations*

AE ..... available energy (R_n + G)

EC..... eddy-covariance method

E_s ..... soil evaporation

ET..... evapotranspiration

ET_0..... FAO grass reference evapotranspiration

G..... soil heat flux

H..... sensible heat flux

HPTFs..... hydro-pedotransfer functions according to Wessolek et al. (2008)

I ..... interception

LAI ..... leaf area index

LE..... latent heat flux

P..... precipitation (measured according to meteorological standards)

P_a ..... annual total of precipitation

PAR..... photosynthetic active radiation

P_c ..... canopy drip

P_d ..... (canopy) drainage

P_n ..... net precipitation

P_s..... stem flow (Chapter 4 and Chapter 5); precipitation in summer months (Chapter 6)

P_t..... (direct) throughfall

R ..... seepage

R_G ..... global radiation

RH ..... relative humidity

R_N ..... net radiation

S_c ..... canopy storage

T ..... transpiration; temperature (consider context)

T_C..... canopy transpiration

T_{EC}..... transpiration derived from EC measurements

T_{max}/T_{min} ... maximum/ minimum of air temperature for the day

T_{SF} ..... transpiration derived from sap flow measurements

VPD ..... vapour pressure deficit

W_a ..... plant available water within the root zone

e..... vapour pressure

g_a ..... aerodynamic conductance

g_c ..... canopy conductance

p_n ..... percentage of P_n related to P

p_t..... throughfall coefficient

u ..... wind speed

$\Re^2$ ..... coefficient of determination

ΔET ..... uncertainty of evapotranspiration

ΔP..... uncertainty of corrected daily precipitation (correction according to Richter 1995)

ΔP_c ..... uncertainty of canopy drip

ΔP_n ..... uncertainty of net precipitation

ΔR ..... uncertainty of seepage

ΔS..... total change of energy storage within the canopy

Θ..... soil moisture, soil water storage

$\Delta\Theta$ ..... change of soil water storage; spatial variation of measured soil moisture (consider context)

σ ..... standard derivation

* Special abbreviations are explained in their respective context

Figures

Tables

References

Ad-hoc-AG Boden (2005): Bodenkundliche Kartieranleitung. 5. Aufl., Schweizerbart'sche Verlagsbuchhandlung, Hannover, 438 pp.

Allen RG, Pereira LS, Raes D, Smith M (2006): Crop Evaporation (guidelines for computing crop water requirements). FAO Irrigation and Drainage Paper No. 56

Ammer C, Albrecht L, Borchert H, Brosinger F, Dittmar C, Elling W, Ewald J, Felbermeier B, von Gilsa H, Huss J, Kenk G, Kölling C, Kohnle U, Meyer P, Mosandl R, Moosmayer HU, Palmer S, Reif A, Rehfuess KE, Stimm B (2005): Zur Zukunft der Buche (Fagus sylvatica L.) in Mitteleuropa – Kritische Anmerkungen zu einem Beitrag von Rennenberg et al. (2004). Allgemeine Forst- und Jagdzeitung, 176: 60-67.

Aubinet M, Grelle A, Ibrom A, Rannik Ü, Moncrieff J, Foken T, Kowalski AS, Martin PH, Berbigier P, Bernhofer C, Clement R, Elbers J, Granier A, Grünwald T, Morgenstern K, Pilegaard K, Rebmann C, Snijders W, Valentini R, Vesala T (2000): Estimates of the Annual Net Carbon and Water Exchange of Forests: The EUROFLUX Methodology. Advances Ecol. Res., 30: 113- 175

Aubinet M, Heinesch B, Yernaux M (2003): Horizontal and Vertical CO2 Advection in a Sloping Forest. Boundary-Layer Meteorol. 108(3): 397- 417

Barner J (1987): Hydrologie - Eine Einführung für Naturwissenschaftler und Ingeniere. Quelle & Meier Verlag, Heidelberg Wiesbaden, 256 pp.

Baumgartner A, Liebscher HJ (1996): Allgemeine Hydrologie – Quantitative Hydrologie, 2. Auflage, Gebrüder Bornträger Berlin Stuttgart, 694 pp.

Beck C, Rudolf B, Schönwiese CD, Staeger T, Trömel S (2007): Entwicklung einer Beobachtungsdatengrundlage für DEKLIM und statistische Analyse der Klimavariabilität. Berichte des Inst. Atmosphäre u. Umwelt, 6, Univ. Frankfurt/M., 107 pp.

Benecke P (1984): Der Wasserumsatz eines Buchen- und eines Fichtenwaldökosystems in Hochsolling. Schriften aus der Forstlichen Fakultät der Universität Göttingen und der Niedersächsischen Forstlichen Versuchsanstalt, 77, J.D. Sauerländer's Verlag Frankfurt am Main, 158 pp.

Benecke P, Ellenberg H (1986): Umsatz und Verfügbarkeit des Wassers im Buchen- und Fichtenbestand. In: Ellenberg H, Mayer R, Schauermann J (Hrsg.): Ökosystemforschung - Ergebnisse des Solling-Projekts 1966-1986. Ulmer Verlag, Stuttgart: 356-374

Bernhofer C (2003): Tharandt- Anchor Station Germany in FLUXNET. In: Integration worldwide CO2 flux measurements. Available via dialog: http://www.fluxnet.ornl.gov/fluxnet/sitepage.cfm?SITEID=404. (accessed Jan. 07th 2008)

Bernhofer C, Aubinet M, Clement R, Grelle A, Grünwald T, Ibrom A, Jarvis P, Rebmann C, Schulze ED, Tenhunen JD (2003a): Spruce forests (Norway and Sitka spruce, including Douglas fir): Carbon and water fluxes and balances, ecological and ecophysiological determinants. In: Valentini R (ed) Fluxes of Carbon, Water and Energy of European Forests, Ecological Studies 163. Springer, Berlin Heidelberg

Bernhofer C, Feigenwinter C, Grünwald T, Vogt R (2003b): Spectral correction of water and carbon flux of EC measurements at the Anchor Station Tharandt. In Bernhofer C (ed): Flussbestimmung an komplexen Standorten. Tharandter Klimaprotokolle Band 8. Eigenverlag der Technischen Universität Dresden, 113 pp.

Bernhofer C, Grünwald T, Köstner B. (2002): Verdunstung. In Bernhofer C (ed): Exkursions- und Praktikumsführer Tharandter Wald – Material zum hydrologisch-meteorologischen Feldpraktikum. Tharandter Klimaprotokolle, Band 6. Eigenverlag der Technischen Universität Dresden, 292 pp.

Bernhofer C (2002): Exkursions- und Praktikumsführer Tharandter Wald. Tharandter Klimaprotokolle, Band 6. Eigenverlag der Technischen Universität Dresden, 292 pp.

Bundesanstalt für Gewässerkunde (2003): Hydrologischer Atlas von Deutschland. Available via dialog: http://maps.wasserblick.net:8080/ (accessed May 10th 2010)

Butter D (2001): 10 Jahre Waldumbau in Sachsen. AFZ/ Der Wald, 55: 995-997

CarboEurope-IP (2008a): Integrated project CarboEurope-IP, Assessment of the European Terrestrial Carbon Balance. Available via dialog: http://www.carboeurope.org/ (accessed Nov. 19th 2009)

CarboEurope-IP (2008b): Ecosystem Component Database. Available via dialog: http://gaia.agraria.unitus.it/database/carboeuropeip/ (accessed Jan./ 22nd 2010)

Čermák J, Kučera J, Nadezhdina N (2004): Sap flow measurements with some thermodynamic methods, flow intergration within trees and scaling up from sample tree to entire forest stands. Trees, 18: 529-546

Clausnitzer F (2008): Personal communication, Sep. 2008

Crockford H, Richardson DP (1987): Factors Affecting the Stemflow Yield of a Dry Sclerophyll Eucalypt Forest, a Pinus Radiata Plantation and Individual Trees within the Forests. Technical Memorandum 87/11, CSIRO, Institute of Natural Resources and Environment, Division of Water Resources Research, Canberra, 82 pp.

Dietz J, Hölscher D, Leuschner C, Hendrayanto (2007): Rainfall Partitioning in Relation to Forest Structure in Differently Managed Montane Forest Stands in Central Sulawesi, Indonesia. Forest Ecology and Management 237: 170-178

Dingman SL (2002): Physical Hydrology, Second Edition. Prentice-Hall, Upper Saddle River, New Jersey, 646 pp.

Dyck S, Peschke G (1995): Grundlagen der Hydrologie, 3. Auflage. Verlag für Bauwesen, Berlin, 536 pp.

Ebermann S (2010): Die Rolle des Wurzelstockes der Buche bei der Infiltration des Stammabflusses – Die Wirkung des Wurzelstockes der Buchen auf die Wasserverteilung im Boden. Diplomarbeit am Institut für Bodenkunde und Standortslehre (Professur für Standortslehre und Pflanzenernährung) der Technischen Universität Dresden

Eichelmann U, Prasse H (2008): Personal communication, Aug. 2008

Eishold B (2002): Überprüfung der Eignung des physikalisch begründeten Ansatzes "BROOK90" für die Berechnung von N-A-Charakteristika in Einzugsgebiet des Weißeritz. Diplomarbeit am Lehrstuhl für Hydrologie und Meteorologie (Professur für Hydrologie) der Technischen Universität Dresden, 88 pp. (and appendix 51 pp.)

Ellenberg H (1996): Vegetation Mitteleuropas mit den Alpen: In ökologischer, dynamischer und historischer Sicht (Uni-Taschenbücher L), 5. Auflage. UTB, Stuttgart, 1095 pp.

Eugster W, Senn W (1995): A Cospectral Correction Model for Measurement of Turbulent NO2 Flux. Boundary- Layer Meteorol., 74(4): 321-340

Falkengren-Grerup U (1989): Effect of Stemflow on Beech Forest Soils and Vegetation in Southern Sweden, Journal of Applied Ecology, 26: 341-352

Federer CA (2002): BROOK 90: A simulation model for evaporation, soil water, and streamflow. Available via dialog: http://home.roadrunner.com/~stfederer/brook/brook90.htm (accessed 16th Nov. 2009)

Feigenwinter C, Bernhofer C, Eichelmann U, Heinesch B, Hertel M, Janous D, Kolle O, Lagergren F, Lindroth A, Minerbi S, Moderow U, Mölder M, Montagnani L, Queck R, Rebmann C, Vestin P, Yernaux M, Zeri M, Ziegler W, Aubinet M (2008): Comparison of horizontal and vertical advective CO2 fluxes at three forest sites. Agric. For. Meteorol., 148: 12-24

Feigenwinter C, Bernhofer C, Vogt R (2004): The Influence of Advection on the Short Term CO2-Budget in and Above a Forest Canopy. Boundary-Layer Meteorol., 113(2): 397-417

Finnigan JJ, Clement R, Malhi Y, Leuning R, Cleugh HA (2003): A Re- Evaluation of Long- Term Flux Measurement Techniques - Part I: Averaging and Coordinate Rotation. Boundary- Layer Meteorol., 107(1): 1-48

FLUXNET (2007): Integration Worldwide CO2 Flux Measurements. Available via dialog: http://www.fluxnet.ornl.gov/fluxnet/index.cfm (accessed 19th Nov.2009)

Foken T (2006): Angewandte Meteorologie: Mikrometeorologische Methoden, 2. überarbeitete und erweiterte Auflage. Springer, Berlin, 326 pp.

Foken T, Wichura B (1996): Tools for quality assessment of surface-based flux measurements. Agric. For. Meteorol., 78 (1–2): 83-105.

Foken T, Wimmer F, Mauder M, Thomas C, Liebethal C (2006): Some Aspects of the Energy Balance Closure Problem. Atmos. Chem. Phys., 6: 4395-4402

Franke J (2009): Risiken des Klimawandels für den Wasserhaushalt – Variabilitätund Trend des zeitlichen Niederschlagsspektrums. Dissertation am Lehrstuhl für Hydrologie und Meteorologie (Professur für Meteorologie) der Technischen Universität Dresden, 107 pp.

Franke J, Bernhofer C, Enke W (2006a): A method to derive future design precipitation on the basis of weather patterns in low mountain range. Meteorological Applications, 16 (4): 513-522

Franke J, Goldberg V, Mellentin U, Bernhofer C (2006b): Risiken des regionalen Klimawandels in Sachsen, Sachsen-Anhalt und Thüringen. Wissenschaftliche Zeitschrift der TU Dresden, 55: 97-104

Franke J, Köstner B (2007): Effects of recent climate trends on the distribution of potential natural vegetation in Central Germany. International Journal of Biometeorology, 52 (2): 139-147

Fuchs S, Lutz M (1999): Empirische Regression. In: Stöcker H. (Ed.) Mathematik, Der Grundkurs, Band 3, Lineare Algebra, Optimierung, Wahrscheinlichkeitsrechnung und Statistik. Verlag Harri Deutsch, 388 pp.

Fürst C, Makeschin F, Eisenhauer DR (2004): Sustainable methods and ecological processes of a conversion of pure Norway and Scots pine stands into ecologically adapted mixed stands. Contr. Forest Sciences, 20: 1-35

FVA [Forstliche Versuchs- und Forschungsanstalt] Baden-Württemberg (2010): Zukunftsorientierte Waldwirtschaft. Available via dialog http://www.zukunftswald.de (accessed 17th Aug. 2010)

Gash JHC (1986): A note on estimation the effect of a limited fetch on micrometeorological evaporation measurements. Boundary- Layer Meteorol. 35(4): 409-413

Gash JHC (1979): An analytical model of rainfall interception by forests. Quarterly Journal of the Royal Meteorological Society, 105: 43-55

Gerold D (2004): Zuwachs und Ertrag der Fichte. AFZ/ Der Wald, 22: 1223-1226

Geßler A, Rienks M, Dopatka T, Rennenberg H (2005): Radial variation of Sap Flow Densities in the Sapwood of Beech Trees (Fagus sylvatica). Phyton-Annales Rei Botanicae, 45 (3): 257-266.

Göckede M, Foken T, Aubinet M, Aurela M, Banza J, Bernhofer C, Bonnefond JM, Brunet Y, Carrara A, Clement R, Dellwik E, Elbers J, Eugster W, Fuhrer J, Granier A, Grünwald T, Heinesch B, Janssens IA, Knohl A, Koeble R, Laurila T, Longdoz B, Manca G, Marek M, Markkanen T, Mateus J, Matteucci G, Mauder M, Migliavacca M, Minerbi S, Moncrieff J, Montagnani L, Moors E, Ourcival JM, Papale D, Pereira J, Pilegaard K, Pita G, Rambal S, Rebmann C, Rodrigues A, Rotenberg E, Sanz MJ, Sedlak P, Seufert G, Siebicke1 L, Soussana JF, Valentini R, Vesala T, Verbeeck H, Yakir D: Quality control of CarboEurope flux data – Part I: Footprint analyses to evaluate sites in forest ecosystems. Biogeosciences Discuss., 4: 4025-4066

Granier A, Biron P, Lemoine D (2000): Water Balance, Transpiration and Canopy Conductance in Two Beech Stands. Agric. For. Meteorol., 100(4): 291-308

Granier A (1985): Une nouvelle méthode pour la mesure du flux de sève brute dans le tronc des arbres. Annales des Sciences Forestieres, 42: 193-200

Granier A (1987): Evaluation of transpiration in a Douglas-fir stand by means of sap flow measurements. Tree Physiology, 3(4): 309-320.

Grelle A, Lindroth A (1996): Eddy- Correlation System for Long- Term Monitoring of Fluxes of Heat, Water Vapour and CO2. Global Change Biol., 2(3): 297-307

Groisman PY, Legates DR (1994): The accuracy of United States precipitation data. Bulletin of the American Meteorological Socienty, 75(3): 215 – 227

Grünwald T (2002): Langfristige Beobachtung von Kohlendioxidflüssen mittels Eddy- Kovarianz-Technik über einem Altfichtenbestand im Tharandter Wald. Tharandter Klimaprotokolle, Band 7. Eigenverlag der Technischen Universtiät Dresden, 150 pp.

Grünwald T (2008): Personal communication, 23rd Jul. 2009

Grünwald T, Bernhofer C (2007): A Decade of Carbon, Water and Energy Flux Measurements of an Old Spruce Forest at the Anchor Station Tharandt. Tellus Series B - Chemical and Physical Meteorol., 59(3): 387-396

Hanewinkel M. (1996): Überführung von Fichtenreinbeständen in Bestände mit Dauerwaldstruktur. AFZ/ Der Wald, 51: 1440-1446.

Hölscher D., Koch O, Korn S, Leuscher C (2005): Sap flux of five co-occuring tree species in a temperate broad-leaved forest during seasonal soil drought. Trees, 19: 628-637.

Horst TW (1997): A Simple Formula for Attenuation of Eddy Fluxes Measured with First- Order-Response Scalar Sensors. Boundary-Layer Meteorol., 82(2): 219-233

IPCC (2007): IPCC WG1 AR4 Report. Available via dialog: http://ipcc-wg1.ucar.edu/wg1/wg1-report.html (accessed 30th Nov. 2009)

Jensen NO, Hummelshøj P (1995): Derivation of Canopy Resistance for Water Vapour Fluxes Over a Spruce Forest, Using a New Technique for the Viscous Sublayer Resistance. Agricultural and Forest Meteorology, 73: 339-352

Kaimal JC, Finnigan JJ (1994): Atmospheric Boundary Layer Flows, Their Structure and Measurement. Oxford University Press, New York, Oxford, 289 pp.

Kaimal JC, Kristensen L (1991): Time- Series Tapering for Short Data Samples. Boundary-Layer Meteorol., 57(1-2): 187-194

Kipp & Zonen (2008): Instruction Manual CNR 1 Net Radiometer. Available via dialog: http://www.kippzonen.com/ (accessed 09th Jan. 2008)

Kölling C, Walentowski H, Borchert H (2005): Die Buche in Mitteleuropa. Eine Waldbaumart mit grandioser Vergangenheit und sicherer Zukunft. AFZ/ Der Wald, 60: 696-701.

Kölling C, Zimmermann L, Walentowski H (2007): Klimawandel: Was geschieht mit Buche und Fichte?. AFZ/ DerWald, 61: 584 - 588

Komatsu H, Tanaka N, Kume T (2007): Do coniferous forests evaporate more water than broad- leaved forests in Japan?. J. Hydrol., 336: 361-375

Köstner B, Granier A, Cermák J (1998): Sapflow measurements in forest stands: methods and uncertainties. Ann. Sci. For., 55: 13-27

Lankreijer H, Lundberg A, Grelle A, Lindroth A, Seibert J (1999): Evaporation and storage of intercepted rain analysed by comparing two models applied to a boreal forest. Agricultural and Forest Meteorology, 98-99: 595-604

Larcher W (1976): Ökologie der Pflanzen, 2. Auflage, Uni-Taschenbücher: 232. Ulmer-Verlag, 320 pp.

Laubach J, McNaughton KG (1998): A Spectrum- Independent Procedure for Correcting Eddy Fluxes Measured With Separated Sensors. Boundary-Layer Meteorol., 89(3): 445-467

Leder B (2002): Strukturreiche Dauerwälder lösen Nadelbaum-Reinbestände ab. LÖBF-Mitteilungen, 2/02: 25-33

Lee X, Massman WJ, Law B (2004): Handbook of Micrometeorology, A Guide for Surface Flux Measurement and Analysis. Atmospheric and Oceanographic Sciences Library Vol. 29., Kluwer Academic Publishers, 250 pp

Lenschow DH, Raupach MR (1991): The Attenuation of Fluctuations in Scalar Concentrations Through Sampling Tubes. J. Geophys. Res. - Atmos., 96(D8): 15259-15268

Leuning R, Judd MJ (1996): The Relative Merits of Open- and Closed- Path Analysers for Measurement of Eddy Fluxes. Global Change Biol., 2(3): 241-253

Leuning R, King KM (1992): Compasison of Eddy- Covariance Measurements of CO2 Fluxes by Open-Path and Closed-Path CO2 Analysers. Boundary-Layer Meteorol., 59(3): 297-311

Leuning R, Moncrieff J (1990): Eddy- Covariance CO2 Flux Measurements Using Open-Path and Closed-Path CO2 Analyzers - Corrections for Analyzer Water - Vapour Sensitivity and Damping of Fluctuations in Air Sampling Tubes. Boundary-Layer Meteorol., 53(1-2): 63-76

Lin HS (2003): Hydropedology: bridging disciplines, scales, and data. Vadose Zone Journal, 2(1): 1–11

Link TE, Unsworth M, Marks D (2004): The dynamics of rainfall interception by a seasonal temperate rainforest. Agricultural and Forest Meteorology, 124: 171-191

Llorens P, Domingo F, (2007): Rainfall partitioning by vegetation under Mediterranean conditions. A reviw of studies in Europe. Journal of Hydrology, 335: 37-54

Lu P, Urban L, Ping Z (2004): Granier's thermal dissipation probe (TDR) method of measuring sap flow in trees: theory and practice. Acta Botanica Sinica, 46(6): 631–646

Lüttschwager D Remus R (2007): Radial distribution of sap flux density in trunks of a mature beech stand. Ann. For.Sci., 64: 431-438.

Massman WJ (1991): The Attenuation of Concentration Fluctuations in Turbulent - Flow Through a Tube. J. Geophys. Res. – Atmos., 96(D8): 15269-15273

Massman WJ (2000): A Simple Method for Estimating Frequency Response Corrections for Eddy Covariance Systems. Agric. For. Meteorol., 104(3): 185-198

Massman WJ, Clement R (2004): Uncertainty in eddy covariance flux estimates resulting from spectral attenuation. In: Lee X, Massman WJ, Law B (ed) Handbook of Micrometeorology; A Guide for Surface Flux Measurement and Analysis. Atmospheric and Oceanographic Sciences Library Vol. 29., Kluwer Academic Publishers: 250 pp.

Mauder M, Liebethal C, Gockede M, Leps JP, Beyrich F, Foken T (2006): Processing and quality control of flux data during LITFASS-2003. Boundary- Layer Meteorol., 121(1): 67-88

McMillen RT (1988): An Eddy- Correlation Technique With Extended Applicability to Non- Simple Terrain. Boundary-Layer Meteorol., 43(3): 231-245

Moderow U, Feigenwinter C, Bernhofer C (2007): Estimating the Components of the Sensible Heat Budget of a Tall Forest Canopy in Complex Terrain. Boundary-Layer Meteorol., 123(1): 99-120

Moncrieff JB, Massheder JM, de Bruin H, Elbers J, Friborg T, Heusinkveld B, Kabat P, Scott S, Soegaard H, Verhoef A (1997): A System to Measure Surface Fluxes of Momentum, Sensible Heat, Water Vapour and Carbon Dioxide. J. Hydrol., 189(1-4): 589-611

Monteith JL, Unsworth MH (1990): Principles of Environmental Physics, Second Edition, Butterworth Heinemann, 291 pp

Moore CJ (1986): Frequency- Response Corrections for Eddy- Correlation Systems. Boundary- Layer Meteorol., 37(1-2): 17-35

Nešpor V, Sevruk B (1999): Estimation of Wind-Induced Error of Rainfall Gauge Measurements Using a Numerical Simulation. Journal of Atmospheric and Oceanic Technology, 16: 450-464

Niemand C, Köstner B, Prasse H, Grünwald T, Bernhofer C (2005): Relating tree phenology with annual carbon fluxes at Tharandt forest. Meteorologische Zeitschrift, 14: 197-202.

Oke TR (1987): Boundary Layer Climates, Second Edition. Cambridge University Press, 435 pp.

Penman HL (1948): Natural Evaporation from Open Water, Bare Soil, and Grass. Proceedings of the Royal Society of London, Series A-Mathematical and Physical Sciences, 193(1032): 120-145

Prasse H, Eichelmann U (2002): Stationsbeschreibungen und historische Ergebnisse. In Bernhofer C (ed): Exkursions- und Praktikumsführer TharandterWald. Tharandter Klimaprotokolle, Band 6, Eigenverlag der Technischen Universität Dresden, 292 pp.

Prescher AK, Grünwald T, Bernhofer C (2010): Land use regulates carbon budgets in eastern Germany: From NEE to NBP. Agricultural and Forest Meteorology, 150(7-8): 1016-1025

Rannik Ü, Vesala T, Keskinen R (1997): On the damping of temperature fluctuations in a circular tube relevant to the eddy covariance measurement technique. J Geophys. Res., 102:12789-12794

Rebmann C, Göckede M, Foken T, Aubinet M, Aurela M, Berbigier P, Bernhofer C, Buchmann N, Carrara A, Cescatti A, Ceulemans R, Clement R, Elbers JA, Granier A, Grünwald T, Guyon D, Havránkova K, Heinesch B, Knohl A, Laurila T, Longdoz B, Marcolla B, Markkanen T, Miglietta F, Moncrieff J, Montagnani L, Moors E, Nardino M, Ourcival1 JM, Rambal S, Rannik U, Rotenberg E, Sedlak P, Unterhuber G, Vesala T, Yakir D (2004): Quality analysis applied on eddy covariance measurements at complex forest sites using footprint modeling. Theor. Appl. Climatol. 80: 121

Rennenberg H, Seiler W, Matyssek R, Geßler A, Kreuzwieser J (2004): Die Buche (Fagus sylva-tica L.) - ein Waldbaum ohne Zukunft im südlichen Mitteleuropa? Allgemeine Forst- und Jagdzeitung, 175: 210-244

Reynolds ERC, Henderson CS (1967): Rainfall Interception by Beech, Larch and Norway Spruce. Forestry, 40(2): 165-183

Richter D (1995): Ergebnisse methodischer Untersuchungen zur Korrektur des systematischen Meßfehlers des Hellmann-Niederschlagsmessers, Berichte der Deutschen wetterdienstes 194. Selbstverlag des Deutschen Wetterdienstes, 93 pp.

Rios-Entenza A, Miguez-Macho G (2010): Moisture recycling and the maximum of precipitation in the spring in the Iberian Peninsula. In: EGU 2010, Book of Abstracts, Vienna, Austria, 02.- 07. May 2010

Rodda JC, Smith SW (1986): The significance of the systematic error in rainfall measurements for assessing wet deposition. Atmospheric Environment, 20(5): 1059-1064

Rutter AJ, Kershaw KA, Robins PC, Morton AJ (1971): A Predictive Model of Rainfall Interception in Forest, 1. Derivation of the Model from Observations in a Plantation of Corsian Pine. Agricultural Meteorology, 9: 367-384

Sachs L (1999): Angewandte Statistik - Anwendung statistischer Methoden, 9. Auflage. Springer, Berlin Heidelberg New York: 881 pp.

Sakai RK, Fitzjarrald DR, Moore KE (2001): Importance of Low-Frequency Contributions to Eddy Fluxes Observed over Rough Surfaces. J. Appl. Meteorol., 40: 2178-2192

Schönwiese CD, Janoschitz R (2008a): Klima-Trendatlas Deutschland 1901-2000. Berichte des Inst. Atmosphäre u. Umwelt/ *4*, Univ. Frankfurt/M., 64 pp.

Schönwiese CD, Janoschitz R (2008b): Klima-Trendatlas Europa 1901-2000. Berichte des Inst. Atmosphäre u. Umwelt/ *7*, Univ. Frankfurt/M., 82 pp.

Schotanus P, Niewstadt FTM, De Bruin H (1983): Temperature measurements with a sonic anemometer and its application to heat moisture fluxes. Boundary- Layer Meteorol., 26(1): 81-93

Schwärzel K, Feger KH, Häntzschel J, Menzer A, Spank U, Clausnitzer F, Köstner B, Bernhofer C (2009a): A novel approach in model-based mapping of soil water conditions at forest sites. Forest Ecology and Management, 258 (10): 2163-2174

Schwärzel K, Menzer A, Clausnitzer F, Spank U, Häntzschel J, Grünwald T, Köstner B, Bernhofer C, Feger KH (2009b): Soil water content measurements deliver reliable estimates of water fluxes: A comparative study in a beech and a spruce stand in the Tharandt forest (Saxony, Germany). Agricultural and Forest Meteorology, 149 (11): 1994-2006

Schwärzel K (2009c): Personal communication, August 14th 2009

Shuttleworth WJ, Wallace JS (1985): Evaporation from Sparse Crops – An Energy Combination Theory. Quarterly Journal of the Royal Meteorological Society, 111: 839-855

Shuttlewoth WJ (1993): Evaporation. In Maidment DR (ed): Handbook of Hydrology. McGraw-Hill Professional, 1424 pp.

Smith DM, Allen SJ (1996): Measurements of sap flow in plant stems. Journal of Experimental Botany, 47(305): 1833-1844

Spank U (2003): Einfluss der Vorfeuchte und der Landnutzung auf das Extremhochwasser im August 2002, Hydrologisch- Meteorologische Projektarbeit am Lehrstuhl für Hydrologie und Meteorologie (Professur für Meteorologie) der Technischen Universität Dresden, 93 pp (and appendix 44 pp)

Spank U, Bernhofer C (2008): Another simple method of spectral correction to obtain robust eddy-covariance results. Boundary-Layer-Meteorology, 128(3): 403-422

Su HB, Schmidt HP, Grimmond CSB, Vogel CS, Oliphant AJ (2003): Spectral Characteristics and Correction of Long-Term Eddy-Covariance Measurements over two mixed Hardwood Forests in Non-Flat Terrain. Boundary-Layer Meteorol., 110: 213-253

The University of Edinburgh [School of GeoSciences, Institute of Atmospheric and Environmental Science] (2001): EdiSol. Available via dialog: http://www.geos.ed.ac.uk/abs/research/micromet/edisol/ (accessed 30th Jan 2008)

The University of Edinburgh [School of GeoSciences, Institute of Atmospheric and Environmental Science] (2007): EdiRe. Available via dialog: http://www.geos.ed.ac.uk/abs/research/micromet/EdiRe/ (accessed 30th Jan 2008)

Thomas C, Mayer JC, Meixner FX, Foken T (2006): Analysis of Low- Frequency Turbulence Above Tall Vegetation Using a Doppler Sodar. Boundary- Layer Meteorol., 119(3): 563-587

Tužinský L (2000): Spruce and beech Forest stands water balance. Ekológia (Bratislava), 19(2): 198-210

Valente F, David JS, Gash JHC (1997): Modelling interception loss for two sparse eucalypt and pine forests in central Portugal using reformulated Rutter and Gash analytical models. Journal of Hydrology, 190: 141-162

Wagner S (2004): Klimawandel- einige Überlegungen zu waldbaulichen Strategien. Forst und Holz, 59: 394-398.

Walter M (2007): Vergleich verschiedener Korrekturverfahren für Eddy-Kovarianz- Daten und ihr Einfluß auf kalkulierte Stoff- und Energieflüsse, Hydrologisch- Meteorologische Projektarbeit am Lehrstuhl für Hydrologie und Meteorologie (Professur für Meteorologie) der Technischen Universität Dresden

Webb EK, Pearman GI, Leuning R (1980): Correction of flux measurements for density effects due to heat and water vapour transfer. Quart. J. R. Met. Soc., 106: 85-100

Weihe J (1984): Wetting and Interception in Beech and Spruce Canopies, IV. The Distribution of Rain Beneath Spruce Canopies (in German: Benetzung und Interzeption von Buchen- und Fichtenbeständen, IV. Die Verteilung des Regens unter Fichtenkronen). Allgemeine Forst- und Jagdzeitung, 155(10-1): 241-252

Weihe J (1985): Wetting and Interception in Beech and Spruce Canopies, V. The Distribution of Rain Beneath Beech Canopies (in German: Benetzung und Interzeption von Buchen- und Fichtenbeständen, V. Die Verteilung des Regens unter Buchenkronen). Allgemeine Forst- und Jagdzeitung, 156(5): 81-89

Wessolek G, Duijnisveld WHM, Trinks S (2008): Hydro-pedotransfer functions (HPTFs) for predicting annual percolation rate on a regional scale. Journal of Hydrology, 356: 17-27

Wilczak JM, Oncley SP, Stage SA (2001): Sonic Anemometer Tilt Correction Algorithms. Boundary-Layer Meteorol., 99(1): 127-150

Wilson K, Goldstein A, Falge E, Aubinet M, Baldocchi D, Berbigier P, Bernhofer C, Ceulemanns R, Dolman H, Field C, Grelle A, Ibrom A, Law BE, Kowalski A, Meyers T, Moncrieff J, Monson R, Oechel W, Tenhunen J, Valentini R, Verma S (2002): Energy balance closure at FLUXNET site. Agric. For. Meteorol., 113: 223-243

Yang D, Goodison BE, Metcalfe JR, Louie P, Leavesley G, Emerson D, Hanson CL, Golubev VS, Elomaa E, Gunther T, Pangburn T, Kang E, Milkovic J (1999): Quantification of precipitation measurement discontinuity induced by wind shields on national gauges. Water Resources Research, 35(2): 491–508

Acknowledgment

The list of people I want to thank is a long one and I apologize that I cannot name everyone individually. I thank my mentor and supervisor Prof. Dr. Christian Bernhofer for his gracious support, his helpful suggestions and his endless patience. In particular I want to thank him that he offered me the opportunity to develop my personality and my abilities. Furthermore, I thank Prof. Dr. Konrad Miegel for reviewing and assessing my study. I also thank PD. Dr. Franz Berger that he arranged to come to my examination despite his full schedule.

The dissertation was supported by the German Science Foundation (DFG) in the frame of the project "Model Based Classification of the Water Balance of Forest Sides in Low-range Mountain Areas" (FE 504/2-2). The measurements at the test sites were supported by a series of EU projects including EUROFLUX (ENVCT 0095-0078), CARBOEUROFLUX (ENVK2-1999-00229) and CARBOEUROPE-IP (GOCE-CT-2003-505572), the BMBF project "VERTIKO" (#07ATF37-UBAS), and the TU Dresden.

I thank Prof. Dr. Karl-Heinz Feger, Dr. Kai Schwärzel, Falko Clausnitzer, PD Dr. Barbara Köstner, Dr. Janet Häntzschel and Alexander Menzer for the fantastic cooperation within the project. Similarly, I thank Dr. Thomas Grünwald, Uwe Eichelmann and Heiko Prasse for their technical assistance and I am grateful to Dr. Sabine Hahn-Bernhofer, Uta Moderow and Christiane Helbig for language assistance. Special thanks go to Mark Sixsmith for proofreading.

Furthermore I want to thank all my colleagues for the likeable and pleasant working environment. Particularly my thanks go to Dr. Ronald Queck for interesting and supporting discussions. Furthermore I thank Klemens Barfus, Cornelia Kurbjuhn and Maik Renner for the nice and inspiring conversations, where they inspired me for a lot of ideas for future tasks.

Last, I want to thank my parents and my life partner Romy Mizera. I thank my parents for the beautiful childhood and the good education. Particularly I am grateful that they offered me the opportunity to find my own way. (Mother, I hope you can see me from heaven.) And I owe thanks to my life partner Romy Mizera for her patience and loyalty even in hard times.